REAL OPTIONS FOR CLIMATE CHANGE INVESTMENTS UNDER UNCERTAINTY

By

LAURENCE GORDON CHAN
(B.Eng.), University of Singapore, (MBA), University of Manchester

A THESIS SUBMITTED

FOR THE DEGREE OF DOCTOR OF PHILOSOPHY

DIVISION OF ENGINEERING AND TECHNOLOGY MANAGEMENT

NATIONAL UNIVERSITY OF SINGAPORE

2013

ACKNOWLEDGEMENTS

"If I have seen a little further it is by standing on the shoulders of Giants"
Isaac Newton (1676)

I would like to thank my thesis supervisor Prof Vladan Babovic for his continuous support and valuable guidance during my doctoral studies. He provided me with the freedom to explore many fascinating areas in my research.

I am also grateful to Prof. Hang CC for providing me with the opportunity to continue my intellectual pursuits.

In addition, I should separately mention the administrative support provided by Singapore Delft Water Alliance office for the outstanding administrative assistant in organizing my seminars.

Special thanks go to all my dear relatives and friends who encouraged me during the whole period of my graduate studies.

Last but not the least, I express my extreme gratitude to my wife, son, and mother, thanks for supporting me with your love, encouragement and understanding.

CONTENTS ii

SUMMARY

Global warming and climate change are mainly attributed to climate forcing from increase in CO2 concentration in the atmosphere. The social costs of global warming from rising sea levels, extreme weather, crop failures, and species extinction are enormous. Scientists and researchers and policymakers are seeking solutions to reduce CO2 emissions.

Managing CO2 emission control policy is a complex problem because of uncertainties in CO2 emission process and CO2 uptake, and irreversibility in investment decisions. As such the timing and conditions to adopt certain CO2 reduction policies become important questions for the policymaker. Real options analysis is an approach which incorporates uncertainties and flexibility in timing. It allows the policymaker to learn and then act when more information is available in future to resolve uncertainties.

This research is an application of real options analysis to CO2 reduction policies with focus on normal and catastrophe events. The goals are to develop a framework and integrated methodology with real options analysis for analyzing the timing and conditions of policy adoption.

In the thesis, I introduced the complexity of analyzing climate change and demonstrated how real options analysis can be applied in a stochastic model for analyzing CO2 reduction policies. I modelled CO2 emission as a stochastic process and used CO2 observation data to statistically estimate the parameters of the stochastic CO2 emission model.

Using real options approach I developed a perpetual or infinite time model to investigate CO2 emission cutback policy and CO2 concentration abatement policy. I solved the closed form analytical model for the option to defer value and illustrated its application in various CO2 reduction rates and discount rates. Next I extended the

perpetual time model to incorporate jump events to represent catastrophe events. The solution is in an equation which could be solved numerically. I studied the impact of jump size and jump intensity of catastrophe events in perpetual time.

As there are time constraints and limited economic resources in practice, I further developed a finite time model with two stopping times: first hitting time and optimal stopping time. I showed how first hitting time can be solved using closed form analytical solutions, and also, how optimal stopping time can be obtained using Monte Carlo numerical solution and least square regression basis function method. I applied these methods to re-analyse CO2 reduction policies in finite time.

For catastrophe events in finite time, I incorporated Poisson jumps to the finite time model. Monte Carlo numerical solution is used to obtain the results. To generate the simulated paths more efficiently, I presented a modified method based on inter-arrival time of the jump events. I showed that the jump diffusion model produces extreme value distribution values in both first hitting time and fixed time. With this jump diffusion model, I investigated the impact of jump events with jump sizes, jump size variances, jump intensities and CO2 reduction rates on CO2 reduction policies. Finally, I showed from the research results that real options analysis is consistent and appropriate for analyzing climate change policies.

List of Figures

List of Tables

Abbreviations and Notations

μ	drift in CO2 concentration level (per annum) When μ is multiplied by X the produce is the CO2 emission rate of stochastic differential equation
μ'	drift in CO2 emission rate after cutback in CO2 emission
σ	volatility of CO2 emission rate of stochastic differential equation (per annum)
α	remaining CO2 emission rate after reduction. (α=1-δ)
α_t, μ_t	parameters in RICE model cost of abatement function (Chapter 7 only)
β_1, β_2, β_3, β_4	roots of homogenous equation in ODE
δ	cutback in CO2 emission rate (Chapter 4 only). δ =0 for no cutback in CO2 emission reduction, δ =1 for 100% cutback in CO2 emission reduction
δ	rate of pure preference (Chapter 2 only)
g	growth rate of GDP per capital (Chapter 2 only)
κ	risk tolerance in discount rate
η	hedging ratio in No Arbitrage theory
γ	elasticity of marginal utility to changes in consumption (Chapter 2 only)
θ	equivalent flow of CO2 concentration to social costs
λ	shape parameter in inverse Gaussian (Chapter 6 only)
Φ	size of the jump
dq	Poisson process event
Υ	rate of change of drift μ (Chapter 4 only)
λ	frequency or intensity of the jump
A_1,A_3,C_1,C_3	constants of homogenous equation in ODE
β_0, β_1, β_2	regression parameters in Longstaff Schwartz Monte Carlo
c_1	constant parameter in reduction cost function
m	power parameter in polynomial of social benefit function
n	CO2 abatement level. n=0 for 100% abatement, n=1 for nil abatement
r	risk free interest rate
z	random variable, normal distributed with mean 0 and variance 1 N(0,1)
B	social benefits
B	constant threshold barrier (Chapter 6 only)
B_m	moving threshold barrier (Chapter 6 only)
CO2	carbon dioxide in the atmosphere
CO2-eq	CO2 equivalent
E(.)	expected value
GHG	greenhouse gas
J_t	summation total of all jump sizes over period t
K	investment cost, adoption cost, exercise cost
LLGHG	long live greenhouse gas (Chapter 3 only)
M	CO2 emission reduction (Chapter 7 only)
N_t	number of jumps in fixed time period t
R	percentage reduction of CO2 concentration in reduction cost function
S	price of asset in financial option pricing
X_0	CO2 concentration level at time t=0
U	uniform probability density function (Chapter 8 only)
V	value of project with no adopt CO2 reduction policy

W	value of project with adopt CO2 reduction policy
X_t	CO2 concentration level at time t
X*	CO2 concentration level at stopping time
Y_i	jump size in i^{th} jump event

1 INTRODUCTION

Since the industrial revolution in 19th century, CO2 concentration level in the atmosphere has been increasing. Recent global warming and climate change are mainly the response to increase in CO2 concentration coming from anthropogenic CO2 emission. IPCC TAR estimates that 60% of additional warming today is due to CO2 increase warming, 20% from methane and 14% from chlorofluorocarbons, and remainder from other greenhouse gases (IPCC TAR, 2001a). The social costs of global warming as a result of rising sea levels, extreme weather events, crop failures, species extinction are enormous. Governments are considering many options to solve this problem. Certainly, the solutions to control or reduce carbon emissions are costly, and this urgent problem is compounded by deep uncertainty of CO2 emission and uptake process.

1.1 Analyzing Climate Change

Policy study in climate change requires a combination of many highly specialised scientific and economic disciplines. In addition to these quantitative approaches, there are also qualitative issues in ethical and political considerations. Furthermore, the vast landscape of research studies in climate change creates a challenging task for researchers. Several methodologies are available to address and analyse specific problems in climate change. The success of these methodologies depends on identifying the issues and accurate modelling of the problem. Therefore it is necessary to outline a suitable research framework, define boundaries of areas for investigation, and focus on important issues.

One approach to analyse climate change policy is to breakdown the problem into 3 stages (Heal & Kriström, 2002). The first stage is to understand the climate process and to make climate forecasts. This is the physical science aspect of

climate study which involves complex interaction of atmosphere, hydrology, and oceanography. Then climate forecasts are made based on physical evidence gathered and analysed. The second stage is to evaluate the economic impact of climate change with economic theory. The traditional approach is to use benefit cost analysis to analyse environmental impact. Societal economic values are expressed as willingness to pay and willingness to accept. Another widely controversial area is the discount rate to be used in calculating the present value of economic policies. The third and final stage is to obtain the optimal policy to control CO2 emission using sensitivity analysis with these models. Usually, the optimized solution is a trade-off of several conflicting objectives and subject to various constraints.

1.2 Uncertainties in Climate Change

Uncertainties are inherent in climate change models. These include uncertainty with regard to future greenhouse gas concentrations (including mitigation efforts), sensitivity of the global climate to greenhouse gas concentrations, and how global climate change will translate to regional climate impacts.

In the physical science report, IPCC AR4 recognizes the importance in uncertainty and presents its studies in a range of confidence levels (IPCC, 2007). The main causes of these uncertainties are unpredictability in chaotic behaviour of complex systems, structural uncertainty in inadequate modelling, and value uncertainty, such as incomplete data and missing parameters.

Kolstad & Toman identify two types of uncertainty in climate change (Kolstad & Toman, 2005). The first uncertainty is parametric uncertainty because some aspects of climate change are not well understood, but would be better understood in future. For example, knowledge of the climate system could be improved with more research. The second uncertainty is stochastic uncertainty. Uncertainties arise because of assumptions in economic or physical processes. No matter how complex

an economic or physical model is some elements are inevitably not modeled. Also the future values of many economic and technology processes can never be unknown, otherwise, there will not be any uncertainty to begin with, and subsequently, the problem will not arise.

Peterson describes the spectrum of uncertainty in climate change range from uncertainty in CO2 emission path, climate forecasts, impacts of climate change to optimal policies (Peterson, 2006). Uncertainty in CO2 concentration level is a stochastic uncertainty caused by misspecification of climate model and the unpredictability of future events. Uncertainty in climate forecasts is parametric uncertainty which is the result of incomplete knowledge of climate change process, especially the parameters and factors affecting climate change. This type of uncertainty can be resolved over time with learning. Uncertainty in impacts of climate change can be analyzed in two ways. In the first instance, there is the environmental impact of climate change. Certain environment impact could be studied in laboratory experiments but it is impractical and expensive to replicate large scale environmental impact without potentially disastrous results. The second impact is economic impact of climate change which requires assessing utility function of environmental goods. This is an even more complex uncertainty because society values and preferences are involved. Therefore, with so many unknown uncertainties it is important to minimize the impact of damages of climate change by hedging against uncertainty (Manne & Richels, 1991). Finally, uncertainty in climate policies could cause the adopted course of action obtained from traditional benefit cost method to be sub optimal and less effective. This is demonstrated in formulating control policies in simulation of the DICE climate model (Nordhaus, 1994) which combines scientific and socioeconomic aspects of climate change for purpose of assessing impacts and policies.

1.3 Irreversibilities in Climate Change

Climate change is impacted by two types of irreversibilities, both of which aggravate the seriousness of the problem.

1.3.1 Irreversibility in Climate Change

CO2 concentration remains in the atmosphere for a long time. Therefore climate change that takes place due to increases in CO2 concentration is largely irreversible for thousands of years after emissions stop (Solomon, Plattner, Knutti, & Friedlingstein, 2009). The above study noted that this long lasting effect will cause persistent decreases in dry-season rainfall and drought in some areas and increases long wet-season rainfall and flooding in other areas. In addition, many coastal cities will be affected by rising sea levels. A recent report by IPCC noted that it is very likely that the frequency of heavy precipitation will increase in the 21st century over many regions (IPCC SREX, 2012). It also warned that economic losses from extreme climate change disasters will continue to increase in future. In summary there is general agreement that the dry regions will get less rainfall and the wet regions will get more rainfall, and there will be rising and extreme sea levels.

A more serious consequence of the long irreversibility of climate change is the build-up of CO2 concentration levels which could trigger off a runaway climate change scenario and herald wide spread catastrophe events.

1.3.2 Irreversibility in Decision Making

The issue of irreversibility in environmental economics was introduced by Arrow & Fisher (Arrow & Fisher, 1974). They show that when future net benefits are uncertain and investment decisions are irreversible, it is preferable to defer the investment because there is a possibility of learning more about future benefits and make better decisions. This value of deferment is known as quasi-option in environmental economics literature. It is the conditional value of information, that is,

a value of information about future net benefits conditional on not investing in the first period because that would bring about uncertain future environmental costs.

In a different approach, Epstein argues that in a firm's consumption and saving, the prospect of greater future information discourages the adoption of an irreversible decision (Epstein, 1980). This means that policymakers view investments as sunk costs because of the possible loss of economic utility in risky investments. Extending Epstein's theory, Narain et al shows that this approach is applicable to decision making in environmental economics problems as well (Narain, Hanemann, & Fisher, 2007).

Pindyck developed the irreversibility thread further (Pindyck, 1991). He compared the irreversible investment opportunity to a financial call option. In his approach the value to future benefits from deferring an irreversible investment becomes a real option for analyzing investments with uncertainty (Dixit & Pindyck, 1994).

1.4 Motivation

The complexity of the problem arising from a combination of multiple uncertainties and irreversibilities creates a number of research questions in analyzing climate change mitigation policies. The main research issues in the thesis are highlighted below.

Adoption of policy that appears appropriate now may turn out to be ineffective once further information becomes available. It is important to balance the timing of adopting the policies with learning and future benefits arising from deferment of adoption. This may suggest that adoption is best pursued with an emphasis on flexibility and with a preference for 'no regrets' options that have benefits regardless of future climate change. For practical reasons, it is also necessary to consider the time horizon in formulating these policies.

The measures and methods of reducing CO2 emissions are important issues in climate change policies. IPCC publishes two separate volumes, one volume on mitigation of climate change, and another volume on impact, adaptation and vulnerability. These two publications describe extensively two approaches to manage problems in climate change: mitigation and adaptation. Mitigation is defined as intervention to reduce human-caused net emissions of greenhouse gases, and adaptation is defined as adjustment in natural or human systems to a new or changing environment (IPCC AR4, 2007a, 2007b). Other than the technical issues in these two reduction approaches, the cost effectiveness of the methods are also important issues for the policymaker.

For many years IPCC warns about the risks of catastrophic or abrupt climate changes which are becoming more serious with increasing extreme weather and climate events (IPCC AR4, 2007b; IPCC SAR, 1996; IPCC TAR, 2001a). Although these catastrophe events have low probability, their impact on economy and human lives are enormous. The costs of damages of such extreme events cannot be ignored and need to be accounted for in policymaking.

Many studies, especially those using Integrated Assessment Models, incorporate uncertainties by assigning pre-specified probabilities and applying Monte Carlo simulations in sensitivity analysis. A more realistic method is to use stochastic process to represent random events in nature.

To address the above mentioned issues, this thesis proposes to use real options analysis, which is based on stochastic process, for investigating economic policies in managing CO2 emissions reduction.

1.5 Research Gaps and Research Scope

The premise of this research thesis is the application of real options analysis to CO2 reduction methods using stopping time approaches. It combines discipline

studies in statistical analysis, economic and financial theory, and climate change. The library of knowledge in each of these disciplines is tremendous, and it is necessary to focus on relevant areas of interest and apply these to further investigate the research gaps.

1.5.1 Relevant parameters in stochastic process

Many research studies (Pindyck, Lin) in climate change policy make use of the values and parameters from Cline's book (Cline, 1992). There are two reasons to revisit these parameters. Firstly, these parameters were obtained from climate science studies with general circulation models which may not be appropriate for use in stochastic processes setting. Secondly, as Cline's book was published some time ago, the parameters need to be updated with new knowledge. Therefore, this research proposes to re-estimate these parameters using up to date CO2 observation data and appropriate statistical estimation methods.

1.5.2 CO2 Reduction Methods

Two reduction methods for atmospheric CO2 proposed in this research are CO2 emission cutback and CO2 concentration level abatement. CO2 emission cutback is an "a priori" method to reduce CO2 concentration level to its present day level. In contrast CO2 concentration abatement can be seen as an "a posterior' method to reduce the effects of CO2 emission which has already taken place. It is common to treat these two CO2 reduction methods as separate problems in policymaking. The first part of this research employs an integrated approach to the problem with a closed form analytical solution in perpetual time. The second part of the research uses a numerical method for the investigation in finite time.

1.5.3 Time Preference and Stopping Times

Time is irreversible and decisions and actions taken earlier cannot be turned back in time. However, a policymaker with foresight of likely future outcomes is able

to make better decisions as uncertainties are resolved exogenously over time. Also, learning takes place with time as more information becomes available endogenously through new knowledge. This research considers time factor using two approaches. The first approach is infinite or perpetual time which also assumes that infinite resources are available for problem solving. The second approach is finite stopping time. The idea of finite stopping times is a more realistic approach for practical policymaking.

Two types of finite stopping time are first hitting time and optimal stopping time. First hitting time is the earliest time CO2 concentration level reaches a pre-determined threshold level. In financial option pricing application the first hitting time is a knock up-out barrier option. Analytical closed form solution is available for first hitting time problem. This approach has not been extensively studied in real options analysis for climate change. Optimal stopping time is an optimized solution of stopping time assuming that the policymaker has considered all the possible outcomes of future events. In financial option pricing application the optimal stopping time is equivalent to the American call option. There is no known closed form solution to optimal stopping time problem. Monte Carlo numerical solution is used to find the option values, actual stopping times, and benefit levels at stopping time.

1.5.4 Catastrophe Events

There is increasing concern of the dangers of low probability and high impact climate change events. These catastrophe events are disastrous to the environment and living species. There have not been many studies of impact of catastrophe events with real options analysis. The perpetual time real options analysis model is extended to include random jump events which simulate catastrophe events. The jump diffusion model is used to investigate the impact of jump factors, such as jump intensity, jump sizes and jump size variance, on the option value to defer.

Furthermore we examine the impact of jump size and CO2 reduction rates on the option value to defer the reduction policy.

1.6 Research Questions

The research uses real options analysis to investigate the flexibility, incentive to defer, and timing decision of implementing CO2 reduction policies. It proposes to answer the following main research questions.

- How effective are CO2 mitigation and CO2 adaptation policies
- What are the effect of CO2 reduction rates on CO2 reduction policies
- How discount rates affect the timing decision to adopt
- How are the decisions affected when there is limited time to act
- What are the impacts of catastrophe events on CO2 reduction policies
- What are the impacts of frequency, magnitude, and magnitude uncertainty of catastrophe events on flexibility and timing decision.

1.7 Organization of Thesis

This thesis is organized into 3 parts. The first part, comprising Chapters 2 and 3, provides the concepts and foundation for the research. Chapter 2 gives an overview of framing climate change policies and theory of real options analysis. Chapter 3 uses CO2 concentration level data in the empirical estimation of parameters for the stochastic CO2 emission model.

The second part consists of Chapters 4 and 5, and focuses on real options analysis in perpetual time. Chapter 4 introduces the mathematical approach of real options analysis to derive a closed form analytical solution for the value of CO2 reduction policy. Chapter 5 extends the perpetual time model to incorporate Poisson jump events.

The final Part C comprises Chapters 6, 7, 8, 9 and 10. These chapters investigate the CO2 reduction problem in finite time using Monte Carlo numerical solution method in real options analysis. Chapter 6 introduces stopping times and CO2 reduction cost functions, and demonstrates the decomposition of option value to defer. This is followed by the study of the two CO2 reduction methods in finite time in Chapter 7. Chapter 8 incorporates Poisson jump events in the finite time model. These jump events are demonstrated to cause extreme value probability distributions. In Chapter 9, catastrophe events are modelled in the jump diffusion model and this is used to study the impacts of the jumps on CO2 reduction methods. The final Chapter 10 summarizes the results of previous chapters, provides a practical guide for the policymaker, describes the limitations and contributions of the research, and suggests potential areas for further research.

PART A

CO2 EMISSION PROCESS AND REAL OPTIONS ANALYSIS

2. CLIMATE CHANGE AND REAL OPTIONS ANALYSIS

Benefit cost analysis (BCA) is an approved method of government agencies for evaluating and making policy decisions on public sector projects. In its basic form, BCA is a static and deterministic approach in which pre-determined net cash flows are discounted to the present value; the decision is made immediately based on the present value of the investment. The weaknesses of BCA method are the assumptions that discount rates, benefit and cost values are known with certainty throughout the period. Therefore BCA method is not suitable when there are deep uncertainties in the problem. An alternative method is to use a stochastic process to account for uncertainties in the problem, and option values to assess the flexibility in the solution. Graham demonstrates that when there are uncertainties the best way to measure societal benefits is by option pricing (Graham, 1981). The option prices are ex ante measures because the society values the policies without knowledge of future events. This approach provides a useful insight into the value of information of future events and value of flexibility in managing policies.

2.1 Framework for Climate Change Policy

There are many complex factors in analyzing climate change policies. Inter related uncertainties in the climatic and economic system limit our ability in predicting the timing and magnitude of future impacts caused by climate change, and formulating effective climate change policies. Furthermore, the policies require time to implement and produce results, and their impact of these policies could last a long time. Therefore a multi facet approach which addresses the many issues in climate change is required for the problem solution.

Cline suggests a three category framework consisting of physical, benefit, and policy (Cline, 1992). The physical category includes economic impact, geographic regions, and technology innovations. The benefit category considers

scaling of estimated benefits, discount rate, and time. And the policy category comprises baseline warming, policy action scenario, risk aversion, adaptation, and weighting.

Dellink proposes a five step framework for analyzing climate change which is based on the requirements of researcher's specification of the problem (Dellink, 2005).

1. The economy can be a real economy with empirical data or hypothetical model.
2. The period under study can be static with a fixed number of dates or dynamic with infinitesimal time periods.
3. The model can be deterministic model or stochastic model with changing uncertainties.
4. The model parameters can be calibrated with real data or assumed by researcher in an example.
5. The study could be a global model or regional focus.

This framework allows the researcher freedom to specify as many models as necessary for the problem.

In real world, policymakers are faced with conflicting objectives, constraints and complex set of courses of actions which include economic, politics, ethics, and financial issues. The final decision needs to balance the interests of all stakeholders. Kann & Weyant propose an unifying framework and holistic approach for analyzing environmental policy models with uncertainty (Kann & Weyant, 2000). Their research is based on a five criteria framework: reduction approach, reduction rate, reduction method, timing, and stakeholder. The following sections describe application of these criteria relevant to the present research.

2.1.1 CO2 Reduction Approaches

Cline classified two models in CO2 reduction (Cline, 2011). These are the top down models and bottom up models. Top down model focuses on the global climate and macroeconomic performance of the reduction policy but ignores innovations in abatement technologies that have been implemented to achieve policy targets. Examples of top down models are Nordhaus's RICE model and EMF 22 models. In the bottom up model the direct costs of carbon emission reductions are given by the marginal and total costs of specific pollution control and abatement technologies in specific industries. The aggregated costs are analysed and assess in the context of their applicability to a wider global climate.

2.1.2 CO2 Reduction Rates

United Nations Climate Change Conference in 1997 Kyoto Protocol set a target rate to reduce greenhouse gas emission to 5°C below 1990 levels by 2012. As this target is unlikely to be achieved, in the 2009 Copenhagen conference leading industry leaders agreed to push back the target date to halve carbon emissions by 2050. The recent 2011 conference in Durban observes that even at the level of 550 ppm it is likely that 2°C would be exceeded (Harvey & Vidal, 2011). The outcomes of many of these international conferences indicate that is not easy to reach an agreement on CO2 reduction policies and reduction rates. Each country has its national interests, and bargaining powers of many countries need to be considered in a compromised solution. Rather than choosing a specific reduction rate, this research explores the entire range of reduction rates from zero reduction to full reduction for sensitivity analysis.

2.1.3 CO2 Reduction Methods

CO2 reduction methods can be driven by technology or government. As proposed in Kyoto protocol the mechanisms for government initiatives include emissions trading, clean development mechanisms, and joint implementation

(UNFCCC, 2009). With technology approach, the reduction method is driven by technology innovation solutions to reduce carbon emission. This research focuses mainly on technology driven approach to CO2 reduction.

The first reduction method is in cutback in the rate of CO2 emission. This is the most common discussed approach in CO2 reduction. Methods of reducing the rate of CO2 at source include technical innovations such as more efficient energy production, alternate renewable energy, and economic measures such as carbon taxes, carbon tariffs, and carbon credit trading.

The second reduction method, which is less frequently mentioned, is CO2 concentration level abatement of atmospheric CO2. There are 2 perspectives in this method. The first perspective requires decreasing the CO2 concentration level in the atmosphere by enhancing the operation of carbon sinks such as reforestation, and carbon sequestration such as capturing and storing CO2 emission at source. In the second perspective, the CO2 concentration level abatement can also be considered as a complimentary solution to CO2 abatement policy. For example, increase in CO2 concentration causes global warming which result in environmental damage such as rising sea levels. The environmental damage could be prevented by investing in adaptation infrastructures such as building sea walls or relocating cities to higher elevations. Although this adaptation to climate change adaption does not reduce the CO2 concentration level, it does alleviate the immediate damage. In example above, the reduction cost in the first approach is in the creation of carbon sinks, and in the second approach the reduction cost is in the adaptation costs of new infrastructure.

2.1.4 Policy Timing

The timing of CO2 emission reduction is an important issue in all United Nations Climate Change Conference and IPCC assessment reports. The Business

as Usual (or “Do Nothing”) attitude is not acceptable as the current situation continues to worsen each day. Clearly, an intervention policy is required.

A rational and cautious policymaker would invest in a project only when the uncertainties have been resolved. If uncertainties can be resolved quickly, then the cost of waiting for more information to be made available is small. If uncertainty cannot be resolved quickly, then costs associated with waiting would be high. To investigate the impact of timing on policymaking this research employs two timing methods: optimal stopping time and first hitting time.

In optimal stopping time approach the objective is to maximize the net benefit of society as a whole. On this basis, adoption can be considered effective if it is done at the least cost, if resources are allocated to activities that generate the greatest net benefit to society, and if the timing of adoption is ‘optimal’. That is, optimal timing decision should be based on the relative costs and benefits of taking action at different points in time. This means the adoption should be deferred as long as the benefits of delay are greater than the associated costs.

In first hitting time approach the objective is to minimize uncertainty and risk of higher unknown costs. In this approach a threshold target is used to monitor the CO2 emission for a hitting event when the CO2 concentration level first reaches the threshold target. This benchmark can also be adjusted continuously with a moving barrier. For example, increasing risk aversion can be represented by a downward sloping barrier which reduces the threshold over time. This is a conservative approach because the first hitting time depends on CO2 concentration level and does not consider the optimization of economic value.

2.1.5 Stakeholder

Mitigation and abatement policies in climate change involve clean air, which is a public commodity, and pollution control, which requires co-operation of individuals. The problem with a public good which is freely available to everyone is that

individuals could fail to manage and protect the common goods. This issue leads to what Hardin calls “the tragedy of commons” (Hardin, 1968). Pollution is one of the common goods highlighted in Hardin’s paper:

> “*The rational man finds that his share of the cost of the wastes he discharges into the commons is less than the cost of purifying his wastes before releasing them. Since this is true for everyone, we are locked into a system of “fouling our own nest,” so long as we behave only as independent, rational, free-enterprisers*.”

This will result in depletion of a shared resource by individuals, acting independently and rationally according to each one's self-interest, despite their understanding that depleting the common resource is contrary to their long-term best interests (Meadows, Meadows, Randers, & Behrens, 1972). Hardin recommends that in a free enterprise society the tragedy of the commons could be prevented by either more government regulation or privatizing the commons property. This research requires the government to act as the agent of various stakeholders change. Societal costs and benefits are simply economic values represented without any specific ownership or equity interests.

In a real options analysis setting, the government is the buyer (investor) and the seller is the producer (for example, industries) of the greenhouse gases and the value is the damage cost resulting from climate change.

2.2 Economic Modelling and Analysis of Reduction Policies

A physical science model and a socio-economic model are the basic building blocks required to assess CO2 reduction policies. The physical science model is used to forecast future climate scenarios. Most research studies use climate forecasts from general circulation models (GCM) as their primary source of climate input, or make certain assumptions of future climate conditions at some future dates. These are used as inputs for the socio-economic model which analyses the economic impact and vulnerability of the environment.

Economic analyses of climate change are frequently performed with integrated assessment models (IAM). These are scientific and socio-economic models for investigating climate change primarily for the purpose of assessing policy options for climate change control. There are two types of IAM. The first type of IAM is policy evaluation models. These simulation models consider the effect of a single CO2 reduction policy on the earth, climate, and sometimes economic systems. The second type of IAM is policy optimization model. These models seek to find the optimal policy which trades off expected costs and benefits of climate change control (regulatory efficiency) or the policy which minimizes costs of achieving a particular goal (regulatory cost-effectiveness).

The disadvantage of IAMs is that the forecasts are available at only certain time and so, economic analysis can only be performed at fixed discrete time. Also, simulation models in IAM could not handle uncertainty effectively because all uncertainty are assumed to be resolved immediately (at the discrete time) in the forward process (Ackerman, DeCanio, Howarth, & Sheeran, 2009). IPCC AR4 recognized this problem and recommended that dynamic and stochastic models should be used for better modelling representation. In a dynamic simulation model, the economy evolves over time and is subjected to random shocks such as technological change, price fluctuations, or even changes in policy-making.

Real options analysis is an alternative approach to manage uncertainties in the project, and to provide flexibility in managing policies. It allows the decision maker to learn and then act when the more information is available to resolve the uncertainties step by step.

2.3 Overview of Real Options Literature and Related Climate Change Literature

The literature of financial option pricing and real options analysis is huge. Furthermore, literature on climate change is even more voluminous. This research focuses only on seminal real options analysis papers and related papers on climate change. In this context there are five strands of literature used in this research: uncertainties in real options, irreversibility in real options, jump events in real options, climate change with real options, and catastrophe events in climate change.

The first strand of literature concerns uncertainties in investments. Uncertainties are represented by random walk events. The random walk is a stochastic process which forms the basics of financial option pricing theory (Black & Scholes, 1973). The Black Scholes formula is a closed form analytical solution for option pricing in fixed time, that is, a European option. In an American option, the exercise time is finite but there is possibility of early exercise.

An early application of real options analysis is the option to expand or growth option. Myers applies the financial option concept to real options in the value of the future value of a firm as the sum of two types of assets: real assets which are the present value of assets which the firm currently owns, and real options which are present value of the growth opportunities to purchase future assets (Myers, 1977). Brennan & Schwarz propose an investment valuation model with real options which can be used to obtain optimal stopping time for investment policies in the case of copper mine (Brennan & Schwartz, 1985). McDonald & Siegel develop a two factor real options model for an investment in a synthetic fuel plant (McDonald & Siegel, 1986). The investment opportunity is the option to invest or a perpetual call option, and the value of the investment opportunity is the option value. They introduced investment timing (exercise of call option) for starting (option to defer) and stopping time for abandoning the investment (option to abandon). Majd & Pindyck extend real

options analysis with staged investments which are made sequentially (Majd & Pindyck, 1987). Paddock et al demonstrate the integration of market price model with real options analysis in an actual case of offshore oil exploration (Paddock, Siegel, & Smith, 1988). Two seminal books on real options were published in the 1990s which brought together the main concepts of real options analysis. Dixit & Pinydck's book provides a theoretical and economic approach to real options analysis (Dixit & Pindyck, 1994), while Trigeorgis' book has a managerial focus on a number of real options analysis applications (Trigeorgis, 1996).

The second strand of literature is irreversibility in sunk cost investments for climate change. Arrow & Fisher argue that in an irreversible investment the expected benefits were reduced if there is flexibility in a quasi-option (Arrow & Fisher, 1974). This quasi option value is the expected value of information gained by delaying an irreversible decision. It establishes the important relationship between irreversibility, uncertainty and option value. The rational decision is to balance the reduced benefits with the cost of flexibility to obtain the optimal stopping time and policy. Bernanke argues that, when the project is irreversible, decision makers would want to wait for more information, so as to avoid the "bad news" (Bernanke, 1983). Furthermore, the uncertainty over project payoff creates an option value to defer the investment and wait for more information to arrive. Pindyck synthesizes irreversibility sunk cost and option to defer with real options idea (Pindyck, 1991). He demonstrates how option pricing method and dynamic programming could be used to solve the investment problem.

The third strand of literature is jump events in real options analysis. In normal real options analysis, the random changes are smooth and continuous. When the changes are sudden and discontinuous, these events become jumps. Cox & Ross approached the jump diffusion process with Poisson jumps in binomial tree solution (J. C. Cox & Ross, 1976), while Merton's jump diffusion model is in continuous time and is based on stochastic calculus (Merton, 1976). Unlike the Black Scholes

formula, there is no general closed form solution for the jump diffusion model with a finite exercise time in both European and American options. For American option with infinite time, closed form solutions have been proposed (Gerber & Shiu, 1998; Mordecki, 1999).

Dixit & Pindyck first introduce jump events in real options analysis (Dixit & Pindyck, 1994). Pennings & Lint use a simplified jump model, comprising a drift and Poisson jump (without diffusion), to study research and development of an optical tape project (Pennings & Lint, 1997). Schwartz & Moon used the jump diffusion model for evaluating research and development of clinical drugs (Schwartz & Moon, 1999). They develop a three factor with uncertainties in cost, price, and a downward jump to failure. In another drug development process case study, Brach & Paxson applied Merton's jump diffusion model to investigate the R&D value of drug discovery (Brach & Paxson, 2001). Koh & Paxson extend the same case study and apply Kou & Wang's double exponential jump diffusion model to value a biotechnology company (Koh & Paxson, 2007). The above survey shows that there are not many real options analysis applications with jump diffusion, and, furthermore, these application studies focus mainly on research and development cases.

The fourth strand of literature is application of real options analysis in climate change. Using real options analysis for climate changes has its origins in the application of real options analysis in environmental natural resources (Brennan & Schwartz, 1985). Later, Dixit & Pindyck develop an economics model and an ecological model for greenhouse emission with real options analysis (Dixit & Pindyck, 1994). Their ecological model is a linear growth model with decay which is based on Nordhaus DICE model (Nordhaus, 1991), and the economic model is a geometric Brownian motion. In their standard formulation of the perpetual time model, the problem is divided into two regions: a no adopt/no exercise region and adopt/exercise region. The optimal solution is obtained from boundary conditions of value matching and smooth pasting. In their numerical example they made use of

values from Cline's work (Cline, 1992), to obtain the optimal CO2 concentration and optimal parameter value to translate CO2 concentration to economic value. Saphores & Carr modify Dixit Pindyck model in a mean reverting stochastic process with square root volatility (Saphores & Carr, 2001) and use this to study the effects of CO2 decay factor. Subsequently, Saphores demonstrates that a lower reflecting barrier affects the optimal solution (Saphores, 2004). Pindyck, in a later paper, separates the problem into two models; one ecological uncertainty, and another economic uncertainty model (Pindyck, 2000, 2002). The ecological uncertainty model follows arithmetic Brownian motion, and partial CO2 emission control is featured in the economic model. Both models are solved by the same methodology as before. Lin et al attempt to synthesize a model with both ecological and economic uncertainties, that is a combination of Pindyck's two separate models (T. Lin, Ko, & Yeh, 2007). However to simplify their solution they assume that the CO2 emission reduces to zero when the policy is adopted.

The fifth and final strand of literature is catastrophe events in climate change under uncertainty. Early studies of catastrophe events in climate change are based on integrated assessment models (Chao, 1995; Gjerde, Grepperud, & Kverndokk, 1999). As noted in the above sections, IAMs models are weak in modelling stochastic process. Baranzini et al examine the impact of catastrophe events on optimal mitigation policy in real options analysis framework (Baranzini, Chesney, & Morisset, 2003). Their concept is that catastrophe events decrease the value of mitigation policy, and the required time to adopt the mitigation policy would be earlier than without catastrophe events. The methodology is based on several scenarios of abatement rate, jump size damages, and damage costs per year. Makropoulou et al incorporate Poisson jumps in Pindyck's work for ecological and economic uncertainties (Makropoulou, Dotsis, & Markellos, 2008). They develop a perpetual time model to examine the impact on mitigation policies with a numerical example which make use of Cline's values (Cline, 1992). However, only scenarios with fixed

jump sizes are illustrated. To study the optimal parameter value for translating CO2 concentration to economic value, Chen & Funke develop an ecological model with linear growth, and the social cost a linear function of CO2 concentration (Chen & Funke, 2010). Their economic model follows a Levy process which comprises mainly small and, occasionally, some large compound Poisson jumps in CO2 concentration level. These jumps are assumed to have instantaneous impact on societal welfare. This approach is in contrast with previous models which are commonly based on Brownian motion process.

The brief survey above reveals several research gaps in using real options analysis for climate change:

a) In general, there is lack of real options analysis studies in finite time using continuous time. It is common in real options analysis with fixed time horizon to assume a fixed date of exercise, that is, early exercise of option is not allowed. This simplifies the problem such that Black Scholes formula can be used directly in the solution but it does not provide optimization of the solution.
b) There is an increasing need to study CO2 mitigation policies in a stochastic framework because of deep uncertainties in climate change (Hallegatte, Shah, Lempert, Brown, & Gill, 2012). Simulation studies using sensitivity analysis are not the same because these assume pre-determined outcomes.
c) Current studies using real options analysis with jump diffusion are limited to simple assumptions. There are no investigations into the inter-dependence impact of jump sizes, jump size variance, and jump variance.
d) There are growing concerns on extreme weather changes and catastrophe climate events. The deep uncertainties in these problems could be investigated in a jump diffusion model. This is a challenging research area because of the complexity in obtaining numerical solutions to the problem.

2.4 Real Options Analysis - Basic Concepts

A real option is the right but not the obligation to take a certain action in the future depending on how uncertainties evolve (Amram & Kulatilaka, 1999). Real options analysis evolves from the financial option pricing theory. The difference between a real option and a financial option is that a real option is an option relating to real things or assets, in contrast, financial options are conceptual assets which are created with standard specifications and traded on financial exchanges. Option pricing theory relates to the derivative price of an underlying asset assuming that asset prices move randomly, and no-arbitrage strategy is available to take advantage of price movements.

The central premise of real options analysis is that, if future conditions are uncertain and changing the strategy later incurs substantial costs, then having flexible strategies and delaying decisions can add value when compared to making all strategies decisions during project planning. Thus, real options provide contingent decisions. It represents this managerial flexibility as 'options on real assets', which can be valued similarly to financial options. Because of this flexibility, the value of the project is increased (Trigeorgis, 1993):

$$\text{Expanded NPV} = \text{Static NPV of Expected Cash Flows } [\text{Discounted Cash Flow}] + \text{Option Value from Managerial Flexibility } [\text{Real Options Analysis}]$$

The real options value includes the related opportunity costs of an investment, so that the critical value of expected discounted benefits of a project is higher using real options analysis than using neoclassical investment analysis. The ability to enhance upside profit potential and limit downsize loss truncates the distribution curve of the net present value and changes the risk profile of the risky project.

Depending on the problem formulation, many types of real options are possible. For example, there are option to defer, option to expand, option to

abandon, option to contract, and sequential options, to name a few (Trigeorgis, 1996). More examples of practical applications of real options analysis can be found in many good texts (Amram & Kulatilaka, 1999; Copeland & Antikarov, 2001; Kodukula & Papudesu, 2006; Trigeorgis, 1996).

Real options analysis is most suitable when the following three key characteristics are present in the problem:

1. Irreversibility

   Investment is a sunk cost because it is not possible, or at least, costly to recover the investment. For example, in climate change, extinction of a plant or animal species is irreversible.

2. Uncertainty

   There are unknown factors or values in the problem which are not known at the present, such as, unknown future costs and benefits of an investment project or missing parameters.

3. Flexibility to defer investment.

   Policymaker does not need to make a now-or-never decision, and that he may delay the investment for some time in order to await new information or better values arising from uncertainty in future benefits.

2.5 Investment Decisions and Real Options

Two important elements in making investment decisions are economic value (whether to invest) and time (when to invest). These decisions depend on the availability and quality of information. Real options analysis combines both value and timing decisions to create managerial flexibility.

In assessing economic value, Myers recommended acquiring options for growth opportunities, abandoning options that are hopelessly out of the money, and

exercising valuable options at the right time and price (Myers, 1977). The type of value decisions available are:

1. Exercise the option — When it is profitable ("in the money")
2. Do nothing/Uncertain — Wait and learn (intrinsic value in option)
3. Expire the option — Result in a loss at end of period ("out of the money")

Time is an exogenous factor in decision making. Forecasts are more uncertain in the distant future than now. The type of timing decisions available are:

1. Decide Now — Immediate action
2. Do nothing — Procrastinate or delay making any decision
3. Decide at Future Date — Review decision at a fixed date in future

By combining these two decision making options, a number of flexible decision making options is created:

Value Decisions	Timing Decisions		
	Present	Wait	Future
Invest	Growth	Learn	Sequential
No Invest	Contract/Abandon	Learn	Restart/Switch
Do Nothing/Uncertain	Defer	Learn	Delay

Table 2-1 Value and Timing Decisions

2.5.1 Rationale of Real Options Analysis for Analyzing Climate Change Policy

In analyzing climate change policy, real options analysis method is relevant because it takes into consideration uncertainty and irreversibility of adopting the policy. It allows the policymaker to defer adopting the policy until the right conditions are in place.

The justifications of using real options analysis are:

a) flexibility in management of policy by avoiding making incorrect decisions prematurely;
b) ability to learn from new information as uncertain outcomes are resolved in future periods ;

c) the above (a) and (b) will lead to optimization in policy making

2.6 Value of a Project under Uncertainty and its Option Value

The concept and theory of financial option pricing theory is applicable in real options analysis. A quick summary of the basic principles is given below.

2.6.1 Stochastic Process

The basic idea in option pricing theory is that uncertain price movements of an asset are represented by a random walk which is characterized by a random variable (*z*) which is also a Markov process. A common form of this random process is known as the Wiener Process which has expected mean of zero and variance equal to time (*t*) (Hull, 2012). A property of Weiner process is that the small movement is proportional to the square root of time, $\Delta z = \epsilon\sqrt{\Delta t}$. The Weiner process is one of the Brownian motion process family in which the small increments have a normal distribution (Neftci, 2000).

In financial option pricing, the asset price, *S*, following a Brownian motion is characterized by a drift component, *μ*, and the diffusion or volatility component, *σ*. One simple form of Brownian motion is the arithmetic Brownian motion $dS = \mu dt + \sigma dz$ but it has the disadvantage that *S* may take negative values. The geometric Brownian process, $dS = \mu S dt + \sigma S dz$, avoids this negative value problem because it can never go below negative value when there is a large change, such as a jump event. For example, a large negative *σdz* value can result a large negative *dS* value which in turn result in negative S.

Similarly, the CO2 emission process can be modelled as a geometric Brownian motion process. In this CO2 emission process model, the CO2 concentration level is *X*, drift of CO2 concentration level is *μ*, and volatility in change in CO2 concentration level volatility is *σ*.

If X follows a log normal process, define $f(X,t) = \ln(X)$ [1]

Therefore,

$$\frac{df}{dX} = \frac{1}{X},\ \frac{d^2y}{dX^2} = -\frac{1}{X^2} \qquad [2]$$

Applying Ito's Lemma

$$df = \left(\frac{df}{dt} + \mu X \frac{df}{dX} + \frac{1}{2}\sigma^2 X^2 \frac{d^2 f}{dX^2} \right) dt + \sigma X \frac{df}{dX} dz$$

$$d\left(\ln X\right) = \left(\mu - \frac{1}{2}\sigma^2 \right) dt + \sigma dz \qquad [3]$$

From equation [3] the path evolution of geometric Brownian motion process is given by

$$X_t = X_0 e^{(\mu - \frac{1}{2}\sigma^2)t + \sigma Z_t} \qquad [4]$$

2.6.2 Valuation Methodology

The option value is the value of investment opportunity to invest in the project. As in neoclassical investment theory, a project is worth investing if it has positive net present value because a project with negative net present value will not consider further, which is as good as a zero value. Projects with zero net present value should be invested immediately because there would not be any further increase in value expected in future periods. Therefore the option value is the maximum of net present value or zero value:

Option Value of Project =

max (Present Value of Project - Present Value of Exercise Cost, 0) [5]

In continuous time the option value of a project is expressed as

$Option\ Value = \max\left[\int_{t=0}^{t=T} e^{-rt} \left(CF - K\right) dt, 0 \right]$, where *CF* is the cash flow at time *t*, and *K* is the cost of project

However, the value of the project needs to be found before the option value can be calculated. As the value of the project is also a stochastic process, it needs to be treated accordingly. Dixit & Pindyck provide an outline to value of a project under uncertainty (Dixit & Pindyck, 1994, Chapters 4 and 6). This thesis adopts a

similar approach but uses mathematical procedures from financial option pricing to value a project.

The approach here is an extension in the application of the basic equation in financial option pricing. This equation is the Black Scholes partial differential equation (Black & Scholes, 1973) from which the Black Scholes formula was further derived. The Black Scholes formula is commonly used in simple real options analysis because it is easy to apply. In the following sections, it is shown that the same form of Black Scholes equation can be derived to value a project.

In the research scheme, let *V* denotes the value of a project (also the value of policy), *X* denotes the value of CO2 concentration level (underlying asset) which *V* depends on, and r denotes the riskless interest rate. Then it can be shown that the value of a project is represented in the following partial differential equation.

$$\frac{\partial V}{\partial t} + \frac{1}{2}\sigma^2 X^2 \frac{\partial^2 V}{\partial X^2} + rX\frac{\partial V}{\partial X} - rV = 0 \qquad [6]$$

Equation 6 is similar in form to Black Scholes equation where *V* becomes option value, *X* is price of the underlying asset, and *r* is the riskless interest rate.

Therefore the same principles and procedures for deriving Black Scholes equation can be used for deriving the equation for the value of project *V*. It requires the setting up of a replicating portfolio with 2 or more assets together with assumptions of risk neutrality or no arbitrage. A replicating portfolio can be constructing in many ways. Two common replicating portfolios are:

- Project Asset and Underlying Asset (CO2 concentration level).

  This is the original Black Scholes approach (Black & Scholes, 1973) and the procedure assumes risk neutrality.

- Project Asset and Riskless Asset (example, a bond).

  This is the generalization of the above method. The procedure assumes no arbitrage.

For validation purposes, both replicating portfolios are used for the mathematical derivations of the value of project.

When the time horizon of the project is infinite, that is, perpetual time, the equation [6] becomes time invariant or time homogeneous (McDonald & Siegel, 1986; Merton, 1973). In this case the project approaches a steady state and the first term in equation [6] approaches zero, and equation [6] becomes an ordinary differential equation.

$$\frac{1}{2}\sigma^2 X^2 \frac{d^2V}{dX^2} + \mu X \frac{dV}{dX} - rV = 0 \qquad [7]$$

Trigeorgis summarizes the various studies which apply the same equation [7] in real options analysis (Trigeorgis, 1996, Section 6.1).

2.7 Mathematical Derivation of Value of Project

This section contains two mathematical derivations for value of project under uncertainty. The value of project is shown to be in the form of a differential equation [6]. The two different approaches used in the derivations produce the same differential equation.

2.7.1 Derivation of Value of Project with No Arbitrage Pricing

The no arbitrage method assumes that there are no arbitrage opportunities between the project and a replicating portfolio comprising the underlying asset and a riskless asset. In this section the binomial lattice model (J. C. Cox, Ross, & Rubinstein, 1979) is used to illustrate and explain the derivation of the value of a project, *V*. This is approach is intuitive and simple to apply.

Let X_t denotes the current value of the underlying asset at time *t* (for example, CO2 concentration level). After one period, *X* can move up to value of *uX* with probability *q* or move down to value of *dX* with probability *(1-q)*.

Suppose a replicating portfolio of the value of the project, *V*, is constructed using *α* units of underlying asset *X* and bonds with value $M and earns interest *r %* per period.

Value of Replicating Portfolio = αX +M [8]

After one period the portfolio value becomes:

V_u = *αuX +rM with probability p* [9]

V_d = *αdX +rM with probability (1-p)* [10]

There are two possible states of the world in this problem: value goes up or goes down. Therefore the project and replicating portfolio are known as contingent claims, Solving [8] and [9] for *α* and *M*,

$$\alpha = \frac{V_u - V_d}{(u-d)X} \geq 0, \qquad M = \frac{uV_d - dV_u}{(u-d)r} \leq 0 \qquad [11]$$

For no arbitrage, the current value of the project *V* must be the same as that of the value of replicating portfolio in [8]. For example, assume that the current value of the project is less than the replicating portfolio value, and then it is possible to make a riskless profit by buying the cheaper project and selling the more expensive replicating portfolio. In this manner, the net profit from these two transactions is guaranteed since the project value and replicating portfolio value cancel each other out at a later period. Therefore the no arbitrage assumption requires

Value of Project = Value of Replicating Portfolio [12]

Substitute [8] in [12] $V_t = \alpha X_{t-1} + M_{t-1}$ [13]

Substitute [11] in [13] and for very small periods *dt*

$$V = \frac{\frac{r-d}{u-d}V_u + \frac{u-r}{u-d}V_d}{(1+r)dt}$$

Rearranging $$V = \frac{\left[pV_u + (1-p)V_d\right]}{(1+r)dt} \qquad [14]$$

Where $p = \frac{r-d}{u-d}$ is called the risk neutral probability as distinguished from the real probability *q*.

Next, the mathematical derivation moves into continuous time.

In continuous compounding, let n be the number of sub periods in one time period, therefore new interest rate in each sub period is (r/n).

When n→∞, $\frac{1}{\left(1+\frac{r}{n}\right)^{n}} = e^{-r}$

Without loss in generality, replace the single time period with a fixed time period *(dt)*

For very small sub periods in time period *dt* : $\frac{1}{\left(1+\frac{r}{n}\right)^{n(dt)}} = e^{-r(dt)}$

Therefore equation [14] becomes $Ve^{r(dt)} = pV_u + (1-p)V_d$

$$Ve^{r(dt)} = p(V_u - V_d) + V_d \qquad [15]$$

and $p = \frac{r-d}{u-d}$ can be written as . $p = \frac{e^{r(dt)} - d}{u-d}$ [16]

Also from an initial period *t* to the next time period *dt* denote the initial value of project as $V=V(X_t)$, $V_u=V(X_{t+dt}{}^u)$ and $V_d=V(X_{t+dt}{}^d)$, where $X^u=uX$ and $X^d=dX$ have the same meanings as before.

Let $u=e^{\sigma\sqrt{dt}}$ denotes the up movement of the project value, and $d=e^{-\sigma\sqrt{dt}}$ denotes the down movement of the project value, that is, $u=1/d$. In this scheme, the up movements are assumed to be same size as down movements.

Using Taylor Series expansion to expand V_u, V_d, e^{rdt}, *u*, and *d*:

$$V_u = V + \frac{\partial V}{\partial X}\left(X_{t+dt}{}^u - X_t\right) + \frac{1}{2}\frac{\partial^2 V}{\partial X^2}\left(X_{t+dt}{}^u - X_t\right)^2 + \frac{\partial V}{\partial t}dt \qquad [17]$$

Note that $\left(X_{t+dt}{}^u - X_t\right) = X_t(u-1)$ [18]

Substitute [18] in [17] $V_u = V + \frac{\partial V}{\partial X}X_t(u-1) + \frac{1}{2}\frac{\partial^2 V}{\partial X^2}X_t{}^2(u-1)^2 + \frac{\partial V}{\partial t}dt$ [19]

Similarly $$V_d = V + \frac{\partial V}{\partial X} X_t (d-1) + \frac{1}{2}\frac{\partial^2 V}{\partial X^2} X_t^{\,2} (d-1)^2 + \frac{\partial V}{\partial t} dt$$

$$V_d = V + \frac{\partial V}{\partial X} X_t (d-1) + \frac{1}{2}\frac{\partial^2 V}{\partial X^2} X_t^{\,2} (d-1)^2 + \frac{\partial V}{\partial t} dt \quad [20]$$

$e^{rdt} = 1+rdt + \ldots$ [21]

$u = e^{\sigma\sqrt{dt}} = 1 + \sigma\sqrt{(dt)} + 1/2\sigma^2(dt) + \ldots$ [22]

$d = e^{-\sigma\sqrt{dt}} = 1 - \sigma\sqrt{(dt)} + 1/2\sigma^2(dt) + \ldots$ [23]

Note also that from [22] $(u-1)^2 = u^2-2u+1$

$= (1+\sigma^2 dt + 2\,\sigma\sqrt{(dt)}..) - 2(1 + \sigma\sqrt{(dt)}\ ..) +1$

Therefore $(u-1)^2 = \sigma^2 dt$ [24]

Similarly $(d-1)^2 = \sigma^2 dt$ [25]

Next, a few intermediate calculations are required to make it easier to make the calculations less messy.

Subtract [19] and [20]

$$V_u - V_d = \frac{\partial V}{\partial X} X_t (u) + \frac{1}{2}\frac{\partial^2 V}{\partial X^2} X_t^{\,2} (u-1)^2 - \frac{\partial V}{\partial X} X_t (d) - \frac{1}{2}\frac{\partial^2 V}{\partial X^2} X_t^{\,2} (d-1)^2 \ldots \quad [26]$$

Substitute [24] and [25] in [26], $$V_u - V_d = (u-d)\frac{\partial V}{\partial X} X_t \quad [26]$$

Multiply by *p* $$p(V_u - V_d) = p(u-d)\frac{\partial V}{\partial X} X_t \quad [27]$$

From [16] $p = \frac{e^{r(dt)} - d}{u - d}$, $$p(u-d) = e^{r(dt)} - d \quad [28]$$

Substitute [28] in [27] $$p(V_u - V_d) = \left(e^{r(dt)} - d\right)\frac{\partial V}{\partial X} X_t \quad [29]$$

Substitute [21] and [23] in [29]

$$p(V_u - V_d) = \left(1 + rdt - 1 + \sigma\sqrt{dt} - \tfrac{1}{2}\sigma^2 dt\right)\frac{\partial V}{\partial X} X_t$$

$$p(V_u - V_d) = \left(rdt + \sigma\sqrt{dt} - \tfrac{1}{2}\sigma^2 dt\right)\frac{\partial V}{\partial X} X_t \quad [30]$$

From [20] $$V_d = V + \frac{\partial V}{\partial X} X_t (d-1) + \frac{1}{2}\frac{\partial^2 V}{\partial X^2} X_t^{\,2} (d-1)^2 + \frac{\partial V}{\partial t} dt$$

Substitute $(d-1) = -\sigma\sqrt{(dt)} + 1/2\sigma^2(dt) + ..$, and $(d-1)^2 = \sigma^2 dt$

$$V_d = V + \frac{\partial V}{\partial X} X_t \left(-\sigma \sqrt{(dt)} \; + \; 1/2\sigma^2 dt \right) + \frac{1}{2} \frac{\partial^2 V}{\partial X^2} X_t{}^2 \sigma^2 dt + \frac{\partial V}{\partial t} dt$$

$$V_d = V - \sigma\sqrt{dt} \frac{\partial V}{\partial X} X_t \; + \; \frac{1}{2}\sigma^2 \frac{\partial V}{\partial X} X_t dt + \frac{1}{2} \frac{\partial^2 V}{\partial X^2} X_t{}^2 \sigma^2 dt + \frac{\partial V}{\partial t} dt \qquad [31]$$

From [15] $Ve^{r(dt)} = p\left(V_u - V_d\right) + V_d$, substitute [31], [21], [26], [23] and [20]

$$V\left(1 + rdt\right) = \left(rdt + \sigma\sqrt{dt} - \tfrac{1}{2}\sigma^2 dt \right) \frac{\partial V}{\partial X} X_t + V - \sigma\sqrt{dt} \frac{\partial V}{\partial X} X_t \; + \; \frac{1}{2}\sigma^2 \frac{\partial V}{\partial X} X_t dt + \frac{1}{2} \frac{\partial^2 V}{\partial X^2} X_t{}^2 \sigma^2 dt + \frac{\partial V}{\partial t} dt$$

$$V + Vrdt = rdt \frac{\partial V}{\partial X} X_t + \sigma\sqrt{dt} \frac{\partial V}{\partial X} X_t - \tfrac{1}{2}\sigma^2 dt \frac{\partial V}{\partial X} X_t + V - \sigma\sqrt{dt} \frac{\partial V}{\partial X} X_t \; + \; \frac{1}{2}\sigma^2 \frac{\partial V}{\partial X} X_t dt + \frac{1}{2} \frac{\partial^2 V}{\partial X^2} X_t{}^2 \sigma^2 dt + \frac{\partial V}{\partial t} dt$$

$$Vr = r \frac{\partial V}{\partial X} X_t + \frac{1}{2} \frac{\partial^2 V}{\partial X^2} X_t{}^2 \sigma^2 + \frac{\partial V}{\partial t}$$

$$\frac{\partial V}{\partial t} + \frac{1}{2} X^2 \sigma^2 \frac{\partial^2 V}{\partial X^2} + rX \frac{\partial V}{\partial X} - Vr = 0 \qquad [34]$$

Now, equation [34] is same as equation [6]. This demonstrates that the Black Scholes equation can be used to value a project, *V*.

Furthermore, for an infinite time horizon equation [34] is reduced to

$$\frac{1}{2} X^2 \sigma^2 \frac{d^2 V}{dX^2} + rX \frac{dV}{dX} - Vr = 0 \qquad [35]$$

The binomial lattice method is pedagogically useful method for an intuitive understanding of the valuation process in discrete finite time. However, it can be seen that the mathematical formulation and derivation in continuous time is challenging and tedious. The original derivation employs stochastic calculus and Ito's Lemma to cut through the steps. The next section shows how to derive the value of a project using hedging method for risk neutral pricing.

2.7.2 Derivation of Value of Project with Risk Neutral Pricing

In Black Scholes' original derivation the replicating portfolio comprise main asset is stock and its underlying asset is option of the stock. It should be noted that the underlying asset can be any asset which the value of the main asset is

dependent upon. For example, the underlying asset in Black Scholes replicating portfolio could even be the corporate bond issued by the same firm of the stock.

In the research scheme, the main asset is the Project, and the underlying asset is CO2 concentration level.

Let *V* = value of the project, *X* is the underlying asset, *μ* = drift of stochastic process, *σ* = volatility or standard deviation, *r*= risk free interest rate.

The geometric Brownian motion of the underlying asset is

$$dX = \mu X dt + \sigma X dz \qquad [36]$$

First Portfolio $\prod_1$ is a replicating portfolio comprising η units of V and one unit of X.

$$\prod_1(t) = E_t\left[\eta V(t) + X(t)\right] \qquad [37]$$

Ito's Lemma

$$dV = \frac{dV}{dX}\left(\mu X dt + \sigma X dz\right) + \frac{1}{2}\frac{d^2V}{dX^2}\left(X dt + \sigma X dz\right)^2 \qquad [38]$$

Substitute [36] in [38]

$$dV = \frac{\partial V}{\partial t} + \mu X\frac{\partial V}{\partial X}(dt) + \sigma X\frac{\partial V}{\partial X}(dz) + \frac{1}{2}\frac{\partial^2 V}{\partial X^2}(\sigma X)^2(dt) \qquad [39]$$

From [36]

$$d\prod_1 = E_t\left[\eta dV + dX\right] \qquad [40]$$

Substitute [39] & [36] in [40]

$$d\prod_1 = \eta\left(\frac{\partial V}{\partial t} + \mu X\frac{\partial V}{\partial X} + \frac{1}{dt}\sigma X\frac{\partial V}{\partial X}(dz) + \frac{1}{2}\frac{\partial^2 V}{\partial X^2}(\sigma X)^2\right)dt + (\mu X dt + \sigma X dz) \qquad [41]$$

Stochastic calculus

$$(dt)^2 = 0, (dz)^2 = dt,\ (dt)(dz) = 0,\ E_t(dz) = 0$$

Simplifying

$$d\prod_1 = \eta\left(\frac{\partial V}{\partial t} + \mu X\frac{\partial V}{\partial X} + \frac{1}{2}\frac{\partial^2 V}{\partial X^2}(\sigma X)^2\right)dt + \mu X(dt) \qquad [42]$$

We eliminate *μ* by setting Hedging Ratio $\eta = -\left(\frac{dV}{dX}\right)^{-1}$ [43]

$$d\prod_1 = \eta\frac{\partial V}{\partial t}(dt) + \eta\mu X\frac{dV}{dX}(dt) + \eta\frac{1}{2}\frac{d^2V}{dX^2}(\sigma X)^2(dt) + \mu X(dt)$$

$$d\prod_1 = \eta\frac{\partial V}{\partial t}(dt) - \left(\frac{dX}{dW}\right)\mu X\frac{dV}{dX}(dt) + \eta\frac{1}{2}\frac{d^2V}{dX^2}(\sigma X)^2(dt) + \mu X(dt)$$

$$d\prod_1 = \eta\frac{\partial V}{\partial t}(dt) - \mu X(dt) + \eta\frac{1}{2}\frac{d^2V}{dX^2}(\sigma X)^2(dt) + \mu X(dt)$$

$$d\prod_1 = \eta\frac{\partial V}{\partial t}(dt) + \eta\frac{1}{2}\frac{d^2V}{dX^2}(\sigma X)^2(dt) \qquad [44]$$

Note that the replicating portfolio is now riskless because the random variate (dz) is no longer in the portfolio (equation 44).

The second portfolio $\prod_2$ comprised η units of *V* and one unit of X. Note that the second portfolio has same portfolio composition as the first portfolio.

Second Portfolio comprises has risk free return.

Second Portfolio $$\prod_2 = r[\eta V + X] \qquad [45]$$

$$d\prod_2 = r(\eta V)(dt) + rX(dt) \qquad [46]$$

For no arbitrage, equate Portfolios $d\prod_1 = d\prod_2$ of equations [44] and [46]

$$\eta\frac{\partial V}{\partial t}(dt) + \eta\frac{1}{2}\frac{d^2V}{dX^2}(\sigma X)^2(dt) = r(\eta V)(dt) + rX(dt)$$

$$\eta\frac{\partial V}{\partial t} + \eta\frac{1}{2}\frac{d^2V}{dX^2}(\sigma X)^2 - rX - r(\eta V) = 0 \qquad [47]$$

Substitute [43] in [47] $$\frac{\partial V}{\partial t} + \frac{1}{2}\sigma^2\frac{d^2V}{dX^2}X^2 + rX\frac{dV}{dX} - rV = 0 \qquad [48]$$

Equation [48] from risk neutral pricing method produces exactly the same equation [34] from the binomial lattice method and Black Scholes equation in equation [6].

For an infinite time horizon equation [48] is reduced to

$$\frac{1}{2}\sigma^2\frac{d^2V}{dX^2}X^2 + rX\frac{dV}{dX} - rV = 0 \qquad [49]$$

The equation [49] from risk neutral pricing method is exactly the same as equation [35] from no arbitrage pricing.

For the real options analysis in perpetual time in Chapters 4 ad 5, the value of the project will employ the risk neutral pricing method described in this section to further derive the specific values of adopt and no-adopt projects. This is necessary because the climate change model contains social costs and benefits, additional items in the replicating portfolios. Therefore the value of the project needs to completely derive again using the risk neutral pricing approach in this section.

2.8 Discount Rates

The issue of discount rate has been a long standing debate (Ramsey, 1928). In neo-classical economics, the discount rate is determined by market forces. A positive discount rate is the result of the premium placed on present versus future goods. This is called the pure time preference theory of interest rate.

In environmental studies, the social discount rate is the rate used to express its inter-generation time preference and to compare the well-being of future generations to the well-being of those alive today. This rate can be less than the individual discount rate for the following reasons:

- Society would want to save more collectively than the sum of individuals' savings decisions.
- Society has different time preferences than individuals in personal role. Thus, individuals are unwilling to pay for common market goods as in the case of "tragedy of commons".
- Individuals have a finite life expectancy act differently from society which has perpetual existence. Thus time preferences of inter-generational discount rates are different.

The social discount rate can thus be described by two parameters: a rate of pure preference for the present δ, and a factor γ that reflects the elasticity of marginal utility to changes in consumption. The social discount rate r is given by:

$$r = \delta + \gamma g \qquad [50]$$

where is δ the rate of pure time preference, γ is factor that reflects elasticity of marginal utility to changes in consumption, g is the rate of growth of GDP per capital.

Hence there exists a wide range of social discount rates for climate change analysis. The possible discount rates in economic analysis range from infinite social discount rate, intergenerational discount rate, intra temporal (within a generation) and

intergenerational discount rates to be the same, zero social discount rate, and negative inter-temporal discount rate (M.L. Weitzman, 1998; M.L. Weitzman & Gollier, 2010).

IPCC AR4 (IPCC AR4, 2007b) described two methods to discounting: a prescriptive approach based on what rates of discount (around 2-3% in real terms) should be applied, and a descriptive approach based on what rates of discount (at least 4% after tax) investors actually apply in their day-to-day decisions. IPCC AR4 (IPCC AR4, 2007b) used discount rates of 4-6% pa for developed countries and 10-12% for developing countries. On the other hand proponents of low discount rate use discount rates ranging from 1.4% in the Stern Review to zero and negative discount rates by Weitzman (M.L. Weitzman, 1998; M.L. Weitzman & Gollier, 2010). Then there is the middle of road approach, for example, the Green Book (Green Book, 2011) which recommends discount rate should decrease from 3.5%pa to 1% pa over time. Dixit & Pindyck use 4% pa discount rate in their real options analysis of CO2 mitigation policy (Dixit & Pindyck, 1994).

A survey of social discount rate used in climate change studies below shows a 4% pa discount rate is quite common.

Stern Review (Stern et al., 2006)	0.1 % pa
UK Government (Green Book, 2011)	1.5 % pa for 201-300 years
IPCC SAR (IPCC SAR, 1996)	2 - 4 % pa
IPCC AR4 (IPCC AR4, 2007a)	4 - 6 % pa
McKinsey's cost function curves (McKinsey, 2009)	4.0 % pa
Nordhaus DICE model (Nordhaus, 2010)	4.0 % pa over 100 years

The rates proposed by these major studies range from 0.1 to1.4 per cent (Stern, et al., 2006) and 1.5 per cent (Cline, 1992) to 4 to 6 per cent (Nordhaus, 1991, 1994).

This research uses a range of nominative discount rate ranging from 0.5% to 10% pa to investigate the effects on CO2 reduction policies in perpetual time.

Instead of joining in an exhaustive debate on the correct discount rate to use, the research assumes a range of risk free interest rates. The real discount rate could be obtained by incorporating a risk tolerance factor to risk free interest rate. In practice either a premium (more) or discount(less) rate is applied to the risk free interest rate to obtain the real discount rate:

real discount rate = risk free interest rate + risk tolerance [51]

real discount rate = risk free interest rate + premium /-discount [52]

This research explores a range of interest rates is used as sensitivity analysis of the results. With this range of interest rates, the policymaker can apply his/her own premium or discount constant to deduce the desired social discount rate for further interpretation of the results.

2.8.1 Indifference Pricing and Discount Rate

The risk tolerance of policymaker may influence risk his preference to adopt CO2 reduction policy, and subsequently, the related risk premium/discount in the discount rate. This is illustrated with pricing curves of CO2 emission rate and risk tolerance. A reduction cost of risk is used to represent the costs to the policymaker.

In the pricing curve of CO2 emission rate, a high emission rate requires a reduction cost and vice versa (Figure 2.1). In the Business as Usual (BAU) scenario, assume that the current reduction cost is R_0 at current CO2 emission rate μ_0. An increased CO2 emission rate μ_1 will have a higher reduction cost at R_1.

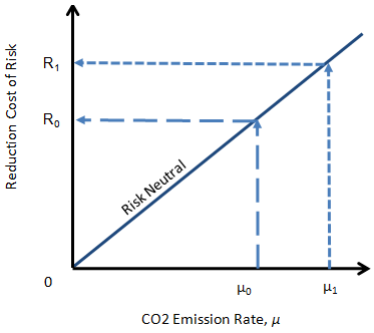

Figure 2-1 Pricing of CO2 Emission Rate

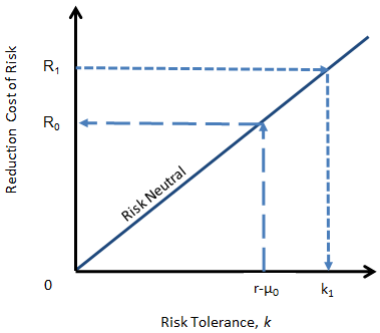

Figure 2-2 Pricing of Risk Tolerance

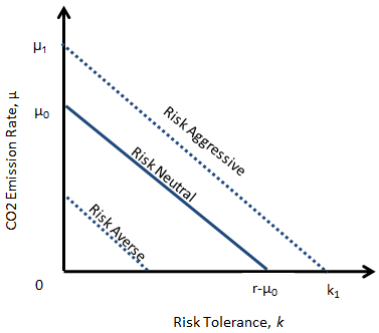

Figure 2-3 Indifference Curves

For a risk neutral policymaker (Figure 2.2), high risk tolerance will eventually result in high reduction costs. At the same reduction cost of R_0 the risk tolerance is (r - μ_0). This means that in the BAU scenario, the policymaker is willing to pay R_0 for a risk tolerance of (r - μ_0), that is, he is willing to accept the risk free rate less the present CO2 emission rate. If the reduction cost is increased to R_1 the new risk tolerance changes to k_1 which is larger than $(r - \mu_0)$. The indifference pricing curves for CO2 emission rate and risk tolerance are shown in Figure 2.3. In this example, the pricing curves, which are assumed to be linear, will produce utilitarian indifference pricing curves. A risk aggressive policymaker will have his pricing curve above the risk neutral. Similarly, a risk averse pricing curve is below the risk neutral curve.

The real discount rate, ρ, of the policymaker as a buyer (or bidder) for the CO2 reduction policy is $\rho = r - k$. where r denotes the riskless rate and k is the risk tolerance in the indifference pricing curve. Similarly, the seller (or asker) discount rate is $\rho = r + k$. This notation is consistent with actuary or insurance pricing where risk tolerance is used.

With this convention of discount rate representation, $\rho = r - k$, the following discount rates can be determined:

For $k = 0$ and $\mu = 0$, therefore $\rho_0 = r$ [53]

For $k = r - \mu_0$ and $u = \mu_0$, therefore $p_\mu = \mu_0$ [54]

It should be noted that $\mu = 0$ does not mean that there is no CO2 emission, but it implies that the net atmospheric CO2 emission rate is zero, in other words, there is no increase in CO2 concentration level.

From the above indifference pricing curves (Figure 2.3), it can be seen that an increase in CO2 emission rate, μ, produces an increase in the risk tolerance, k. With a very large k value, it is possible that the discount rate, $\rho = r - k$, could become negative.

As an example, assume that the increase in CO2 emission rate, $\Delta\mu$, causes the risk tolerance to increase by Δk. Then the new tolerance risk $k1 = r - \mu_0 + \Delta k$, and the new discount rate is:

$$\rho = r - k_1 = r - k1 = r - r + \mu_0 - \Delta k = \mu_0 - \Delta k$$

Therefore the condition for discount rate ρ to be negative is $\Delta k > \mu$ in this simple example. The exact conditions for negative discount rates will depend on the various pricing curves and sensitivity of risk tolerance to changes of CO2 emission rates.

From the above equations it can be seen that negative discount rates will be produced when future generations are worse off than present generation either because of higher CO2 emission rates. As an example in climate change policy, improper implementation of climate change policy may reduce benefits for future generations.

This research focuses mainly on positive discount rates because the policymaker is assumed to be a rational decision maker and is unlikely to be risk aggressive.

3. STOCHASTIC PROCESS OF CO2 EMISSION

The core of real options analysis is the stochastic process which characterizes the behaviour of the uncertainty and evolution of future events. Basic stochastic processes, such as arithmetic Brownian motion (ABM), and geometric Brownian motion (GBM), comprise a drift and a diffusion component. Other common stochastic processes are Ornstein Uhlenbeck (OU) process which exhibits mean reverting properties, arithmetic OU, geometric OU, squared root (Cox Ingersoll Ross, CIR model), and Vasicek model.

In climatology, sophisticated physical science models are used to project CO2 concentration level. However these climate models may not be appropriate for real options analysis application because different principles are used in modelling the climate system. This thesis proposes and develops a CO2 emission process model based on stochastic process. The parameters of the model are calibrated using observed CO2 concentration data and statistical estimation analysis. The new model could then be used for real options analysis.

3.1 Greenhouse Gas, CO2 and Global Warming

Greenhouse gas (GHG) is contributes to most of the radiative forcing which result in global warming. The important long lived greenhouse gases (LLGHG) are CO2, methane (CH4), nitrous oxide (NO2), chlorofluorocarbons (CFC11 and CFC12) (Figure 3.1). Other species which contribute to positive forcing are ozone, water vapour, and black carbon, while aerosols tend to reduce radiative forcing. These GHG are measured in CO2-equivalent (CO2-eq).

IPCC definition of CO_2-equivalent is that it is the concentration of CO_2 that would cause the same amount of radiative forcing as a given mixture of CO_2 and other forcing components (IPCC AR4, 2007c, Synthesis Report, Section 2.1). It is derived by summing the total amount of atmospheric global warming potential from

all the greenhouse gases and expresses the sum in terms of the equivalent amount of CO2 needed to give that same warming effect.

The three major LLGHG are CO2, CH4, and N2O which contribute to 64%, 18%, and 6% of the total radiative forcing by LLGHG. The relative global warming potential (GWP) are CO2 (1), CH4 (25), and N2O (298). Therefore, even though CO2 is causing the most warming on a weight -for-weight basis, reductions in CH4 or N2O emissions provide a lot more climate relief than those of CO2. For example, reducing methane emissions by one ton would be equivalent to reducing CO2 emissions by 25 tonnes; thus, its CO2-eq is 25 tonnes. In the case of N2O, its CO2-eq is 298 tonnes of CO2. As these three LLGHG have different rates of emissions, their makeup composition in LLGHG and their GWP will also vary. Finally, the cost of reduction of each LLGHG is different; this implies that cost effectiveness of each LLGHG reduction program is different.

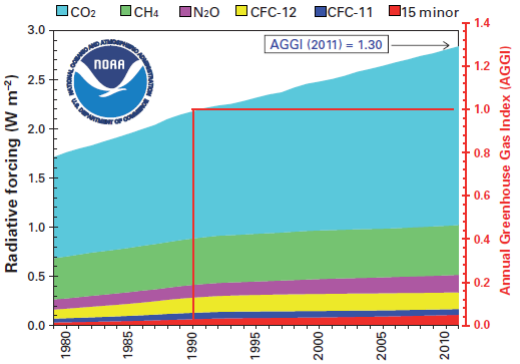

Figure 3-1 Atmospheric radiative forcing relative to 1750

Reference: NOAA Annual Greenhouse Gas Index (NOAA, 2012)

This methodology for estimation of parameters is applicable for each of LLGHG. However, this research focuses mainly in CO2 because this is the main LLGHG which attracts the most interest in climate change policies.

3.2 Stochastic Differential Equation Parameters Estimation

The Ito stochastic differential equation of Brownian motion is given by:

$$dX_t = h(t, X_t; \theta)\,dt + g(t, X_t; \theta)\,dZ_t \qquad [1]$$

Assume the Markovian process with observations X_t with $t=1,2,..,T$ are i.i.d. (independent identically distributed), and their transition density function $p(X, \theta)$. In

estimation of parameters the observation data are sampled at discrete time events for a stochastic process in continuous time.

3.2.1 Maximum Likelihood Estimation (MLE)

MLE is based on Jensen inequality that for any alternative distribution *p(X, θ')*

$$E\left[\ln p\left(X,\theta^{'}\right)\right] \le E\left[\ln p\left(X,\theta_0\right)\right] \text{ where } E[X] = \int X.p\left(X,\theta_0\right)dX \quad [2]$$

Define the likelihood function as:

$$L\left(\theta\right) = \ln p\left(X,\theta\right) \quad [3]$$

In the likelihood function, *X* samples are independent variables, and the model parameters, *θ*, are dependent variables, and *p(X, θ)* is an unknown transition density (Silverman, 1986).

For independent identical distributed samples of *X*, the parameters of the stochastic model equations are obtained by maximizing *θ* in the log likelihood function given by

$$\frac{1}{T}L\left(\theta\right) = \frac{1}{T}\ln\prod_{t=1}^{T} p\left(X_t,\theta\right) = \frac{1}{T}\sum_{t=1}^{T}\ln p\left(X_t,\theta\right) \quad [4]$$

The parameters are estimated from the sample observation data from *t=1* to *T*:

$$\theta = \arg\max\frac{1}{T}\sum_{t=1}^{T}\ln p\left(X,\theta\right) \quad [5]$$

If *X* sample data is assumed to have a kernel density which are normally distributed with mean *μ*, and variance, σ^2.

The log likelihood for the sample X_t , *t=1,2,..,T* is:

$$L\left(\theta\right) = \sum_{t=1}^{T}\left[\ln\frac{1}{\sqrt{2\pi\sigma^2}} - \frac{\left(X_t-\mu\right)^2}{2\sigma^2}\right] \quad [6]$$

By maximizing the log likelihood function, the best parameter estimate is given by

$$\hat{\theta} = \arg\max_{\theta} L\left(\theta\right) \quad [7]$$

3.2.2 Scheme for Parameter Estimation

As the transition density, *p*, is an unknown distribution a Monte Carlo scheme is used to approximate the transition density. The following algorithm is provided by (Picchini, 2007):

1. for the time interval (t_{i-1}, t_i) and divide it into *M* subintervals of length $h = (t_{i-1}, t_i)/M$.
2. approximate *X* at t_i by integrating on this discretization by using a standard algorithm (e.g. Euler-Maruyama, Milstein) by taking x_{i-1} at time t_{i-1} as the starting value.

   Euler Maruyama approximation is given by:

$$X_t = X_{t-1} + h\, f\left(X_{t-1}\right) + g\left(X_{t-1}\right)\Delta W_{t-1} \qquad [8]$$

   where $\Delta W_t = W(t) - W(t-1)$ and is normally distribute $N(0,h)$ and $W(t_0)=0$, $t=0,1,2,\ldots,T-1$.

   A more efficient and accurate numerical method is the Milstein scheme:

$$X_t = X_{t-1} + h\, f\left(X_{t-1}\right) + g\left(X_{t-1}\right)\Delta W_t + \frac{1}{2} g\left(X_{t-1}\right) g'\left(X_{t-1}\right)\left[\Delta\left(W_t\right)^2 - h\right]$$

   In this research the second order finite difference approximation of Milstein scheme is used but a higher order finite difference approximation procedure could also be employed.
3. integration is repeated *R* times, thereby generating *R* approximations of the *X* process at time t_i starting from x_{i-1} at t_{i-1} to obtain the approximate X values, $X^1_{ti}, \ldots, X^R_{ti}$
4. the simulated values $X^1_{ti}, \ldots, X^R_{ti}$ are used to construct a non-parametric kernel density estimate of the transition density $p\left(t_i, x_i; t_{i-1}, x_{i-1}, \theta\right)$

$$p^R\left(t_i, x_i; t_{i-1}, x_{i-1}, \theta\right) = \frac{1}{Rh}\sum_{r=1}^{R} K\left(\frac{x_i - X^r{}_{t_i}}{h_i}\right) \qquad [9]$$

   where h_i is the kernel bandwidth at time t_i and $K(\cdot)$ is a suitable symmetric,

non-negative kernel function enclosing unit mass; a normally distributed kernel will be

$$K(u) = \frac{1}{\sqrt{2\pi}} \exp\left(\frac{-u^2}{2}\right) \quad [10]$$

A faster integration method is to assume a parametric kernel density with of uniform distribution, but this method cannot be used with the Milstein scheme.

5. the previous procedure is repeated for each x_i and the $p^R(t_i, x_i; t_{i-1}, x_{i-1}, \theta)$ thus obtained used to construct the log likelihood function

$$L^R(\theta) = \prod_{i=1}^{n} p^R(t_i, x_i; t_{i-1}, x_{i-1}, \theta) \quad [11]$$

6. the log likelihood function $L^R(\theta)$ is maximized with respect to θ to obtain the approximate Maximum Likelihood Estimate given by $\hat{\theta} = \arg\max_\theta L^R(\theta)$

3.3 Data Source

Scripps Institution of Oceanography, University of San Diego, which collaborates with National Centre for Atmospheric Research (NCAR) in its climate research studies, maintained several observation sites for collecting CO2 atmospheric data. The two well-known observation sites are Mauna Loa, Hawaii, and Antarctica, South Pole. These two sites represent the northern and southern hemispheres respectively (Scripps Institution of Oceanography). Another data source is Carbon Dioxide Information Analysis Centre (CDIAC) which maintains a comprehensive data base of greenhouse gas data records since 1978.

Scripps' Antarctica observation site in South Pole has the longest record of in-situ and flask CO2 sample data. The CO2 concentration level in Mauna Loa is consistently higher than South Pole because of higher pollution in the industrialized northern hemisphere and lack of vegetation in the frozen Antarctica. But the trend and characteristics of CO2 concentration level are similar at both sites.

For the parameter estimations of the stochastic CO2 model, 54 continuous annual field atmospheric CO2 data observations were obtained in South Pole from January 1958 to January 2011. These records represent the longest scientifically observed data for CO2 concentration available. The raw CO2 concentration level data is measured in parts per million. To allow ease in data handling the calculations and results in this research are also represented in parts per million CO2 (ppm CO2).

3.4 Methodology

The drift and diffusion parameters of Brownian motion processes (arithmetic and geometric), and mean reverting processes (CIR, OU) are estimated with MATLAB SDE Toolkit (Picchini, 2007). The kernel density is assumed to be normally distributed. A step size of 0.001 was used with 1000 simulated Monte Carlo paths (Higham, 2001).

The stochastic processes investigated in the statistical experiment were:

Brownian Motion Processes	Mathematical Form
Arithmetic Brownian Process (ABM)	$dX = \mu\, dt + \sigma\, dz$
Geometric Brownian Motion (GBM)	$dX/X = \mu\, dt + \sigma\, dz$
Mean Reverting Processes	**Mathematical Form**
Ornstein Ulhenbeck Process	$dX = \eta\,(\mu - \delta X)dt + \sqrt{(\sigma X)}\, dz$
Arithmetic Mean Reverting Process	$dX = (\mu - \delta X)dt + \sigma\, dz$
Vasicek Model	$dX = \eta\,(\mu - \delta X)dt + \sigma \sqrt{(X)}\, dz$

where μ denotes drift, σ denotes volatility, δ denotes mean reversion, and η denotes speed of reversion.

Using MLE method, the parameters of the above stochastic models are obtained and evaluated. The mean reverting processes are not able to provide any parameter estimations. The reason is that the observed data are continuously increasing in an upward trend, and the data trends do not show any indications of

mean reversal. In this case, decay factor is zero which reduces mean reverting process to Brownian motion process.

3.5 Results and Analysis

In the initial analysis Euler Murayama was used to obtain a preliminary estimation of the parameter values because the solution convergence is fast. Then the initial parameter estimates were used as inputs to Milstein scheme to obtain better estimates.

	Euler Murayama		Milstein	
SDE Parameters	ABM	GBM	ABM	GBM
Drift	1.3760	0.003907	1.3833	0.003957
Volatility (%)	0.1794	0.000486	0.1767	0.000479
Simulated Data	ABM	GBM	ABM	GBM
Mean Value	387.27	386.68	387.67	387.69
Variance	1.752	1.927	1.670	1.878
Skewness	1.28×10^{-13}	9.32×10^{-3}	2.61×10^{-13}	9.18×10^{-3}
Kurtosis	2.73	2.73	2.73	2.73

Table 3-1 Statistical Results of Parameters Estimation

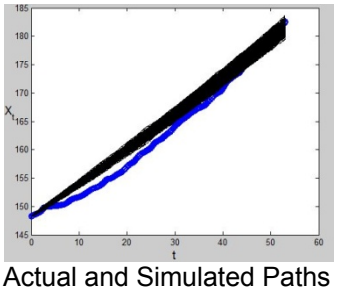

Actual and Simulated Paths

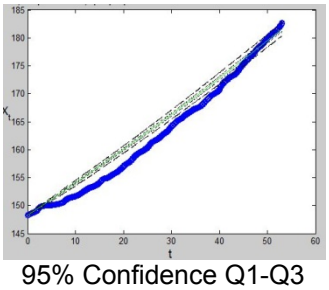

95% Confidence Q1-Q3

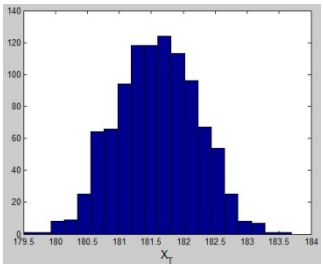

Histogram 95%

Figure 3-2 Euler Murayama Method - Geometric Brownian Motion

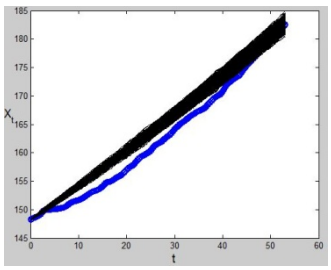

Actual and Simulated Paths

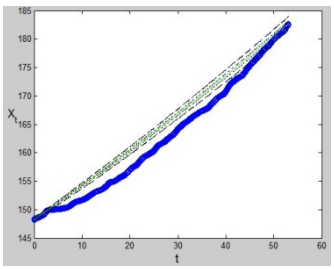

95% confidence Q1-Q3

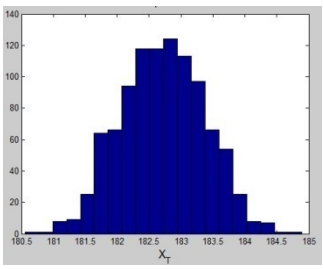

Histogram 95%

Figure 3-3 Milstein Method - Geometric Brownian Motion

The choice between ABM and GBM models is marginal because the differences are insignificant. The skewness of ABM is less than GBM, this suggests that the ABM has a longer left tail than GBM. As future climate change is likely to have more extreme events, the distribution and histogram should have a longer right tail as in the GBM case. Another advantage of GBM is that GBM process does not allow CO2 concentration to be negative value; this is more realistic in the physical world. Also, analytical models and applications based on GBM model are easier to analyse than ABM models. For the above reasons, GBM model is selected for subsequent research work with the following parameter estimates shown below.

	Mean	95% confidence level	
Drift	0.003956817	0.0038228	0.0040923
Volatility (%)	0.000479211	0.0004509	0.0004950

3.6 Discussion of CO2 Emission Process

The different parameter values estimated with stochastic differential equation and simple regression using the same CO2 observation data are shown in Table 3.2.

Estimation Method	Mean Drift	Variance (%)
Linear Least Square Regression (A)	0.008093	0.003080
Stochastic Differential Equation (B)	0.003957	0.000479
Difference (A/B) -1	105%	543 %

Table 3-2 Comparison of SDE and LS parameters

The differences in the estimations of the two parameters between the two methods are indeed significant. This indicates that parameters estimated with linear least square regression are not compatible for use in real options analysis models.

3.6.1 IPCC SRES Scenarios

A qualitative assessment of the validity of the results could be made by comparing the projected CO2 concentration from CO2 emission model (Figure 3.5) with IPCC SRES scenarios (Figure 3.4). IPCC develops four scenarios to year 2100 based on growth assumptions of economic growth, population growth, technology

innovations, society affluence, and narrowing of income gap among nations. The projections of these scenarios are shown in the Table below (IPCC TAR, 2001b).

SRES scenarios	CO2 conc ppm	Temperature Increase	Sea Level Rise
A1	600-950	1.4 to 6.4 C	20 to 59 cm
B1	550	1.1 to 2.9 C	18 to 38 cm
A2	850	2.0 to 5.4 C	23 to 51 cm
B2	600	1.4 to 3.8 C	20 to 43 cm

Table 3-3 IPCC SRES Scenarios

The CO2 concentration evolution path and projection from CO2 emission model are displayed together with IPCC SRES scenarios for ease of comparison (Figures 3.4 and 3.5).

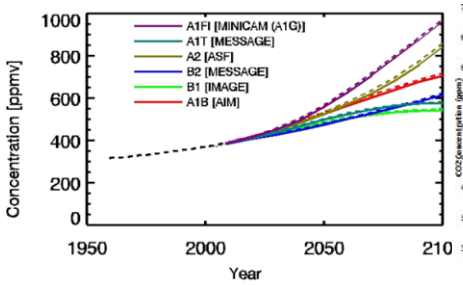

Figure 3-4 IPCC SRES (2001)

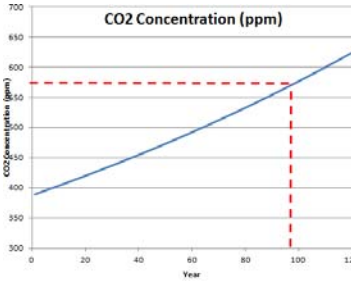

Figure 3-5 CO2 Emission Model to 2100

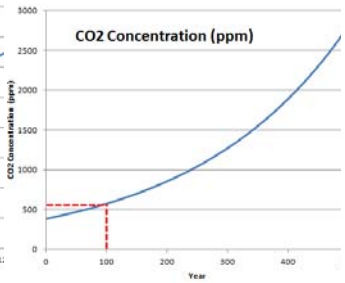

Figure 3-6 CO2 Emission Model to 2600

In the next 100 years to year 2100, CO2 concentration is 570ppm from CO2 emission model (Figure 3.5) and 550ppm in B1 scenario to 600ppm in B2 scenario (Figure 3.4). Compared with other IPCC SRES scenarios the CO2 concentration from the model appears low. The reason could be that the model does not take into account other factors such as water vapour, greenhouse gases and ocean circulation system which are included in IPCC models. Also, the mathematical model assumes that the industry, economy and world population trends continue unchanged. Nevertheless the CO2 emission model is compatible with the lower range of IPCC SRES scenarios, that is, B1 scenario.

The B2 storyline describes a growing world population in which the emphasis is on local and regional solutions to economic, social and environmental sustainability. In B1 scenario storyline, there is a overall low population growth that

peaks in mid-century and declines but with rapid changes in economic structures toward a service and information economy, with reductions in material intensity, and the introduction of clean and resource-efficient technologies. The emphasis is on global solutions to economic, social, and environmental sustainability, including improved equity, but without additional climate initiatives. The projected temperature increased in the 21st century is between 1.1C to 2.9C with best estimate of 1.8C, and projected sea level rise in the range 18cm to 38 cm (IPCC SRES, 2000).

For the policymaker the CO2 emission model can be used as a conservative model for projecting CO2 concentration levels. For projections yielding higher concentration levels the policymaker could increase the value of the drift parameter μ to produce higher CO2 emission rates.

PART B

CLIMATE CHANGE INVESTMENTS

IN PERPETUAL TIME

WITH REAL OPTIONS ANALYSIS

4. CO2 REDUCTION IN PERPETUAL TIME

In this Chapter, an integrated model of real options analysis in perpetual time, which incorporates both CO2 emission cutback and CO2 concentration abatement policies, is developed using continuous time stochastic process. The derivation of the model follows the approach used in Section 2.7 and the full step-by-step mathematical derivation is shown in Appendix 1. This CO2 emission model is used to analyse CO2 reduction policies with varying discount rates and reduction rates.

4.1 Method of Value of CO2 Reduction Policies in Perpetual Time

The real options analysis in this research is a one factor model with one uncertainty in the volatility of CO2 emission process. This geometric Brownian motion model is similar to Pindyck's ecological model (Pindyck, 2000, 2002) except the Pindyck's model used arithmetic Brownian motion. Although there are earlier studies (T. Lin, et al., 2007; Pindyck, 2002; Saphores & Carr, 2001) using the Pindyck's framework, these studies focus only in CO2 emission reduction and not CO2 concentration abatement. There is a research gap covering CO2 concentration abatement policies. This research attempts to fill this research gap with an integrated solution in closed analytical form which can be used for both CO2 emission reduction and CO2 concentration abatement. In addition, the Pindyck's framework employs dynamic programming in formulating the problem. This research approaches the problem using risk neutral pricing. This method is introduced in Chapter 2 is now used to obtain the value of CO2 reduction policy and, subsequently, its option value.

To recap the CO emission model, let X denotes CO2 concentration level which follows a geometric Brownian motion process comprising CO2 emission rate with drift (μ), and diffusion (volatility), σ, given by the stochastic differential equation:

$$dX = \mu X dt + \sigma X dz \qquad [1]$$

In the stochastic process it is assumed that evolution of the stochastic paths follows a Markovian process. In other words the information of future CO2 concentration level is based solely on its present state as well as the past history. In addition, it is assumed that there are no other external factors, such as interference from the policymaker, before the process stops.

In more complex models, the drift could be non-stationary and changes with time. The trend of drift can be estimated with sufficient data. Assume that trend is linear, then $d\mu/dt = Y$ or $\mu_t = Y\,t + \mu_0$ where μ_t is the drift at time t, and is the trend at time, *t=0,* and is the trend of the drift. This additional equation can be used in the ordinary differential equation of perpetual time. However the numerical solution may be required.

As shown in Section 2.6, the value of a CO2 reduction project, *W*, of a stochastic process in perpetual time is represented in terms of its CO2 concentration (*X* terms) in the ordinary differential equation (see also equation [6] in Section 2.6):

$$\frac{1}{2}\sigma^2 X^2 \frac{d^2W}{dX^2} + \mu X \frac{dW}{dX} - rW = 0 \qquad [2]$$

where μ denotes drift of CO2 emission rate, σ denotes volatility (standard deviation), and *r* is the discount rate.

Next, the social benefits produced by the CO2 reduction policy needs to be established. The build-up of CO2 concentration level produces pollution damages to society and environment. The social costs and damages caused by CO2 emission have economic values and impacts on society and environment. To mitigate the social costs of pollution, a CO2 reduction policy is proposed to counter the negative effects of CO2 concentration increase. This policy is adopted when social benefits equal to the social costs. In effect, the social costs are equivalent measures of social benefits.

To translate the CO2 concentration level, *X*, to real economic loss value, the damage function of social costs is defined in terms of X_t. Assume the damage cost

damage function be in the form $-\theta X^m$, this is a convex polynomial function with power parameter m ($m \geq 2$), and, θ, is a constant parameter for equivalent flow of CO2 concentration value to social costs (Pindyck, 2000). The corresponding social benefit function, B, is

$$B = \theta X^m \qquad [3]$$

The benefit function [3] is based on the widely used Cobb Douglas production function in economics (Cobb & Douglas, 1928). This cost function has been used in real option analysis studies on climate change (Dixit & Pindyck, 1994; T. Lin, et al., 2007; Pindyck, 2002). Pindyck studied the critical values θ using different volatility values (σ) , and found that critical value θ converges to the value $\theta = 1$ as CO2 concentration level increases to very large values (Pindyck, 2002, page 1693, figure 1).

At any time, the value of investment opportunity of the CO2 reduction project is given by:

Value of Investment Opportunity = Social Benefits – Investment Cost [4]

where K denotes the investment cost (cost of adoption). The value of the project (W), which produces the social benefits, is also same as the value of B. For the policymaker deciding upon an investment, a CO2 reduction project is adopted when social benefits equals or exceeds the investment cost, that is, once the investment opportunity value of project equals or greater than zero value.

By similar analogy, a project which *do not adopt* the CO2 reduction policy, V, have a similar mathematical expression but with V replacing W in [2]. Also the cost of damages will have the same value, θX^m, from [3].

The graphical illustration to show how to use real options analysis to obtain stopping time of adoption of CO2 reduction policy and option value is shown in the following example. The CO2 reduction policy problem comprises two projects: a ADOPT project (W) and a NO-ADOPT project (V). In each project there are two regions: an ADOPT region and a NO-ADOPT region. When the value of the policy is

above the curves, there is an investment opportunity, and the policy will be adopted because the value exceeds the boundary of the project (Figures 4.1a and 4.1b). Likewise, the policy will not be adopted when the value of the policy is below (less than) the boundary value of the project, that is, there is no investment opportunity.

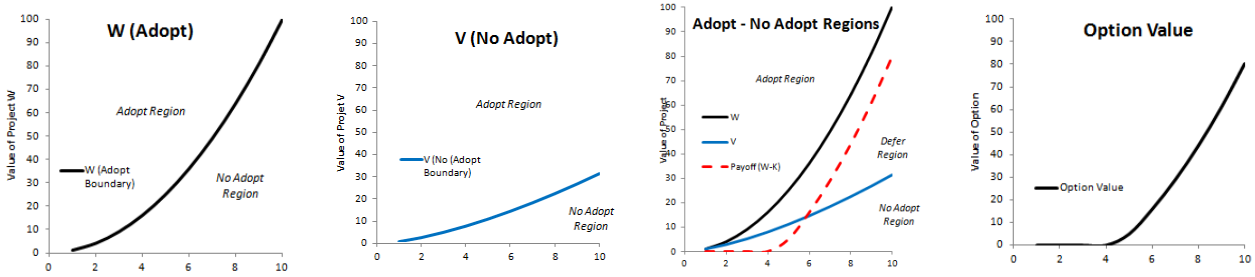

Figure 4.1a Figure 4.1b Figure 41c Figure 4.1d

Figure 4-1 Graphical Illustration of Methodology

The stopping time to adopt the policy is where the two regions meet tangentially (Figure 4.1d) (Dixit, 1993). However there is common area on the right where it is a Adopt Region in the NO-ADOPT project (Figure 4.1a) and Adopt Region in the ADOPT project (Figure 4.1b). In the ADOPT project indicates that there is an investment opportunity but the NO-ADOPT project indicates that there is no investment opportunity. This uncertain area in Figure 4.1c is the option to defer region. In this situation the policymaker is in a dilemma whether to adopt or not to adopt the policy. So the best option is to defer the decision and wait for further information to arrive to clear the uncertainty. The combined payoff of both projects is obtained from *max(V-K, W-K, 0)* where *K* is project cost. The option value of the policy is the payoff value of the combined projects shown in Figure 4.1d. This option profile in Figure 4.1d is the same as to a call option of a financial option.

Next, it is necessary to incorporate the effect of continuous contribution of the benefit-cost values (equation 3) in the value of the project (equation 2) into the two projects, ADOPT (*W*) and NO-ADOPT (*V*). The above approach is first described in Dixit & Pindyck's book ((Dixit & Pindyck, 1994; Pindyck, 2000) and is called Pindyck's framework in this thesis. The following sections show how equation 2 can be

extended to complete the problem formulation. Detailed step-by-step mathematical derivations can be found in Appendix 1.

4.1.1 No Exercise - No Adopt Project

The economic idea of the equation in this region is that the evolution of CO2 concentration, *X*, produces damages to the environment.

Assume that there is a project, *V*, which does not adopt the CO2 reduction policy. Let *V* denotes the economic value of this project not adopting. The cost of damages resulting from this project is the same as the benefits foregone in adopting a project which produces benefits $B=\theta X^m$ (see equation [2]).

At general equilibrium of asset values, the value of the project *V* is represented by the differential equation shown in equation [5]. The mathematical derivation of equation [5] is shown in Appendix 1.

$$\frac{1}{2}\sigma^2 X^2 \frac{d^2V}{dX^2} + \mu X \frac{dV}{dX} - \theta X^m = rV \qquad [5]$$

The intuitive interpretation of equation [5] in economic terms is as follows: *rV* represnts interest earned from investing equivalent V amount at interest rate *r*, $\mu X(dV/dX)$ represents the growth in value of project *V*, $½(\sigma^2X^2)(dV^2/dX^2)$ represents increase in the growth value of the project, and θX^m represents the cost of damages.

4.1.2 Exercise - Adopt Project

The economic idea of the equation for adopt project is similar to the no adopt. However in this case the let *W* be the economic value of the project which adopts CO2 reduction policy. This ADOPT project will result in a new CO2 emission process after the adoption of the policy. The mathematical derivation of equation [6] is shown in Appendix 1.

$$\frac{1}{2}\sigma^2 X^2 \frac{d^2W}{dX^2} + \alpha\mu X \frac{dW}{dX} - \theta X^m = rW \qquad [6]$$

Let δ denotes the cutback in CO2 emission rate, and as a result, the remaining CO2 emission rate is α. Therefore, $\alpha = 1 - \delta$. If there is no cutback in CO2 emission, then $\delta = 0$, and $\alpha=1$, and the CO2 emission continues as before. On the other hand, if there is 100% cutback in CO2 emission, then $\delta=1$, and $\alpha=0$, and the CO2 emission is eliminated.

The intuitive interpretation of equation [6] in economic terms is as follows: rW represents interest earned from investing equivalent W amount at interest rate r, $\alpha\mu X(dW/dX)$ represents the growth in value of adopt project V, $1/2(\sigma^2X^2)\ (dW^2/dX^2)$ represents increase in the growth value of the adopt project, and θX^m represents the social benefits produced by the adopt project.

4.2 Method of Implementing CO2 Reduction Policies

Next, the mathematical modelling of the two types of CO2 reduction policies in the real options analysis model is described below. It is assumed that both CO2 reduction policies are separate and independent.

4.2.1 Carbon Emission Cutback

Theoretically, there are two cases with zero CO2 emission, $\alpha=0$. First case is when there is still the possibility of uncertainty in CO2 emission from the stochastic process, $\sigma > 0$. This means that the first term with the second derivative and volatility still remains. Second case is when the uncertainty in CO2 emission is removed entirely, $\sigma = 0$, and the first term with the second derivative is also eliminated. This research assumes that the first case, that is, there is uncertainty in CO2 emission remaining and σ remains unchanged.

4.2.2 Carbon Concentration Level Abatement

CO2 level abatement involves reduction of CO2 concentration level, X, at the time of exercise/adoption of policy. A full abatement means decreasing the current CO2 concentration level to the original level, X_0, at starting time, t_0. In the model and

also in practice, CO2 mitigation policies assume that the current CO2 level is left unchanged, that is the abatement is zero. In other words, the two reduction methods are assumed to be independent.

4.3 Solution of Adopt Project and No Adopt Project Values

The perpetual time solution can be found by solving the ordinary differential equations [5] and [6] with boundary conditions at the adoption time of reduction policy.

4.3.1 No Exercise - No Adopt Project Value

NO-ADOPT region is first defined and the perpetual value in this region by solved from equation [5]. For simplicity, θ=1 is assumed in the equation (see Section 4.1). Therefore equation [5] reduces to:

$$\frac{1}{2}\sigma^2 X^2 \frac{d^2V}{dX^2} + \mu X \frac{dV}{dX} - rV = X^m \qquad [7]$$

This is an inhomogeneous non-constant coefficient second order ordinary differential equation. Equation [7] can be solved using standard methods in differential calculus, such as Laplace Transform, Fourier Series or Power Series. The method of variation parameters is used here to find the solution.

Applying the general solution from Appendix 2 to [7]:

$$\mathrm{V} = \mathrm{A}_1 \mathrm{X}^{\beta_1} + C_1 X^{m+2} \qquad [8]$$

where

$$\beta_1, \beta_2 = \frac{-\left(\mu - \frac{1}{2}\sigma^2\right) \pm \sqrt{\left(\mu - \frac{1}{2}\sigma^2\right)^2 + 2\sigma^2 r}}{\sigma^2} \qquad [9]$$

$$C_1 = \left[\frac{1}{(\beta_1 - 1)(4 - \beta_1)} + \frac{1}{(\beta_2 - 1)(4 - \beta_2)}\right] \qquad [10]$$

And $\mu > \sigma > 0$, and $0 > \beta_1 > \beta_2$.

4.3.2 Exercise - Adopt Project Value

Next, the solution of the ADOPT region is obtained using the same method above:

$$\frac{1}{2}\sigma^2 X^2 \frac{d^2W}{dX^2} + \mu' X \frac{dW}{dX} - rW = X^m \qquad [11]$$

where μ' denotes the new CO2 emission after exercise - adoption of policy.

Applying the general solution from Appendix 2 to [11]:

$$W = A_3 X^{\beta_3} + C_2 X^{m+2} \qquad [12]$$

Where

$$\beta_3, \beta_4 = \frac{-\left(\mu' - \frac{1}{2}\sigma^2\right) \pm \sqrt{\left(\mu' - \frac{1}{2}\sigma^2\right)^2 + 2\sigma^2 r}}{\sigma^2} \qquad [13]$$

$$C_2 = \left[\frac{1}{(\beta_3 - 1)(4 - \beta_3)} + \frac{1}{(\beta_4 - 1)(4 - \beta_4)}\right] \qquad [14]$$

And $\mu' > \sigma > 0$, and $0 > \beta_3 > \beta_4$.

4.4 Boundary Conditions of Solution

The exercise-adoption condition is determined by the point of contact where the boundaries of No-Exercise-No Adopt Region and Exercise-Adopt Region meet and touch each other tangentially. This is the stopping time for adoption of the CO2 reduction policy at CO2 concentration *X**.

4.4.1 Exercise Condition

At the stopping time, the value of adopt project, W*(X*)* less the investment cost, *K*, is equal to the value of the no adopt project, V*(X*)*:

$$V(X^*) = W\left(X^*\right) - K \qquad [15]$$

This means that the net value of the adopt project (W(X) less K) is equal to the value of value of no adopt project. In other words, the net benefits produced by the adopt

project is equal to the damage cost caused by no adopt project. The graphical representations of CO2 emission cutback is shown in Figure 4.1a.

The graphical illustration of the CO2 reduction policies resembles the stabilization wedges described by Wigley et al (Wigley, Richels, & Edmonds, 1996). These wedges are produced as a result of increasing benefits over time after CO2 emission reduction takes effect. The triangular areas between the 2 solid curve and dashed curve on the right hand side of Figures 4.1a and 4.2b illustrate the benefits obtained from adoption of the two reduction policies over time.

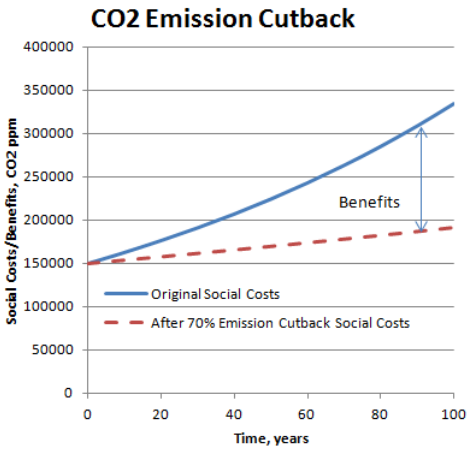

Figure 4.1a

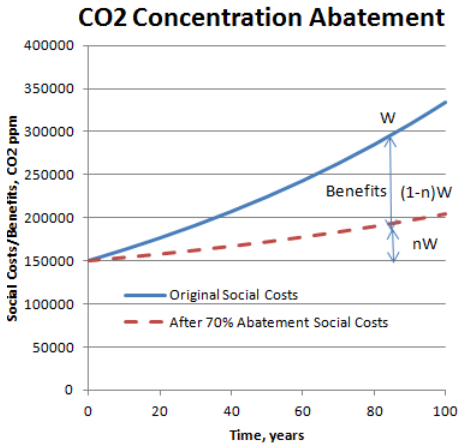

Figure 4.1b

Figure 4-2 CO2 Reduction Policies

For partial abatement of CO2 concentration level, the exercise condition is modified to:

$$V\left(X^*\right) = nW\left(X^*\right) - K \qquad [16]$$

The abatement in CO2 concentration level is *n*, where *1 > n > 0*, where *n=0* for full abatement of CO2 concentration level, and *n=1* for no abatement. For partial abatement, to reduce the cost damages to *n* level will require abatement of the order of *(1-n)* of the current CO2 concentration level. A partial abatement for *n<1* will result in a discontinuity at X=X*, which is similar to downward jump from *W(X*)* to *nW(X*).* The graphical representations of CO2 emission cutback is shown in Figure 4.1b.

The adoption time is determined by the free boundaries in *W(X)* and *V(X)*. The values of these two boundaries change stochastically with the CO2 concentration level *X.* Therefore, Black Scholes formula cannot be used in this problem because in the Black Scholes problem the exercise boundary is a fixed boundary, and its option payoff is a linear function of the underlying asset. But in this research the benefit function is convex and payoff is non-linear.

4.4.2 Boundary Conditions

To recapitulate, the two policy regions are defined as:

No Exercise-No Adopt $$V = A_1 X^{\beta_1} + C_1 X^{m+2} \quad [17]$$

Exercise-Adopt $$W = A_3 X^{\beta_3} + C_2 X^{m+2} \quad [18]$$

4.4.2.1 Boundary Condition 1 Value Matching

At the time of adoption, *X*=*X**;

$$V\left(X^*\right) = nW\left(X^*\right) - K \quad [19]$$

$$A_1 K^{\beta_1} + C_1 K^4 = n\left(A_3 X^{\beta_3} + C_2 X^4\right) - K \quad [20]$$

The abatement in CO2 concentration level is *n*, where *1 > n > 0*, where *n=0* for full abatement of CO2 concentration level, and *n=1* for no abatement. For partial abatement, to reduce the cost damages to *n* level will require abatement of the order of *(1-n)* of the CO2 concentration level at time t=0. A partial abatement for n<1 will result in a discontinuity at *X*=*X**, which is similar to downward jump from *V(X*)* to *nV(X*).*

4.4.2.2 Boundary Condition 2 Smooth Pasting

Point of contact of two curves is tangential for continuous transition at $X=X^*$. Notwithstanding the possible discontinuity of equation [19] from Boundary Condition 1, it is a valid assumption to have the two curves to have the same slope at $X=X^*$.

$$\frac{dV}{dX^*} = \frac{dW}{dX^*} \qquad [21]$$

Substitute [17] in [21] $$\frac{dV}{dX^*} = A_1\beta_1 X^{*\beta_1 - 1} + (m+2)C_2 X^{*(m+1)} \qquad [22]$$

Substitute [20] in [21] $$\frac{dW}{dX^*} = A_3\beta_3 X^{*\beta_3 - 1} + (m+2)C_2 X^{*(m+1)} \qquad [23]$$

Equating [22] and [23] $$A_1\beta_1 K^{\beta_1 - 1} + (m+2)C_1 K^{(m+1)} = A_3\beta_3 K^{\beta_3 - 1} + (m+2)C_2 K^{(m+1)} \qquad [24]$$

Using the boundary conditions [equations 19 to 24] with the exercise conditions [equations 17 and 18], the values of A_1 and A_3 can be obtained (see Appendix 3).

4.5 Complete Solution of Perpetual Value

The derivation of the complete solution of the two regions is shown in Appendix 3 and the final solution is shown below.

No Exercise-No Adopt $$V = A_1 X^{\beta_1} + C_1 X^{m+2} \qquad [25]$$

Exercise-Adopt $$W = A_3 X^{\beta_3} + C_2 X^{m+2} \qquad [26]$$

$$\beta_{1,2} = \frac{-\left(\mu - \frac{1}{2}\sigma^2\right) \pm \sqrt{\left(\mu - \frac{1}{2}\sigma^2\right)^2 + 2\sigma^2 r}}{\sigma^2}$$

$$\beta_{3,4} = \frac{-\left(\mu' - \frac{1}{2}\sigma^2\right) \pm \sqrt{\left(\mu' - \frac{1}{2}\sigma^2\right)^2 + 2\sigma^2 r}}{\sigma^2} \qquad [27]$$

$$C_1 = \left[\frac{1}{(\beta_1 - 1)(m+2-\beta_1)} + \frac{1}{(\beta_2 - 1)(m+2-\beta_2)}\right] \qquad [28]$$

$$C_2 = \left[\frac{1}{(\beta_3 - 1)(m+2-\beta_3)} + \frac{1}{(\beta_4 - 1)(m+2-\beta_4)}\right] \qquad [29]$$

$$A_1 = \frac{K^{(m+2)-\beta_1}}{\beta_3 - n\beta_1}\left[C_1\left([m+2]n - \beta_3\right) - C_2 n\left([m+2] - \beta_3\right) - \frac{\beta_3}{K^{(m+1)}}\right] \qquad [30]$$

$$A_3 = \frac{K^{(m+2)-\beta_3}}{\beta_3 - n\beta_1}\left[C_1\left([m+2]-\beta_1\right) - C_2\left([m+2]-n\beta_1\right) - \frac{\beta_1}{K^{(m+1)}} \right] \quad [31]$$

The solution form in [25] to [30] is the stopping time for policy adoption which depends on CO2 concentration level, *X*, and cost of reduction, *K*, but not the actual time dimension. In other words, the actual time for policy adoption is indeterminate in the perpetual time model.

4.5.1 Option Value for Policy Adoption

Option Value of Reduction Policy is given by the following equations,

For *X*<*K*, $$\mathrm{F}(\mathrm{V}) = \max(\mathrm{V} - K, 0) \quad [32]$$

For *X*>*K*, $$\mathrm{F}(\mathrm{W}) = \max(\mathrm{nW} - K, 0) \quad [33]$$

4.5.2 Critical Discount Rates

It is obvious that the values of $\beta_1, \beta_2, \beta_3, \beta_4$ in equation [28] and [29] cannot be 1 or (m+2), otherwise C_1, C_2 becomes infinite and the solution will explode.

Let $\beta_1 = 1$, $\beta_2 = 1$ in equation [9], and $\beta_3 = 1$, $\beta_4 = 1$ in equation [10] respectively,

$$-\left(\mu - \frac{1}{2}\sigma^2\right) \pm \sqrt{\left(\mu - \frac{1}{2}\sigma^2\right)^2 + 2\sigma^2 r} = \sigma^2 \quad [34]$$

Solving for r in [34],

$$r = \mu \quad [35]$$

$$r = \mu' \quad [36]$$

Similarly, when m=2, let $\beta_1 = 4$, $\beta_2 = 4$ in equation [10], and $\beta_3 = 4$, $\beta_4 = 4$ in equation [13] respectively,

$$-\left(\mu - \frac{1}{2}\sigma^2\right) \pm \sqrt{\left(\mu - \frac{1}{2}\sigma^2\right)^2 + 2\sigma^2 r} = 4\sigma^2$$

Solving for r,

$$r = 4\mu + 6\sigma^2 \quad [37]$$

$$r = 4\mu' + 6\sigma^2 \qquad [38]$$

For parameters A_1 and A_2 from [30] and [31], the critical value is $\beta_3 - n\,\beta_1 = 0$. For $0<n<1$, the value of $(\beta_3 - n\,\beta_1)$ is an increasing function, and A_1 and A_2 are monotonic increasing positive values. If $n = 1$ for zero abatement, then $\beta_1 = \beta_3$. For $n<0$, numerical analysis, shows $\beta_1 < \beta_3$. Also for all discount rates, the only possible solution is $\beta_1 = \beta_3 = 0$. This implies that there is no critical discount rate in A_1 and A_2 parameters.

4.6 Example of CO2 Emission Model in Perpetual Time

The objective of the following example is to study the impact of CO2 reduction policies and discount rates on the two CO2 reduction policies. The CO2 emission cutback policy targets the source of emission by modifying the drift, μ, of the stochastic process. This is the widely used policy approach which can be implemented with more energy efficient plants and machineries. The CO2 concentration abatement policy achieved this by varying the abatement parameter n. For example, this could be achieved by innovative ways of storing CO2 and absorption of atmospheric CO2 with plants. The numerical example will provide the policymaker a better understanding of the interactive effects of reduction cost, CO2 concentration level, and discount rate on the reduction policies.

4.6.1 Data Parameters

The measurement units of benefits and costs in this research are parts per million CO2 (ppm CO2). Although these could be expressed in monetary units by multiplying the carbon values by the social cost of carbon, the ppm CO2 unit is used here because there is a wide range of social cost of carbon estimations which would further complicate the solution. The parameters used in the example are summarized below:

μ, original drift in CO2 emission 0.003957

σ, volatility of drift in CO2 emission	0.000479
X_0, initial CO2 concentration (Jan 2011)	387.19 ppm CO2
μ' CO2 emission after adoption	0 to1.0 [varying CO2 emission cutback]
n, CO2 concentration level abatement	0 to1.0 [varying CO2 conc abatement]
r, discount rate	0.1 to 10% pa [varying]
θ, theta	1.00 [assumed]

4.6.2 Adoption / Reduction Cost for CO2 Reduction

In the perpetual time model, the reduction cost (K) which must be specified in order to obtain a solution. But the reduction cost also depends on the time horizon because the implementation cost of the policy increases with time. For this example, the reduction cost is set to be equal to the CO2 concentration level in year 500. As CO2 concentration level follows the stochastic process in the CO2 emission model, the cost of reduction in ppm CO2 is also given by:

$$Reduction Cost = \left[X_0 exp^{(\mu - \frac{1}{2}\sigma^2)t + \sigma\sqrt{t}} \right]^2 \qquad [39]$$

Using parameters of CO2 emission model from above, the reduction cost at year 500 is estimated to be 8.00×10^6 ppm CO2.

4.6.3 Critical Discount Rates

As noted in Section 4.6.2, critical discount rates have big impact on solution. Using the above CO2 data parameters, when $\beta=1$ and $\beta=4$, the critical discount rates are determined to be 0.394% pa and 1.576 % pa respectively. Caution must be exercised in using discount rates around these critical values as the solutions are not well behaved. Except for brief periods in economic history, interest rates are usually above these critical levels. Abnormally low interest rate will revert back to higher interest rates in the long term. In this Chapter 4 and Chapter 7 a range interest rates is used for sensitivity analysis, and in Chapters 6, 8 and 9the interest rate is set at 4% pa. to simplify the analysis,

4.7 Results and Discussion of CO2 Emission Model Example

4.7.1 Option to Defer Value in Real Options

The typical solution space of the analytical model comprised two main regions: NO-ADOPT region and the ADOPT region (Figures 4.3 and 4.4). Note that value of the Y-Axis is in logarithm scale; otherwise, the two figures are similar to Figure 4.1 in Section 4.1. This allows the two curves to shown clearer than with a normal scale. The NO-ADOPT is upward sloping because increase in CO2 concentration level increases the social costs. The ADOPT curve is also upward sloping with the boundary condition is fixed at *V(0)=0* and *W(0)-K=0*. This means that adoption of policy at high CO2 concentration level requires high benefits to justify. This implies that an early adoption of policy, when CO2 concentration is low, is economically more attractive because of lower costs.

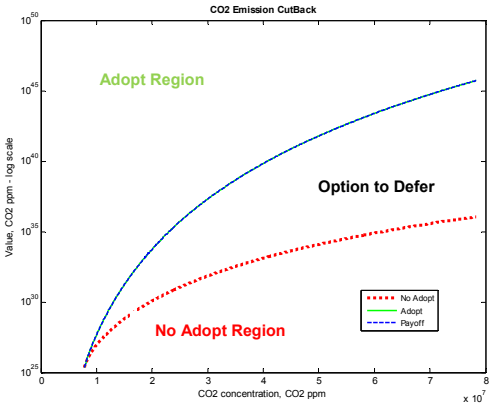

Figure 4-3 CO2 Emission Cutback

[50% CO2 emission cutback, 0% CO2 concentration abatement, reduction costs 8.00E06 ppm CO2]

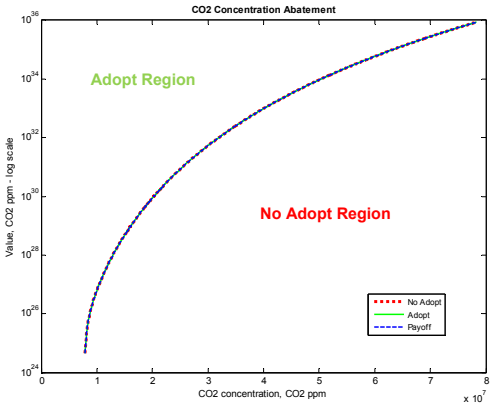

Figure 4-4 CO2 Concentration Abatement

[50% CO2 concentration abatement, 0% CO2 emission cutback, reduction costs 8.00E06 ppm CO2]

NO ADOPT Region

NO-ADOPT region is the area between the horizontal axis and the NO-ADOPT curve. Therefore the decision is should be against adoption of the reduction policy.

ADOPT Region

ADOPT Region is the area above both the ADOPT and NO-ADOPT curves. Therefore the decision should be adoption of reduction policy immediately.

Option to Defer Region

For CO2 emission cutback policy there is an additional area space between the two regions (Figure 4.3). This area is the option to defer, and it arises from the uncertainty of CO2 emission rate which gives the additional value using real options analysis. For CO2 concentration abatement, the two curves collapse into one curve (Figure 4.4), and there is no option to defer region because the CO2 concentration level is assumed to exist in the atmosphere and there is no uncertainty of its value. There are an infinite number of possibilities in this option to delay region. However, the best option is to adopt is at the upper boundary, that is, the boundary of ADOPT region, where the benefit values are the largest.

Another way to look at this option to defer is to draw a vertical line with a fixed CO2 concentration in Figure 4.3. Moving up from bottom to top with increasing benefit levels, the decision maker will move upwards above the no adopt boundary curve to extract higher values to reach the adopt boundary curve above. The benefit level at adopt boundary curve is larger than no adopt boundary curve at this fixed CO2 concentation level. From the above analysis it can be seen that the real options analysis approach is able to extract larger benefits for the same reduction cost and CO2 concentration level. However, the results also show that there is no option to defer value for the CO2 concentration abatement policy.

4.7.2 Discount Rates Effects on CO2 Reduction Policies

Discount rate is an important factor in economic analysis. In the following example, the reduction cost is fixed, and a range discount rates and CO2 emission cutback rates are used. The objective of this section is to understand the impact of discount rates and CO2 reduction policies on option to defer values.

4.7.2.1 CO2 Emission Cutback

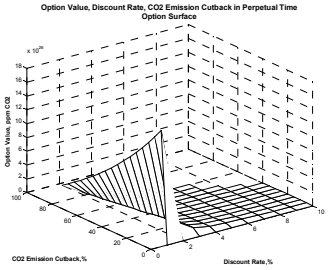

Figure 4-5 CO2 Emission Cutback and Discount Rates-Option Value

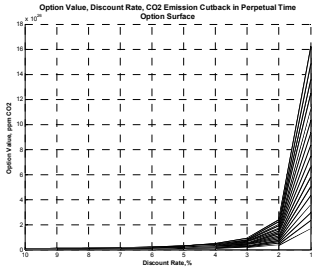

Figure 4-6 CO2 Emission Cutback Effect

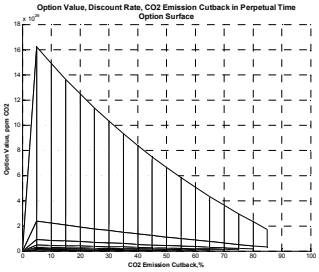

Figure 4-7 Discount Rates Effect

CO2 emission cut back: 0% to 100%, reduction costs 0 to 8.00E06 CO2 ppm, 0% CO2 concentration abatement, r=1-10%pa

High option values are produced with low discount rates and low CO2 emission cutback rates (Figure 4.5). The maximum option value is obtained with combination of both low discount rates and low CO2 emission cutback rate. In low discount rate environment, the option value is high because the opportunity cost of waiting is low and, hence, the incentive to defer is high (Figure 4.6). This indicates that the flexibility of implementing the policy is greatest at low discount rates and low reduction rates. The option values and flexibility decrease rapidly with higher discount rates but are still positive. However there is no feasible adoption policy when there is high discount rates and high CO2 emission cutback rates (blank area in the upper right corner of Figure 4.5). In these cases, the high rate of CO2 emission cutback has already solved the CO2 reduction problem, and coupled with high discount rates, there is solution for the option value.

At low discount rates, the rate of change of option value in CO2 emission cutback rate (as indicated by the steeper slopes in Figure 4.6) is more sensitive than in discount rate (as indicated by the gentler slopes in Figure 4.7); this suggests the option to delay is more sensitive to changes of CO2 emission rates than discount rate changes. This indicates that the flexibility is more sensitive and decreases more quickly with changes in discount rates, which are below 3% to 4%, than with changes

in reduction rates. Also the change in flexibility is proportionally linear with reduction rates.

Impact of negative discount rates is assessed by extending the results from low positive discount rates. It can be deduced that negative discount rates will make the option values even larger. This would provide the policymaker even more incentive to defer to adopt CO2 reduction policy because the future benefits will be less than the current benefits. So the policymaker will prefer to spend the money on other promising projects than the CO2 reduction policy. Also, if future generations would want to the reduction policy to be adopted now, they will have to pay the present generation to implement the policy. This is a difficult proposition to achieve in reality.

4.7.2.2 CO2 Concentration Abatement

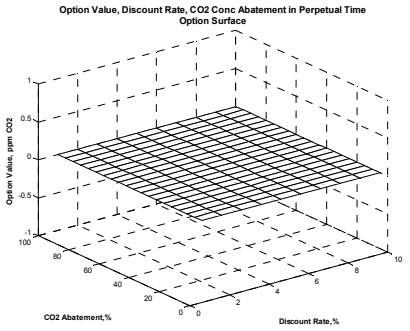

CO2 concentration abatement: 0% to 100%, reduction costs 0 to 8.00E06 CO2 ppm, CO2 emission cutback 0%, r=1-10%pa

Figure 4-8 CO2 Concentration Abatement and Discount Rates

There is no option value to defer for CO2 concentration abatement for all discount rates (Figure 4.7). This agrees with the same result shown in Figure 4.3. Discount rates have no impact on option values in CO2 concentration abatement because there is no uncertainty of the CO2 concentration in perpetual time. This indicates that there is no flexibility in deferring implementation of policy, in other words, the policy must be implemented immediately.

4.7.3 CO2 Emission Cutback vs CO2 Concentration Abatement

The cost effectiveness of the two reduction policies is investigated in this section for their value of information and value of managerial flexibility. As in the example above, the maximum reduction cost is 8.00×10^6 ppm CO2, and the range of

reduction costs is from 0% to 100%. The investigation is performed in two separate parts by controlling one reduction policy whilst varying the reduction rate of the other reduction policy, and vice versa. For example, the first part is to evaluate CO2 concentration abatement policy. The range of reduction costs and CO2 concentration abatement rates are used to obtain option value whilst CO2 emission cutback is fixed at zero. The second part is to evaluate CO2 emission cutback with the same procedure. The range of reduction costs and CO2 emission cutback rates are used to obtain option value whilst CO2 concentration abatement is fixed at 0%.

4.7.3.1 Value of Information in CO2 Reduction Policies

Using the same reduction costs, the option values of the two CO2 reduction policies are compared to assess their value of information. Both policies have maximum option values with low reduction costs below $2x10^5$ ppm CO2. This suggests that even relatively low reduction costs produce high value of information (Figures 4.9 and 4.10).

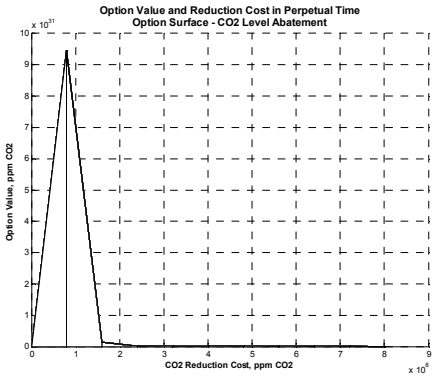

Figure 4-9 CO2 Concentration Abatement - Reduction Cost and Option Value

CO2 concentration abatement from 0% to 100%
reduction costs 0 to 8.00E06 CO2 ppm
0% CO2 emission cutback, discount rate 4%pa

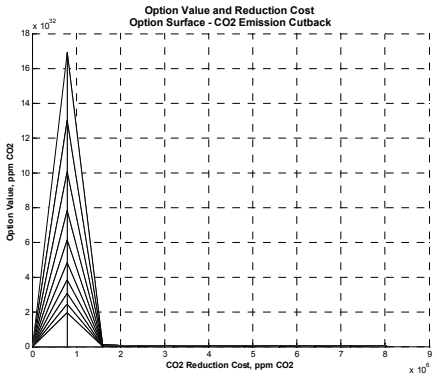

Figure 4-10 CO2 Emission Cutback - Reduction Cost and Option Value

CO2 emission cutback from 0% to 100%,
reduction costs 0 to 8.00E06 CO2 ppm
0% CO2 concentration abatement, discount rate 4%pa

The maximum option value in CO2 emission cutback, which depends on the reduction costs, is $17x10^{32}$ ppm CO2 carbon (Figure 4.10). But the maximum option value in CO2 concentration abatement is $9x10^{21}$ ppm CO2 (Figure 4.9). Therefore

the value of information in CO2 emission cutback is higher than CO2 concentration abatement. The reason is that CO2 emission cutback is directed at solving the source of uncertainty in CO2 emission; whereas in CO2 concentration abatement the CO2 reduction is aimed at solving the existing problem caused by released CO2 concentration, while the source of CO2 emission remains unchanged. The policymaker can make use of the value of information to invest in research and development projects and to acquire better quality information.

4.7.3.2 Value of Flexibility in CO2 Reduction Policies

In CO2 concentration abatement (Figure 4.11) the option value remains the same at all CO2 concentration abatement rates. In other words, flexibility to adopt the project does not change with reduction costs and rate of CO2 concentration abatement.

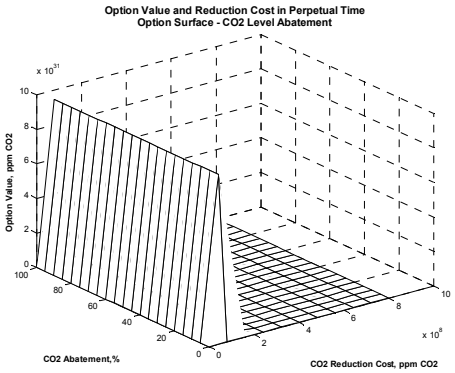

Figure 4-11 CO2 Concentration Abatement and Option Value

CO2 concentration abatement 0-100%,
reduction costs 0 to 8.00E06 CO2 ppm
0% CO2 emission cutback, discount rate 4%pa

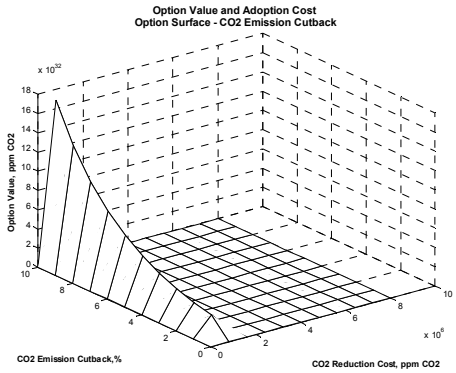

Figure 4-12 CO2 Emission Cutback and Option Value

CO2 emission cutback 0-10%
reduction costs 0 to 8.00E06 CO2 ppm
0% CO2 concentration abatement, discount rate 4%pa

In CO2 emission cutback (Figure 4.12), the option values rise steadily from zero CO2 emission cutback, then increase exponentially to $17x10^{22}$ ppm CO2 at 10% CO2 emission cutback rate. The increasing option values with CO2 emission cutback suggests that flexibility increases with reduction costs and CO2 emission cutback rate. With higher reduction rates planned for the future, there is more flexibility to adjust CO2 emission cutback policy. In some discount rates, the

flexibility does not exist when the adoption cost is above a threshold level. The reason is that the adoption cost will always be larger than the benefits obtained from the reduction policies. The take away for the policymaker is that flexibility to adopt the reduction policy depends on both adoption cost and discount rate exists.

4.8 Discussion of CO2 Damage Cost with Delayed Damage Impact

The CO2 damage cost function of equation [3] in Section 4.1 assumes that the impacts from the damages are instantaneous. In reality, the resulting impact may continue to increase for many more years.

The continuing damage of CO2 emission after CO reduction can be taken into account in the model by allowing the CO2 reduction cost to be less effective in each subsequent period.

For example the modified CO2 reduction cost function can be an exponential decay function, Ke^{-kt}, and the CO2 damage cost function becomes:

$$B_t = B_0 - K\exp^{-\kappa t} \qquad [40]$$

where κ denotes a growth parameter of the original CO2 damage cost, B_0, K denotes the reduction in CO2 concentration level, and t denotes the elapsed time since implementation of CO2 reduction.

It is assumed that the modified CO2 reduction cost reduces every year because of damage impact of CO2 has not stopped (Figure 4.13). Therefore the cost of CO2 damages continues although at a slower rate over time (Figure 4.14).

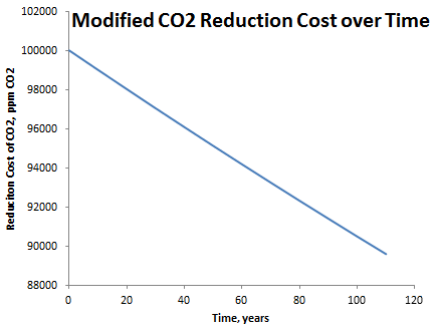

Figure 4-13 Modified CO2 Reduction Cost

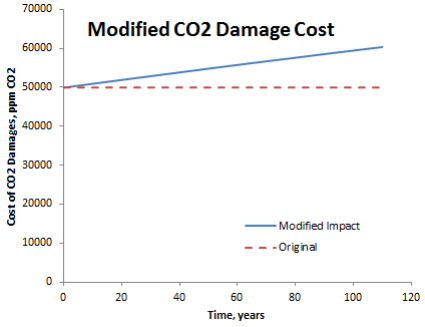

Figure 4-14 Cost of CO2 Damages over time

This modified CO2 reduction cost, Ke^{-kt}, can be substituted for K in the finite time model. An analytical solution for perpetual time is not possible because of time variable in the differential equations.

4.9 Recommendations for the Policymaker

Adaptation policy, as in CO2 concentration abatement, is the least cost effective policy solution. The policy has to be implemented immediately because there is no uncertainty that the problem has arrived.

Mitigation Policy, as in CO2 emission cutback, provides the most flexibility for the policymaker to defer implementation of policy. It does not mean that the policymaker does nothing. The policymaker can gather new information and learn about the uncertainties or develop solutions for the problem. This means that the policymaker needs to invest as research and development. However by doing so will reduce some of the option value to defer and hasten the time of policy implementation.

Adoption time of CO2 mitigation policy varies proportionately, linearly and inversely with the rates of CO2 reduction. For example, if the policy is to make small CO2 emission cutbacks, then there is little incentive to implement this policy early. However if the policy is to make big CO2 emission cutbacks, the policymaker needs to implement this quickly, otherwise the implementation cost or damage cost will increase higher in future.

Low discount rates will increase the likelihood to defer adopting the CO2 reduction policy because there is a lot of flexibility available for the policymaker. It is tempting to use low opportunity costs as an excuse to ignore the problem. However discount rates above 3% to 4% pa are not likely to affect the results much. Therefore it is recommended to use discount rates 4% pa and above if the policymaker is sensitive to changes to what discount rate to use.

4.10 Contributions and Summary

Results from real options analysis showed that low rates of CO2 emission cutback and CO2 level abatement produced the greatest flexibility. One precaution in interpreting the results is that the high flexibility may lead the policymaker to adopt a 'do nothing, wait and see' strategy. The model shows that a zero emission cutback rate has zero value. Therefore, the best adoption strategy is to undertake a low CO2 emission cutback rate, and at the same time, gathering information and learning more about the environment. The analytical model also reveals that there are critical values of discount rates at 0.394% pa and 1.576 % pa which cause instability and discontinuity in the solution.

Between the cost effectiveness of the two reduction policies, it is found that value of information in CO2 emission cutback is higher than CO2 concentration abatement. The results also show that, unlike CO2 emission cutback policy, the flexibility in CO2 concentration abatement policy does not change with reduction rates.

5. RARE EVENTS IN PERPETUAL TIME

A recently IPCC publication highlights the risks and dangers of extreme events in climate change (IPCC SREX, 2012). Based on climate records, past global warming has resulted in increase in frequency and magnitude of extreme events. Furthermore, IPCC AR4 cautions "the possibility of abrupt climate change and/or abrupt changes in the earth system triggered by climate change, with potentially catastrophic consequences, cannot be ruled out" (IPCC AR4, 2007b).

To model catastrophe event in a stochastic process, it is common to represent these rare events as Poisson jumps. Although rare events are difficult to define and specify in practical terms, this Chapter characterizes rare events in 2 dimensions: jump size and jump intensity. Jump size is used to represent the magnitude or cost of the event, and jump intensity is the probability of occurrence (frequency or return period of the event).

So far only one study has been found to use the Pindyck's framework in catastrophe events for climate change (Makropoulou, et al., 2008). However the study does not provide an analytical solution and, as a result, considers only specific scenarios of catastrophe events. There is a research gap in investigating s full a spectrum of impacts caused by different jump sizes and jump intensities. This research aims to fill this research gap with more thorough analysis using a semi numerical solution.

5.1 Discontinuous Stochastic Process Model in Perpetual Time

5.1.1 Poisson Process

Poisson process is frequently used to model random shocks of jump events in discontinuous stochastic process. A compound Poisson process (without diffusion) is represented by:

$$dX = \mu dt + \varphi dq \qquad [1]$$

where μ denotes the drift of Brownian motion process, φ denotes the size of the jump, *dq* denotes the Poisson process event, and λ denotes the frequency or intensity of the jump.

Let the small change from jump in time *dt* be *df*

$$df = f(X_{t+dt}, t+dt) - f(X_t, t) \quad [2]$$

Substitute [2] in [1]

$$df = (f(X_t + \varphi, t) - f(X_t, t))dq + (f_t + \mu f_X)dt$$

$$df = (f_t + \mu f_X)dt + (f(X_t + \varphi, t) - f(X_t, t))dq \quad [3]$$

When there is jump, let the jump event with probability λdt with jump size $(\varphi-1)$

$$f(X_t + \mu dt + \varphi, t+dt) - f(X_t + \mu dt, t+dt)$$

$$= f(X_t + \varphi, t) - f(X_t, t) \quad [4]$$

When there is no jump, let the no jump with probability $(1-\lambda)dt$ with jump size =0

$$f(X_t + \mu dt, t+dt) - f(X_t + \mu dt, t+dt) = 0 \quad [5]$$

The above is the derivation of Ito's Lemma for Poisson Processes.

5.1.2 Jump Diffusion Model

The real options analysis perpetual time model is now extended to include random shocks in CO2 concentration level. The jump diffusion process comprises geometric Brownian process and Poisson process and is *cadlag* (right continuous with left limits). In addition, the two processes are assumed to be independent processes. Following Merton's jump diffusion model (Merton, 1976), the CO2 emission process can be written as:

$$dX = \mu X dt + \sigma X dz + (\varphi - 1) X dq \quad [6]$$

where *dq* denotes the Poisson process with value *dq=1* when there is jump event, and *dq=0* when there is no jump, and φ denotes the size of the jump with $\varphi>1$ for a positive upward jump. It should be noted that the jump events are instantaneous or impulse events, and the jump size variance is zero.

The remainder of the real options analysis model follows the geometric Brownian motion model which is described in Chapter 3. To recap, the social benefit function, *B*, is

$$B = \theta X^{m} \qquad [7]$$

Following the same procedure and analysis in Chapters 2 and 4, it can be shown that the value of the project *V* in a jump diffusion model is given in the ordinary differential equation,

$$\frac{1}{2}\sigma^2 X^2 \frac{d^2V}{dX^2} + \mu X \frac{dV}{dX} - \theta X^2 + \lambda V(\varphi - 1) - \lambda V = 0 \qquad [8]$$

where $\varphi = (V_{n+1} / V_n - 1)$, $m=2$, and $\varphi>1$, is the proportionate increase of CO2 concentration level after the jump, λ is the frequency of the jump or intensity of Poisson process.

In addition, the value of the no adopt project *V* defining the NO-ADOPT region is given by:

$$\frac{1}{2}\sigma^2 X^2 \frac{d^2V}{dX^2} + \mu X \frac{dV}{dX} - \theta X^2 + \lambda V(\varphi - 1) = rV + \lambda V \qquad [9]$$

Similarly, the value of the adopt project *W* defining the ADOPT region is given by:

$$\frac{1}{2}\sigma^2 X^2 \frac{d^2W}{dX^2} + \mu\alpha X \frac{dW}{dX} - \theta X^2 + \lambda W(\varphi - 1) = rW + \lambda W \qquad [10]$$

As in the continuous geometric Brownian process problem, the ODEs in [9] and [10] can be solved by separating the solution into homogenous solution and particular solution.

The homogenous solution has a general form $V_h = AX^{\beta}$. Details of the solution are shown in Appendix 4. However the roots, β_1 and β_2, of the homogenous solution are in a more complex function, and can only be obtained by numerical method in [11].

$$\frac{1}{2}\sigma^2\beta^2+\left(\mu-\frac{1}{2}\sigma^2\right)\beta-(r+\lambda)+\lambda(\varphi-1)^{\beta}=0 \quad [11]$$

The particular solution is the same as in the continuous geometric Brownian solution.

Once the values of β_1 and β_2 are obtained, these can be substituted into the solution:

No Exercise-No Adopt $\mathrm{V}=\mathrm{A}_1\mathrm{X}^{\beta_1}+C_1X^4$ [12]

Exercise-Adopt $\mathrm{W}=\mathrm{A}_3\mathrm{X}^{\beta_3}+C_2X^4$ [13]

where

$$C_1=\left[\frac{1}{(\beta_1-1)(4-\beta_1)}+\frac{1}{(\beta_2-1)(4-\beta_2)}\right] \quad C_2=\left[\frac{1}{(\beta_3-1)(4-\beta_3)}+\frac{1}{(\beta_4-1)(4-\beta_4)}\right] \quad [14]$$

The values of A_1 and A_3 are found by using the same exercise condition with boundary conditions as in the continuous geometric Brownian process:

Exercise Condition $V(X^*)=nW(X^*)-K$ [15]

Value Matching Boundary Condition 1 $X=X^*$ [16]

Smooth Pasting Boundary Condition 2 $\frac{dV}{dX^*}=\frac{dW}{dX^*}$ [17]

where $V(X^*)$ denotes the CO2 concentration level at adoption time.

The complete solution is similar to the continuous geometric Brownian process as shown in Appendix 3.

$$A_1=\frac{K^{4-\beta_1}}{\beta_3-n\beta_1}\left[C_1(4n-\beta_3)-C_2n(4-\beta_3)-\frac{\beta_3}{K^3}\right]$$

$$A_3=\frac{K^{4-\beta_3}}{\beta_3-n\beta_1}\left[C_1(4-\beta_1)-C_2(4-n\beta_1)-\frac{\beta_1}{K^3}\right] \quad [18]$$

Option to Defer Value of CO2 Reduction Policy is given by the following equations,

For $X<K$, $\mathrm{F}(\mathrm{V})=\max(\mathrm{V}-K,0)$ [19]

For $X>K$, $\mathrm{F}(\mathrm{W})=\max(\mathrm{nW}-K,0)$ [20]

5.2 Example of Jump Diffusion Model in Perpetual Time

The objective of this example is to investigate the interactions between jump size and jump intensity, the two dimensions characterizing rare events, on the value of the reduction policy and its option value in the jump diffusion model. The results will be useful in planning CO2 reduction policies for catastrophe events.

Using the same parameters from Chapter 3, the parameters values are drift (μ) of CO2 emission 0.003957, volatility (σ) of CO2 emission 0.000479, initial CO2 concentration level (X_0) 387.19 ppm CO2, discount rate (r) 4% pa, and theta (θ) value 1. It is not possible to obtain observational data of rare events in nature and perform empirical statistical analysis to estimate the jump parameters. Therefore a range of jump sizes and jump intensities are used to simulate their behaviour under various jump scenarios. As before the cost of CO2 reduction or cost of adoption policy is a function of CO2 emission path (see Section 4.6.2 equation [39]):

$$Reduction\ Cost = \left[X_0 exp^{(\mu - \frac{1}{2}\sigma^2)t + \sigma\sqrt{t}} \right]^2$$

Assuming a 500 years' time frame, the reduction cost is 8.00 x10^6 ppm CO2.

5.3 Discussion and Analysis of Jump Diffusion in Perpetual Time

5.3.1 Jump Size and Jump Intensity Factors

The joint conditional impacts of jump size and jump intensity on option value is investigated with a fixed reduction cost in this section.

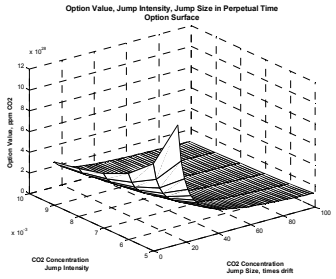

Figure 5-1 Jump Size, Jump Intensity, Option Value

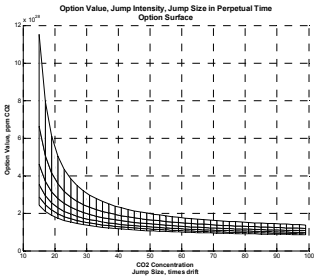

Figure 5-2 Jump Size and Option Value

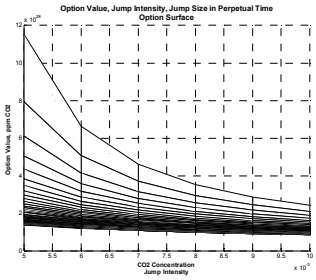

Figure 5-3 Jump Intensity and Option Value

CO2 emission cutback 50%, zero CO2 abatement, discount rate 4% pa, reduction costs 8.00E06 CO2 ppm (equivalent of CO2 concentration level at year 500), Jump Intensity 0.001 to 0.01, Jump Sizes 15 -100 times drift

Figure 5.2 shows that changes in option values with jump sizes from 15 to 100 times of drift in CO2 emission rate. Low jump sizes have higher option values than high jump sizes. There is a negative "exponential like" relationship between jump sizes and option values. Similar observation of the negative non-linear relationship is made with jump intensity and option values in Figure 5.3. However the functional relationship is more a "polynomial like" function. Comparing the relative sensitivity of jump size and jump intensity impact on option values, it can be seen from the gradients of the curves that jump intensity (Figure 5.3) produce higher option values than jump size (Figure 5.2).

In other words there is greater sensitivity in the flexibility in the reduction policy with uncertainty in low jump size than for uncertainty in jump intensity. Therefore the policymaker should monitor jump sizes carefully because the flexibility tend to disappear very fast.

On the other hand jump intensity is less sensitivity than jump size. Its flexibility declines slowly even for higher return periods. The policymaker could invest more in research or in obtaining information on frequency of catastrophe events so as to reduce this uncertainty. This investment is warranted because low probability events could even be more disastrous than high probability events. IPCC AR4 "Mitigation of Climate Change" Chapter 2 page 128 (IPCC AR4, 2007b) noted

that “a policy which risked a catastrophically bad outcome with a very low probability might be valued higher than one which completely avoided the possibility of catastrophe and produced merely a bad outcome, but with a very high probability of occurrence.”

With very high jump sizes and high jump intensities, the options to defer values have low positive values and do not change much. The implication of these extreme values is that there is little incentive to defer, and wait and learn for “good news” of future events is not recommended. The damage costs of the catastrophe events are high and could reduce the benefits of adoption of reduction policy.

5.3.2 CO2 Emission Cutback and Jump Size

The previous study is continued by varying jump sizes and reduction rates to obtain option values. In addition, sensitivity analysis is performed with jump intensity.

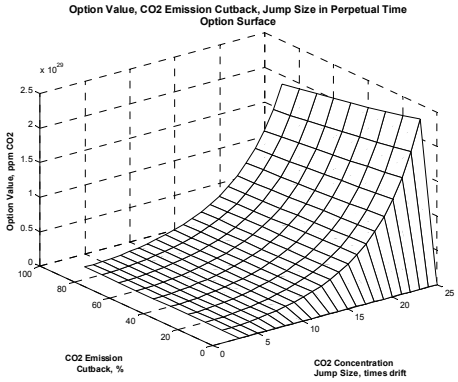

Figure 5-4 Jump Size, CO2 Emission Cutback, Option Value: Jump Intensity 0.001

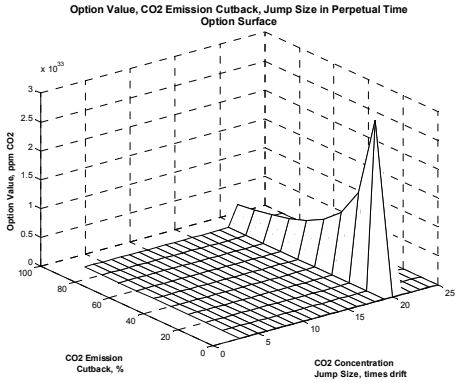

Figure 5-5 Jump Size, CO2 Emission Cutback, Option Value: Jump Intensity 0.002

CO2 emission cutback 50%, zero CO2 abatement, discount rate 4% pa, reduction costs 8.00E06 CO2 ppm (equivalent of CO2 concentration level at year 500), Jump Intensity 0.002 and 0.01, Jump Sizes 3 -25 times drift

With a low jump intensity of 0.001 (1 in 1000 year event), the option values increase with jump size and reaches a maximum value of 2.5×10^{29} ppm CO2 at jump size of 25 times (Figure 5.4). The option values continue to increase with jump intensity and with a jump intensity of 0.002 (1 in 500 year event), it reaches a maximum of 3×10^{33} ppm CO2 (Figure 5.5). Also, the option values increase with

decrease in low reduction rates. This is the same observation in Section 4.7.2.1 for the model with no jump.

The results suggest that there is high incentive to defer adoption of the policy because of higher uncertainties in both jump size and jump intensity. This means that the policymaker also has more flexibility in managing more serious catastrophe events. For example, the policymaker would have more time to prepare several contingent plans and build up emergency measures to handle large scale disasters.

5.3.3 CO2 Emission Cutback and Jump Intensity

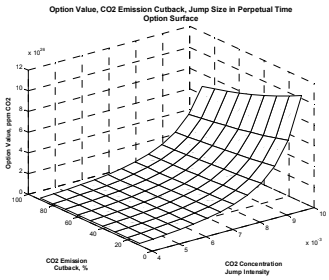

Figure 5-6 Jump Intensity, CO2 Emission Cutback, Option Value - Jump Size 5X

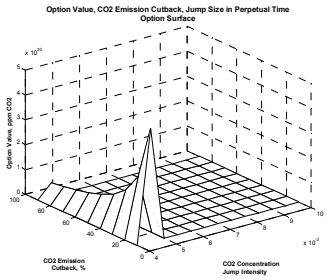

Figure 5-7 Jump Intensity, CO2 Emission Cutback, Option Value - Jump Size 10X

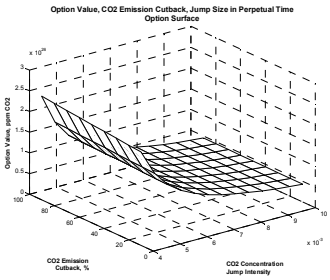

Figure 5-8 Jump Intensity, CO2 Emission Cutback, Option Value - Jump Size 20X

zero CO2 abatement, discount rate 4% pa, reduction costs 8.00E06 CO2 ppm (equivalent of CO2 concentration level at year 500), Jump Intensity 0.004 to 0.01, Jump Size 5x, 10X, 20X drift

The final study investigates varying CO2 emission cutback rates and jump intensities on option values (Figures 5.6, 5.7, and 5.8). For jump sizes up 20X drift of CO2 emission, the results (Figures 5.6 and 5.7) are identical the previous section. However for jump sizes above 20X drift, the option values decline with increasing jump intensity. This means that beyond jump sizes above 20X drift there is little flexibility for the policymaker and the policy should be adopted as soon as possible. The policymaker has less time to adopt the policy because the potential damages of these catastrophe events exceed the value of flexibility.

The results suggest that there is a range of jump sizes around 20X to 25X drift that could trigger the policymaker to adopt the policy quickly.

5.3.4 Evaluation of Catastrophe Events with Normal Events

The normal event model (Section 4) and catastrophe event model can now be compared to assess the additional impact of catastrophe events.

The following example studies the option values of both models by varying the reduction costs for 50% reduction in CO2 emission rate when the CO2 concentration level is at 7.86×10^5 ppm CO2. The option values are for normal event and catastrophe event model are obtained using the same reduction costs.

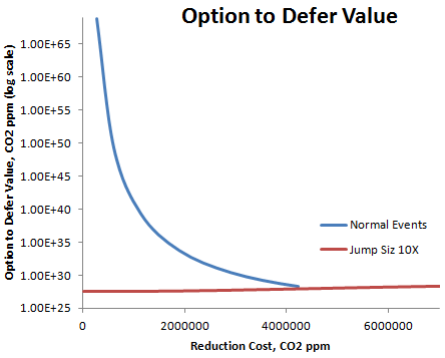

Figure 5-9 Compare Normal and Jump Events

zero CO2 abatement, discount rate 4%pa, 50% CO2 emission cutback

The option values in normal event are many time higher than the catastrophe event (Figure 5.9). This shows that there is relatively little flexibility in catastrophe because of the sudden occurrence in nature. Therefore the policymaker should take the possibility of catastrophe events seriously in his reduction policy.

5.4 Recommendations for the Policymaker

The policymaker can monitor the likelihood of catastrophe events by monitoring the changes in magnitude of CO2 emission rate and frequency of such magnitude increases.

In his planning the policymaker should pay more attention to jump magnitude than jump intensity. In other words, there is greater urgency to act with higher jump magnitudes because implementation time decreases very quickly with jump magnitude. For example, for policy with estimated jump magnitude about 20 X drift, should be implemented immediately. Generally, small jump magnitude and low reduction rates allow high incentive to defer and increases stopping time, while large jump magnitudes and high reduction rates discourages policymaker to delay

implementation. Extremely rare events with large jump magnitudes and high jump frequency need immediate implementation by the policymaker. In summary higher priority is required for catastrophe events than normal events.

As flexibility declines rapidly for jump sizes above 20X, the policymaker should adopt a conservative and prudent policy with regards to jump size. In the words of Gollier & Treich “one should not wait for conclusive evidence of a risk before putting control measures in place designed to protect the environment”(Gollier & Treich, 2003).

One important observation in perpetual time model is that the option values are extremely high. The reason is that the perpetual time solution takes into account each and every one of the finite time solutions. Although the perpetual time model provides elegant closed form solutions, it is of limited practical application. A finite time real options analysis is more useful for analyzing CO2 reduction policies in practice. The remaining chapters in this research focus on the finite time model.

PART C

CLIMATE CHANGE INVESTMENTS

IN FINITE TIME WITH REAL OPTIONS ANALYSIS

6. STOPPING TIMES FOR CO2 REDUCTION POLICIES

In the perpetual time model, the analytical solution depends of CO2 concentration level and the cost of CO2 reduction. These two variables are time dependent, this means a longer adoption time will result in higher CO2 concentration level and higher cost of CO2 reduction. In such case, it is not possible to obtain an optimal solution of an increasing monotonic process in perpetual time because there is no time boundary. Furthermore the results may not be realistic because as the time frame increases reduction costs also increases and becomes unreasonably high. In a fixed time model, the solution is confined by the time restriction and bounded by CO2 concentration level or cost of CO2 reduction. With these additional conditions, an optimal solution of the stopping time could be possible.

Traditional benefit cost analysis assumes there are no uncertainties in the decision making process and, hence, the decision can be made immediately. When uncertainties exist, it is preferable to defer the decision until the uncertainties clear up using new information which are available in future periods. Eventually this process needs to be stopped some time in future.

The stopping time in stochastic process is a random time in which the process is terminated when it satisfies certain boundary conditions. While the process is still alive, learning takes place when more information is available and uncertainties are resolved. Two types of stopping times are used in this research. In first hitting time, learning and information stopped immediately when the process reaches a certain threshold level. On the other hand, if full information is available for the entire time period, it is possible to deduce backwards and learn how to arrive at the optimal stopping time.

6.1 First Hitting Time for CO2 Reduction Policy

CO2 emission process is assumed to move in a random walk as a Brownian motion - a martingale in which the available information in a filtered space is used to determine information up to the next period. When the process is stopped, the learning and information is only available up to that time. Therefore the first hitting time can be considered as a conservative policy decision because it does not make any forecast or assumption of future events. Although it is possible that a few future events may fall below the threshold level because of volatility in the process, the positive drift in the process ensures that re-entry time is short and brief.

6.1.1 Real Options with First Hitting Time

The features of first hitting time can be used in CO2 reduction policy to provide flexibility to the policymaker within a window of opportunity to decide and implement the reduction policy. It also allows the policymaker to monitor the progress and learn more about the uncertainties, and decide on the appropriate response. It is assumed that the policy takes effect immediately at adoption. In real world, implementation takes time, but this can be minimized by closely monitoring the events leading up to the first hitting time and making early preparations for early implementation.

The first hitting time provides a signal to trigger an adoption event of the policy. The signal is set off by the first instance which the CO2 concentration path in its random walk reaches a specific CO2 concentration level at the earliest event and is absorbed or stopped at the threshold barrier. In real options analysis application, this threshold barrier is the reduction cost.

The option value is $max(V_t - K, 0)$, where V denotes the value of the project and K denotes the reduction cost. In first hitting time the adoption condition is $V_t = K$, where t is the stopping time of first hitting time. As the CO2 emission model is a stochastic model with uncertainty in its diffusion component, there is also uncertainty

in the stopping time when CO2 concentration level would reach the threshold level. Therefore there would be an option value in first time hitting because of this uncertainty.

First hitting time is a forward induction progress without knowledge of future events; it sets a lower boundary in stopping time for adopting the policy. Therefore it is shortest, earliest stopping or extreme stopping time event. On the other hand, the perpetual time is the upper boundary in stopping time because it has an infinite time value.

6.1.2 Literature Survey of First Hitting Time

Early analysis of first hitting time are in the papers of statistical and probability theory of sequential analysis of Markov chain. The closed form solution of first hitting time of a constant fixed barrier is provided by Cox & Miller (D. R. Cox & Miller, 1965). A more detailed analysis of first hitting time and Brownian motion is found in Karlin & Taylor (Karlin & Taylor, 1975). First hitting time of moving barrier is described by Tuckwell & Wan who also present a closed form solution for a sloping linear barrier (Tuckwell & Wan, 1984). The results from these studies lay the foundation of its application in financial option theory (Ingersoll, 1987).

In financial option theory, first hitting time is known as first passage time and the financial options are commonly known as barrier options. There are four basic types of barrier options: down and out option, down and in option, up and out in, and up and in options. The differences refer to the relative position of the state with respect to the barrier and the value upon exercise. Closed form analytical solutions of option values are available for many barrier options (Haug, 2007; Merton, 1973; Rubinstein & Reiner, 1991).

First hitting time is introduced very briefly in real options analysis by Dixit & Pindyck as barriers in stochastic processes (Dixit & Pindyck, 1994). A real options analysis application of first hitting time is incorporated into a study of migration

strategies of technical innovations by a firm (Grenadier & Weiss, 1997). First hitting time is used as the earliest time which a technical innovation arrives in the market. In their paper, the optimal stopping time is also used in the migration strategies. The only study related to climate change is a work from Saphores which shows that a lower reflecting barrier on the level of the stock pollutant may significantly impact the threshold of adoption policy (Saphores, 2004).

This research fills a gap in applying first hitting time in real options analysis with climate change. First hitting time is equivalent to the earliest stopping time. As such it can be considered an extreme event of a process. It can be used to answer the question, what is the earliest time to adopt CO2 reduction policy in view of uncertain events.

6.2 Analysis of First Hitting Time

First hitting time, also known as first passage time, first exit time, is the stopping time which a random motion process hits a boundary from below (upper boundary), or from below (lower boundary). It has many practical applications ranging from actuarial studies, nuclear physics, chemical processes and to financial options.

6.2.1 Probability Density Function of First Hitting Time

The probability density function of the first hitting time, *t*, is an Inverse Gaussian distribution (also known as Wald distribution) with two parameters: μ, mean, and λ, shape parameter. The Inverse Gaussian distribution is given by:

$$p(t;\mu,\lambda) = \sqrt{\frac{\lambda}{2\pi t^3}} \quad \exp\left[-\frac{\lambda}{2\mu^2 t}(t-\mu)^2\right] \qquad [1]$$

The inverse Gaussian is a skewed distribution, and like the log normal distribution, it converges asymptotically, that is, as $(\lambda/\mu) \rightarrow \infty$ the distribution of *t* is asymptotically normal with mean μ and variance (μ^3/λ). When the skewness is significant, the inverse Gaussian distribution is an alternative for lognormal, Weibull and gamma

distributions. The fat tails distribution suggests that there is a predominance of extreme events.

6.2.2 First Hitting Time Constant Barrier

The threshold in constant barrier is a fixed level (B) which can be above the current level (upper barrier, $X_0<B$) or below the current level (lower barrier, $X_0>B$). The lower barrier ($X_0<B$) approaches zero (non-negative) in most cases, but upper barrier ($X_0<B$) needs to be specified. As the CO2 emission process has a positive drift, only the upper barrier, $B>X_0$, is applicable.

The first hitting time of geometric Brownian motion is defined as:

$$T^* = \inf\left(t > 0; X_t = B\right) \qquad [2]$$

6.2.2.1 Probability of Hitting

The probability of first hitting (Pr) of a constant barrier (B) is:

$$Pr\left(X > B \mid X_0 \mid\right) = \exp\left[-\frac{2\left(\mu - \frac{1}{2}\sigma\right)\left(log\frac{B}{X_0}\right)}{\sigma^2}\right] \qquad [3]$$

The solution of first hitting time is based on reflection principle of the random motion at the barrier (Harrison, 1985; X. S. Lin, 2006) and solved using Fokker-Planck and Kolmogorov equations (D. R. Cox & Miller, 1965; Kwok, 2008).

6.2.2.2 Expected First Hitting Time

Expected first hitting time of an upper barrier $B>X_0$ is given by :

$$E\left[T^* \mid X = B\right] = \frac{1}{\left(\mu - \frac{1}{2}\sigma^2\right)} log\left(\frac{B}{X_0}\right) \qquad [4]$$

The geometric Brownian motion stochastic process with random variables defined by X^m, as $X^m_0, X^m_1, X^m_2 \ldots, X^m_n$ with $0<n<inf$ and $m>0$ has first hitting time of an upper barrier $B>X^m_0$ given by:

$$E\left[T^* \mid X^m = B\right] = \frac{1}{m}\frac{1}{\left(\mu - \frac{1}{2}\sigma^2\right)} log\left(\frac{B}{X^m{}_0}\right) \quad [5]$$

When $\sigma^2 = 2\mu$, the denominator becomes zero, and the expected hitting time is infinite. Therefore, the condition for a first hitting time solution is $\sigma^2 < 2\mu$.

Variance of first hitting time is given by:

$$var\left[T^* \mid X = B\right] = \frac{\sigma^2}{2\left(\mu - \frac{1}{2}\sigma^2\right)^3} log\left(\frac{B}{X_0}\right);$$

$$var\left[T^* \mid X^m = B\right] = \left[\frac{\sigma^2}{2\left(\mu - \frac{1}{2}\sigma^2\right)^3} log\left(\frac{B}{X^m{}_0}\right)\right]^{\frac{1}{m}} \quad [6]$$

6.2.3 First Hitting Time Moving Barrier

Let the threshold level be a moving barrier in the linear form, $B_m = \alpha t$, where α is linear slope of the barrier. There are two cases:

Case 1 $\alpha > \mu - 0.5\,\sigma^2$:

moving barrier and carbon emission path diverge, there is no hitting solution

Case 2 $\alpha < \mu - 0.5\,\sigma^2$:

moving barrier and carbon emission paths will almost surely converge

Expected mean and variance of first hitting time of a moving barrier is given by (Tuckwell & Wan, 1984):

$$E\left[T^m \mid X = B_m\right] = \frac{1}{\left(\mu - \frac{1}{2}\sigma^2 - \alpha\right)} log\left(\frac{B_m}{X_0}\right);$$

$$var\left[T^{m|} X = B_m\right] = \frac{\sigma^2}{2\left(\mu - \frac{1}{2}\sigma^2 - \alpha\right)^3} log\left(\frac{B_m}{X_0}\right) \quad [7]$$

Analytical solution of moving barriers for first hitting time is only known to be available for linear moving barrier.

6.3 Numerical Solution for Option Value in First Hitting Time

Although closed form analytical formulas are available for barrier options, these formulas are derived with linear payoff function. But in this research benefit function is non-linear (quadratic polynomial), therefore, these formulas could not be used. The methodology in this research is to use Monte Carlo numerical solution to obtain the option value. In this scheme, the social costs are obtained from simulated CO2 concentration paths. The first hitting time occurs when the social costs equal the reduction costs of the policy. The option price is obtained from $max(V_t - K, 0)$ in each path, and the average option value is the mean of all option values from the simulated paths. Compared with other studies described in Section 6.1.2, this methodology is flexible in that it allows the actual stopping time to be obtained.

6.4 Optimal Stopping Time for CO2 Reduction Policy

Optimal stopping time is a stopping time which is based on sequentially observed random variables of a Markov chain in order to maximize expected benefits or to minimize expected costs. It is the main feature in American option which allows the option holder the right to exercise the option at any time ("early exercise"). The flexibility in optimal stopping time can be incorporated in CO2 reduction policy so that adoption of policy is deferred until the option value, and also net benefit value, is maximum. This additional flexibility to adopt at any time has an added economic value to the CO2 reduction policy.

Optimal stopping time requires all sequential information of the possible paths during the option period, to be known in advance. Starting from the last period, the optimal stopping time is obtained by recursively working backwards searching for the

best solution in each preceding period. Since optimal stopping time allows adoption of policy to be deferred as long as possible, therefore, the optimal stopping time should be longer, if not equal to, than the first hitting time.

Under normal conditions, it is never optimal to exercise early an American call option. This feature arises from the linear payoff function in the financial option model. However, the CO2 emission model has a convex payoff function which allows early adoption for optimal stopping time.

6.4.1 Real Options with Optimal Stopping Time

The solution setup of optimal stopping time is similar to the perpetual time model. In the optimal stopping time problem the time dimension is non-homogenous whereas in perpetual time problem the time element is time invariant. Therefore the same principles are applicable for real options analysis in optimal stopping time.

In financial option theory and real options analysis, optimal stopping time is a free boundary problem. Here the free boundary, which is also the optimal boundary for adoption, is an unknown boundary curve (to be determined) which divides the domain ($0<x<\infty,\ 0<t<T$) and benefits of the policy ($0 < V < \infty$) into two parts: the No-Adopt (continuation) region, and the Adopt (stopping) region. This is similar to the concept of the perpetual time model (see Section 4.1).

Let the value of a project (policy) be V and reduction cost be K. When V is in the No Adopt region, the option value is greater than the payoff at adoption, $Option\ Value > (V - K)^+$, therefore the policymaker should continue to keep the option alive to avoid incurring costs and losses. When V is at the boundaries of the Adopt and No Adopt regions, the option value equals the payoff at adoption, $Option\ Value = (V - K)^+$, therefore, the policymaker should adopt the policy immediately to capture the benefits.

Since the policymaker can adopt any time, τ, during the option period, the option value is given by:

$$Option\ \ Value = sup\, E_{\tau}\left[e^{-r\tau}\, max\left(V_{\tau} - K\right), 0 \right] \qquad [8]$$

The above *suprenum* is reached at the optimal stopping time, τ^*, so that this is the first time the option value exceeds the net benefit (payoff) value:

$$t = inf\left[t \le \tau^* \le T : max\left(V_{\tau^*} - K\right), 0 \right] \qquad [9]$$

The solution of optimal stopping time is more difficult because the option value, at each time period, needs to be determined together with the value of the project *V*. In other words, the optimal boundary at adoption depends on both the time period and the value of the project *V*. Many studies have attempted to find a closed form analytical solution of the option value of optimal stopping time but there is no known solution to date.

6.4.2 Literature Survey of Optimal Stopping Time

Optimal stopping time is first studied by Wald in statistics for sequential probability ratio test (Wald, 1945), and its application is generalized by Snell (Snell, 1952). As the option value of optimal stopping time problem is the same as valuation of American option, this brief survey also includes American call option literature. The first mathematical analysis of the optimal stopping time is from McKean who consider the problem of a discounted American call option as a heat flow equation in a long uniform thin bar problem (McKean Jr, 1965). He shows that the stopping problem could be converted into a free boundary problem.

A more intuitive approach to the optimal boundary at adoption decomposes the American option value as the corresponding European option plus the gain from early adoption ("early exercise premium") (Jacka, 1991; Kim, 1990). The gain from early adoption is the present value of the benefits in the ADOPT region less the risk free interest losses on the costs incurred upon adoption.

Brennan & Schwartz describe a real options analysis study of a copper mine valuation involving several American type options (Brennan & Schwartz, 1985). They

solve the problem by backward induction using finite difference method of the partial differential equation. Subsequently, the copper mine valuation real options problem is analysed using Monte Carlo numerical simulation method (Cortazar, 2001; Sabour & Poulin, 2006). Their results from Monte Carlo method are compatible with finite difference method.

Certain real options analysis in a finite time horizon can be analysed using Black Scholes option formula (European options). However, real options analysis using Black Scholes option formula are strictly restricted to problems with a predetermined adoption time, for example, real estate leases and contracts with specified expiry dates. In most practical applications, the optimal stopping time is more realistic because it allows the policymaker to exercise any time.

As noted in the literature survey of previous chapters, studies involving real options analysis related to optimal stopping time are mainly limited to perpetual time problems. Therefore these studies are not realistic for investigating climate change problems which need urgent solutions. This research fills a gap in applying real options analysis for climate change problems to answer the question, what is the optimal stopping for adopting the CO2 reduction policy within a limited time horizon.

6.5 Numerical Solution for Option Value in Optimal Stopping Time

There is no closed form analytical solution for option value of optimal stopping time, but several approximate and numerical schemes are available to obtain the option value. A survey of American call option literature reveals four basic approaches to option valuation (Ahn, Bae, Koo, & Lee, 2011):

1. Analytical approximation methods

   Geske & Johnson (Geske & Johnson, 1984) propose using compound options. MacMillian (MacMillian, 1986), Barone-Adesi & Whaley (Barone-Adesi & Whaley, 1987) suggest using quadratic approximation.

2. Lattice Trees methods

   Cox, Ross Rubinstein (J. C. Cox, et al., 1979) propose binomial lattice method to discretized the Brownian motion. Trinomial tree method is another version of lattice tree method (Trigeorgis, 1996). The lattice tree method is used to generate the evolution of possible asset prices or values. The optimal solution of stochastic process is obtained by optimizing the final results and folding them in a backward recursive manner, as in dynamic programming, into the current decision.

3. Finite difference schemes

   Schwartz (Schwartz, 1977) propose using finite difference equations to approximate the partial derivatives. Forward difference, backward difference, or central difference schemes can be used in the solution. The finite differences can be made with Euler or Crank Nicholson discretization method.

4. Monte Carlo simulation method

   Boyle (Boyle, 1977) introduces Monte Carlo simulation method to obtain value of financial options. This method is well suited to handle multi-dimensional problems which could be difficult for lattice trees and finite differences methods.

In summary, lattice tree method is easy to implement but it has difficulty in handling multi-dimensional problems. The computation can get unmanageable when there are too many branches in a complex problem. The finite difference method is suitable when the problem can be setup as a mathematical model (Duffy, 2006). Monte Carlo is a flexible method for handling complex problems but it requires computational resources and power (Glasserman, 2004).

6.6 Monte Carlo Numerical Solution for Real Options Analysis

Monte Carlo numerical method is one of the popular numerical solution method for optimal stopping time problem because of its flexibility in handling many dimensions, and various type of stochastic processes and boundary conditions.

6.6.1 Procedure of Monte Carlo Simulation Paths

The general procedure for generating Monte Carlo paths is:

Step 1 Initialize parameters

drift (μ), volatility (σ), time period (T), number of sub periods (N), and $dt = T/N$.

Step 2 Generate random variate (dz) with normal distribution $N(0,1)$ for each period at each sub period.

Step 3 Compute value of the project, V_t , at each sub period

$$V_t = V_{t-1}\, exp\left(\left[\mu - 0.5\sigma^2\right]dt + \sigma\sqrt{dt}\right)$$

Step 4 Continue with Step 2 until end of time period.

The efficiency of a Monte Carlo scheme can be greatly enhanced through the use of various variance reduction techniques in generating the random paths such as variance reduction, antithetic variates, control variates, and low discrepancy sequences (Glasserman, 2004).

6.6.2 Optimal Stopping Time Numerical Solution

Monte Carlo numerical solution method for optimal stopping time or American option poses a special problem in determining the optimal time for stopping (adoption) on each path. The no adoption (continuation) value of the option at that instance is unknown because of the free boundary condition. To solve this problem, several schemes have been proposed for the American option problem. These schemes include bundling and sorting algorithm (Tilley, 1993), dimension reduction bin technique (Barraquand & Martineau, 1995), Broadie & Glasserman algorithm

(Broadie & Glasserman, 1997), and, least squares regression method via basis functions (Longstaff & Schwartz, 2001).

The bundling and sorting algorithm approximates the early adoption boundary based on average future values (Tilley, 1993). At each instance, the price levels of all paths are reordered and grouped into a number of bundles/bins. The continuation value is computed as the average of present value of future cash flows for the bundle/bin. Broadie & Glasserman method is to find the upward and downward biased price estimators and find confidence intervals which reduce to a point estimate asymptotically as the number of simulation paths increases (Broadie & Glasserman, 1997).

Longstaff & Schwartz propose to use a set of basis functions to approximate the continuation value. At each instance on each simulation path, the discounted future value is regressed against basis functions to obtain an approximate analytic form, and the adoption decision is made by comparison with the current intrinsic value and the value of the approximate analytic form of the continuation value (Longstaff & Schwartz, 2001). The method, also known as least squares Monte Carlo (LSMC), starts the analysis at the final time period. The value of continuing to hold the option past the current time period is determined by the least squares technique from regression. All paths that would return a profit in the current time period are regressed to form a single function that gives the value of continuing to the next period. Then, each path that is in the money is evaluated using the function to determine if the option should be exercised at the current time period or held to a future date. Finally, the algorithm moves to the next previous time period and continues the analysis. The algorithm of LSMC is summarised in Appendix 6.

Monte Carlo numerical solution method has been successfully implemented and reported in several papers. Cortazar uses the dimension reduction bin technique for American options in the copper mine problem (Brennan & Schwartz, 1985; Cortazar, 2001), while Sabour & Poulin use the least squares method in the same

problem (Sabour & Poulin, 2006). Alessi investigates the application of least squares method for real options analysis in multi dimensions problems (Alesii, 2008).

Currently there is a research gap in the application of LSMC in real options analysis. The methodology of using LSMC in real options analysis in this research is novel, especially in climate change studies. This requires writing computer codes from scratch to ensure that the programming solution perform to specifications. In this research, MATLAB programming is used in the numerical solution.

6.7 Illustration of Real Options Analysis Values

The numerical example is an illustration of the application of two different stopping times for analyzing option values for CO2 concentration abatement. The results are obtained by Monte Carlo numerical solution, and optimal stopping time by LSMC.

(CO2 ppm)	First Hitting Time	Optimal Stopping
Discount Rate, % pa	4.0%	4.0%
Duration Time Period, years	500	500
Original social benefits, *Vo*	149,916	149,916
Reduction Policy (20% reduction of CO2 concentration level)		
Reduction Cost, (C), CO2 ppm	87,234	87,234
Stopping Time, years	136	159
Decomposition of Option Values, CO2 ppm		
Benefit Value at Exercise V*, (B)	87,582	106,175
Net Payoff, (A) = (B) - (C)	348	18,941
PV of Option Value (Option to Defer)	1.48	28

Table 6-1 Analysis of Values in First Hitting Time and Optimal Stopping Time

Table 6.1 shows that first hitting time is earlier than optimal stopping time. Furthermore the benefit value at optimal stopping time is higher than first hitting time because the uncertainties in first hitting time are smaller than optimal stopping time. By discounting net benefit payoff in first hitting time to its present value, the option value is obtained. In the case of optimal stopping time, the option value has to be found in each period and discounted to year 500.

6.8 Analysis and Discussion

To complete the above numerical example, the reduction cost is now varied from $8.00x10^4$ ppm CO2 up to maximum value of $8.00x10^6$ ppm CO2.

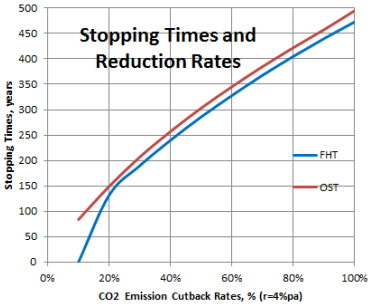

Figure 6-1 First Hitting Time and Optimal Stopping Time - Stopping Times

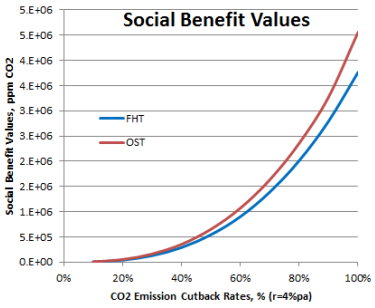

Figure 6-2 First Hitting Time and Optimal Stopping Time - Benefit Values

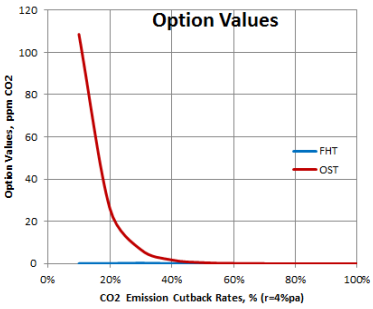

Figure 6-3 First Hitting Time and Optimal Stopping Time - Option to Defer

First Hitting Time and Optimal Stopping Time for CO2 emission cutback
0-100% CO2 emission cutback, discount rate 4%pa, finite time horizon 500 years

For stopping times (Figure 6.1), the first hitting time curve is always below the optimal stopping time, because optimal stopping time has the flexibility to delay adoption whereas the first hitting time is the earliest time for adoption of policy. Furthermore the optimal stopping time method produces higher benefit values than first hitting time with the same cost of reduction (Figure 6.2). The rate of change of stopping times with reduction cost is the greatest when the reduction costs are low, while, the same rate of change is almost linear for reduction costs above $4x10^6$ ppm CO2. For example, reduction costs decrease from 2 $x10^6$ ppm to zero ppm CO2 the stopping times decrease about 120 years. At the other end, the same reduction costs from 8 $x10^6$ ppm CO2 to 6 $x10^6$ ppm CO2 result in 70 years decline.

Furthermore the option values in optimal stopping time is very large at low reduction cost but decreases rapidly when the reduction costs become larger (Figure 6.3). This implies is that low reduction costs have low opportunity costs of waiting, high incentive to defer adoption, and high flexibility for the policymaker. In contrast

the option value in first hitting time is relatively insignificant, that is, there is little flexibility in first hitting time for the policymaker.

6.9 Recommendations for the Policymaker

The policymaker could apply the concepts of first hitting time and optimal stopping time in formulating CO2 reduction policies.

First hitting time is a conservative policy which requires the policy to be implemented once the CO2 concentration level reaches a threshold level. It is easy to understand and simple to implement. The policymaker only needs to monitor the CO2 concentration level to alert him of the adoption event. The disadvantage is that it may not be the most cost effective policy.

Optimal stopping time is a rationale economic policy which allows for “best decision” after considering all possible future outcomes. It is difficult to apply in practice because the policymaker is required to make many assumptions. Also, the “best decision” may not be the most practical solution. However, it does provide the most cost effective solution.

7. CO2 REDUCTION POLICIES IN FINITE TIME

The perpetual time model in Chapters 4, 5 and 6 are useful for understanding the characteristics and behaviour of CO2 reduction policies with real option. It demonstrates the flexibility produced by real options in deciding how soon to adopt reduction policies, and how catastrophe events should be planned. As the perpetual time model also assumes infinite resources availability in infinite time, the stopping times for policy adoption are unrealistically high of practical use. Therefore it is necessary to constraint the time for adoption of the policy so that useful results could be obtained for the policymaker.

This Chapter looks into greater details CO2 reduction policies with the first hitting time and optimal stopping time. It re-investigates the same research questions as in Chapter 4 but in finite time. In addition, there is no known application of Monte Carlo numerical method with LSMC solution to obtain the solutions for optimal stopping time in real options analysis. This research fills a research gap in the application of LSMC in real options analysis.

7.1 CO2 Reduction Cost Function

The four important factors in climate change policy analysis are CO2 emission rate, CO2 concentration level, temperature increase, and cost function of CO2 reduction. Of these four factors, the reduction cost function is, perhaps, the most subjective because valuation of environmental damages and forecasting technology innovation are very difficult.

In this research a convex cost reduction function is used because it is able to optimize the solution of CO2 reduction policy. A convex cost function is a monotonic increasing function, that is, it is convex downward (or concave upwards). The first derivative of the function is positive, that is the slope is increasing, and the second derivative is greater than zero. In neoclassical economic theory, the Arrow Debreu

model employs convex cost functions or concave production functions. It allows buyers to maximize their utility and benefits, and producers to make units of a good so that the cost of producing the incremental or marginal unit is just balanced by the revenue it generates.

7.1.1 Survey of Cost Reduction Functions

Cline identifies two categories of cost abatement function for carbon abatement (Cline, 2011). They are the top down models and bottom up models. Examples of top down models, in which the carbon abatement are based on economy performance, are Nordhaus's RICE (Nordhaus, 2010) model and EMF 22 (Energy Modelling Forum, Stanford University) models. The bottom up models, such as McKinsey model (McKinsey, 2009), focus on the abatement costs of specific energy industries. This research focuses on global climate change environment, therefore, the top down model is more appropriate.

According to Cline, the power function equation of the total cost of carbon abatement in the RICE model is

$$Total\,Cost\ of\ Abatement = \alpha_t \mu_t^{2.8}\,\mathrm{GDP}_t \qquad [1]$$

where μ_t denotes the future CO2 emission rate, GDP_t denotes the forecast gross domestic product, and α_t denotes a multiplicative factor that declines over time to reflect the widening choices of technological alternatives. In its form in equation [1], the cost function also requires forecast of future GDP. The power parameter has been found to be fairly constant over various time periods and countries.

7.1.2 Proposed CO2 Reduction Cost Function

For this research, an effective CO2 reduction cost function should be able to provide a feasible solution to the CO2 reduction problem. If the reduction cost is too high relative to benefit values, the reduction policy will never be adopted. On the other hand, setting a very low exercise cost relative to benefit values will not result in any deferment option because the policy will be adopted immediately and are no

interesting results. In the last case, using benefit cost analysis is sufficient for the problem.

The top down reduction cost function in equation [1] is a function of time and economic activity. However the CO2 emission model is a one factor stochastic model. Introducing a time dimension in the reduction cost function will make the CO2 concentration model more complex and real options analysis more difficult to solve in continuous time. Therefore, two assumptions are used in the proposed cost reduction function to simplify the analysis.

The first assumption is that the reduction policy must be adopted sometime within the time horizon of the policy. For example, a fixed budget of reduction costs can be set based on the final benefits targeted to be achieved at the end of the duration time period. The policymaker is required to adopt the policy within this time period. But there is possibility that the adoption could be earlier if the CO2 concentration level increases at a faster rate.

The second assumption is to simplify the cost function to a modified form which is similar to equation [1]:

$$K = c_1 R^{2.8} \qquad [2]$$

where *K* denotes cost of reduction, *R* denotes the percentage reduction CO2 concentration level, c_1 denotes a parameter which is depends on total reduction cost of adopting the policy at a specific time period. In other words, an increase in percentage of CO2 concentration requires a non-linear increase in reduction cost.

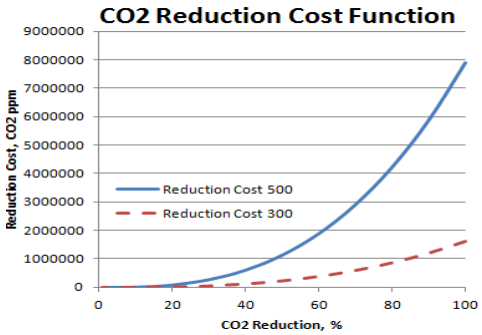

Figure 7-1 CO2 Cost Reduction Function

To calibrate the cost function in equation [2], it is assumed that there is 100% reduction in a period of 500 years. At year zero, the reduction cost of CO2 emission is 1.50×10^5 ppm CO2 and at end of year 500, the social of CO2 emission is 8.00×10^6 ppm CO2 (see Section 4.6.2), that is, a net total reduction of 7.86×10^5 ppm CO2 is required. Substituting this in equation [2], c_1 parameter is 19.85:

$$K = 19.85R^{2.8} \qquad [3]$$

This reduction cost function will be used in all investigations of finite time CO2 reduction policy in Chapters 7, 8 and 9.

The reduction costs used of real options analysis with climate change in the literature surveyed in Section 2.3 assume predetermined fixed costs based on certain assumptions in their problems. In one of the studies a cost reduction function based on GDP projections is used to produce a range of reduction costs (Makropoulou, et al., 2008). In this research the proposed cost reduction function is easier to apply because it does not require additional forecasts of other variables such as GDP or population growth.

7.2 Numerical Example of CO2 Reduction in Finite Time

In Chapter 4 the perpetual time model was used to investigate CO2 reduction policies, this Section now continues with CO2 reduction policies with finite time model using different discount rates.

The benefit value and value of CO2 reduction policy are obtained as follows:

	CO2 emission cutback	CO2 conc abatement
Reduction Rate	*m* m=1 for 0%, m=0 for 100%	*n* n=1 for 100%, n=0 for 0%
Original social cost value without reduction	$V = X_0^2$	$V = X_0^2$
Reduced social cost value after reduction	$V_e = X_e^2$	$V_e = (1-n) X_a^2$
Benefit value from CO2 reduction	$V - V_e$	$V - V_e$
Value of reduction policy, Option to Defer value	$V - V_e - K$	$V - V_e - K$
Remarks	X_e is CO2 conc level at time, t, with reduced CO2 emission rate from μ to $m\mu$	X_a is CO2 conc level at time, t, with reduced CO2 concentration level at (1-n%)

Table 7-1 Calculation of Benefit Value and Option Value

Note that at adoption time the net benefit equals value of CO2 reduction policy. The same methodology can be used for a mixture of multiple gases (see Appendix 7 for more details).

The parameters used in the numerical example are:

CO2 emission model	Geometric Brownian motion
Reduction cost function	Equation [3]
Duration time period	500 years
Discount Rates, *r*	0.5 to 10% pa
Maximum reduction cost	8.00×10^6 ppm CO2 (100%)
Reduction rates	10% to 100%
Solution Methods	
First Hitting Time	Monte Carlo numerical solution
Optimal Stopping Time	Monte Carlo numerical solution (LSMC)
Numerical Simulation	
Method	Euler discretization
Number simulated paths	10,000
Time sub-period	1 year

For studying the cost effectiveness of CO2 emission cutback and CO2 concentration abatement, the reduction cost is assumed to be the same at each level of reduction in both cases.

7.3 Analysis and Discussion - CO2 Concentration Abatement

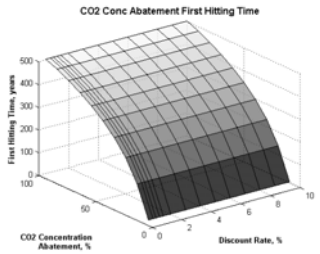

Figure 7.2a
Stopping Time - First Hitting Time

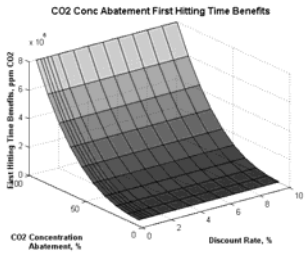

Figure 7.2c
Benefit Value - First Hitting Time

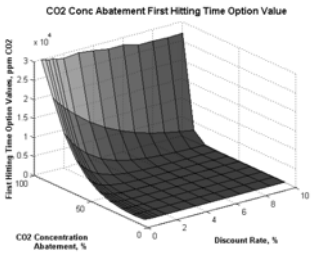

Figure 7.2e
Option Value - First Hitting Time

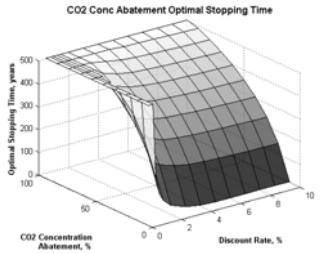

Figure 7.2b
Stopping Time - Optimal Stopping Time

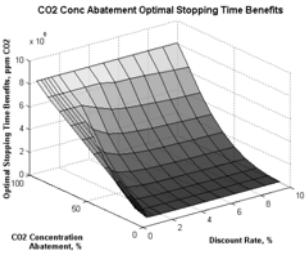

Figure 7.2d
Benefit Value - Optimal Stopping Time

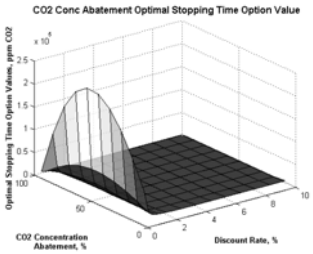

Figure 7.2f
Option Value - Optimal Stopping Time

Figure 7-2 CO2 Concentration Abatement and Discount Rates

7.3.1 Stopping Times

When reduction rates increase (Figure 7.2a and 7.2b), stopping times increase as higher reduction costs require higher benefits which could only be attained at later dates when CO2 concentration levels are higher. Both stopping times have convex shaped upwards with increasing reduction rates, otherwise the effect of higher discount rates is relatively flat for both first hitting time and optimal stopping time. For optimal stopping time, the stopping times are more sensitive at very low discount rates as can be seen in the upturn corner in Figure 7.2b.

7.3.2 Value of Benefits

Benefit values increase rapidly with reduction rates (Figures 7.2c and 7.2d), in order to match higher reduction costs, but there is little impact from varying discount rates. Also, low discount rates for optimal stopping time provide higher benefit values than higher discount rates. The suggests that there is no difference in benefits received when the discount rate is high but at low discount rate the optimal stopping time provides the highest benefit values at adoption of policy.

7.3.3 Option to Defer Values

In general, first hitting time option value (Figure 7.2e) is much lower than optimal stopping time's (Figure 7.2f). Larger option values are obtained at high CO2 concentration abatement rates, but discount rates have a smaller impact than CO2 concentration abatement rates. The implication is that the policymaker should set the 100% reduction rate in CO2 concentration abatement. With this reduction rate the policymaker have the maximum flexibility to adjust the reduction rates lower.

The option value of optimal stopping time is highest at low discount rates. For high discount rates the option value is zero except when the CO2 reduction rates are low. This suggests that there is high flexibility when discount rates and reduction rates are low because of low opportunity costs and low reduction costs.

7.4 Analysis and Discussion - CO2 Emission Cutback

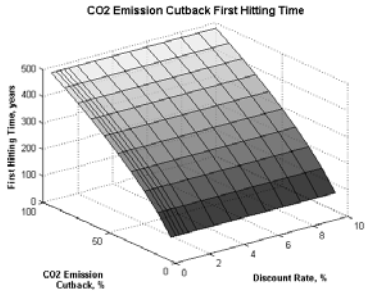

Figure 7.3a
Stopping Time - First Hitting Times

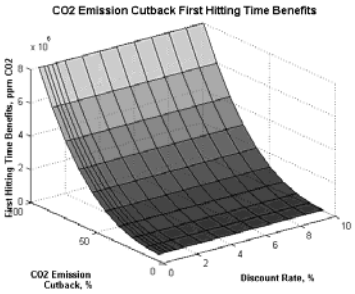

Figure 7.3c
Benefit Value - First Hitting Times

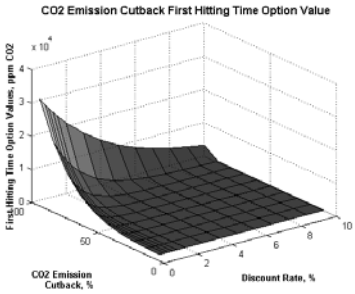

Figure 7.3e
Option Value - First Hitting Times

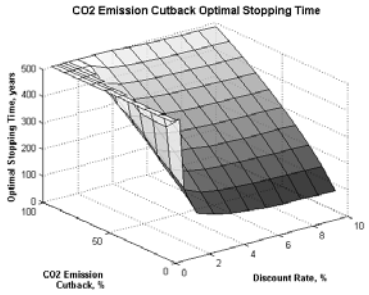

Figure 7.3b
Stopping Time - Optimal Stopping Time

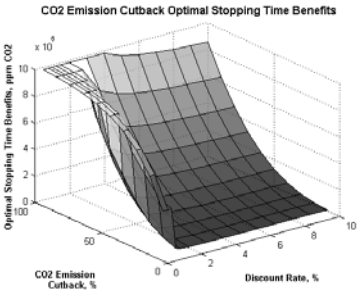

Figure 7.3d
Benefit Value - Optimal Stopping Time

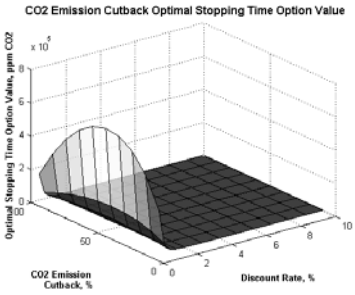

Figure 7.3f
Option Value - Optimal Stopping Time

Figure 7-3 CO2 Emission Cutback and Discount Rates

7.4.1 Stopping Times

The two stopping times increase with CO2 reduction rates. In first hitting time the stopping times are almost constant at a particular CO2 reduction rate for all discount rates (Figure 7.3a). In optimal stopping time the stopping time is largest at very low discount rates and CO2 reduction rates (Figure 7.3b). This indicates that adoption of policy can be deferred for a longer time when the discount rates are low, and especially at low CO2 reduction rates

7.4.2 Benefit Values

In general, the benefit values of optimal stopping time are higher than first hitting time, and increase with CO2 reduction rates (Figures 7.3c and 7.3d). However, the benefit value of optimal stopping time is largest at low discount rates. This is the result of low discount effect and also the increase in CO2 social benefit caused by deferment of policy adoption.

7.4.3 Option to Defer Values

The option value of first hitting time is small (about 10 times smaller) compared with optimal stopping time option value (Figure 7.3e). As expected this indicates that the policymaker has higher flexibility with optimal stopping time than first hitting time. Both low discount rates and high CO2 emission cutback rates produce higher option values. These results are similar as in the perpetual time model.

The option value in optimal stopping time shows the highest value at low discount rates and peaks around 50% CO2 reduction rates (Figure 7.3f). The low discount rate and low opportunity cost creates incentive to defer adoption. This suggests that the optimal reduction rate in optimal stopping time is 50%. At this rate the policymaker has maximum flexibility to adjust the policy rate upwards or downwards.

The option value in CO2 emission cutback (Figure 7.3f) is much larger (10 times larger) than CO2 concentration abatement's option value (Figure 7.2f). Again this indicates that CO2 emission cutback has higher flexibility than CO2 concentration abatement.

The feature of the option value plot in Figure 7.4 is identical to a European call option (vanilla call option) (Figures 7.5 and 7.6). However option values in optimal stopping time have larger values than European call option because of the flexibility of adopting the policy at an earlier time.

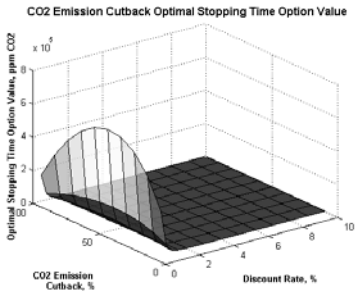

Figure 7-4 Option Value - Optimal Stopping Time of CO2 Emission Cutback

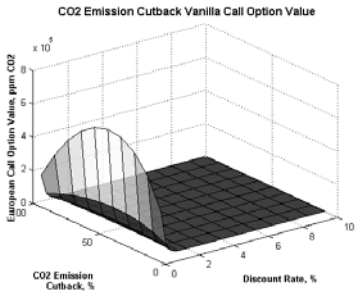

Figure 7-5 European Call Option of CO2 Emission Cutback

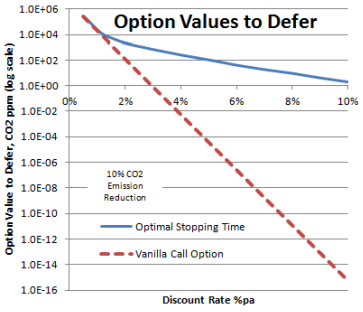

Figure 7-6 10% CO2 emission cutback

7.5 Evaluation of CO2 Reduction Policies in Finite Time

The two CO2 reduction policies with optimal stopping time (Sections 7.3 and 7.4) are compared and analysed to highlight the interesting features and differences.

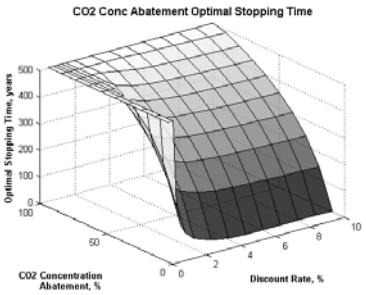

Figure 7.7a
Optimal Stopping Time

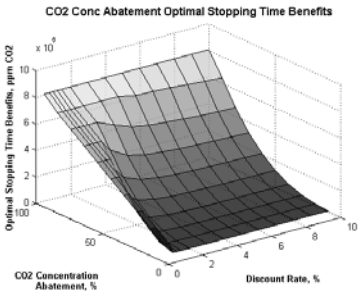

Figure 7.7b
Benefit Value

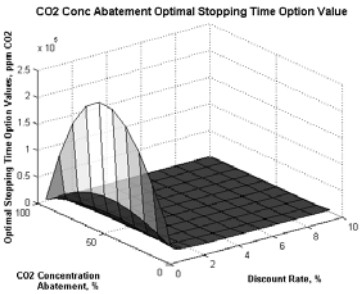

Figure 7.7c
Option Value

Figure 7-7 CO2 Concentration Abatement Policy with Optimal Stopping Time

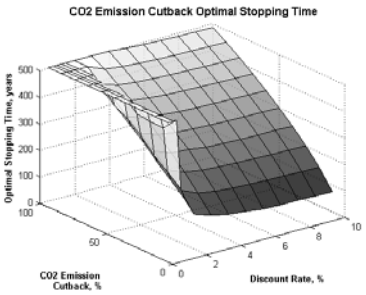

Figure 7.8a
Optimal Stopping Time

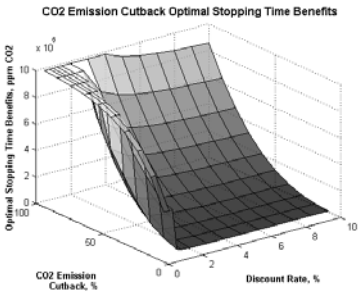

Figure 7.8b
Benefit Value

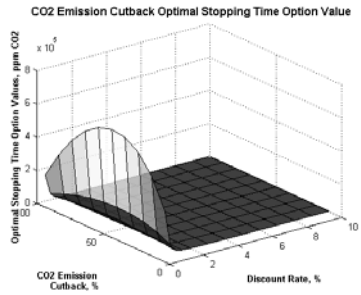

Figure 7.8c
Option Value

Figure 7-8 CO2 Emission Cutback Policy with Optimal Stopping Time

Figure 7.8a shows that the stopping times at low discount rates in CO2 emission cutback are larger than CO2 concentration abatement (Figures 7.7a and 7.8a). However this feature reverses when the discount rates increases at high discount rates; the CO2 concentration abatement stopping time (Figure 7.7a) is more convex upwards than CO2 emission cutback (Figure 7.8a). This implies at low discount rates that the implementation time of CO2 concentration abatement policy is earlier than the CO2 emission cutback policy, and vice versa.

The benefit values at stopping time of CO2 emission cutback are higher than CO2 concentration abatement (Figures 7.7b and 7.8b). This is evident in the higher values at the upper edges of the plot in Figure 7.8b. This suggests that higher

benefits from reduction policy are obtained at low discount rates with CO2 emission cutback, but these benefits are achievable only when the reduction policy is adopted at larger stopping times.

Finally the option values of CO2 emission cutback (Figure 7.8c) are larger than CO2 concentration abatement (Figures 7.7c) - the maximum option values are $5x10^5$ ppm CO2 and $1.8x10^5$ ppm CO2 respectively. This suggests that the flexibility to adopt CO2 emission cutback policy is higher than CO2 concentration abatement policy at low discount rates.

7.6 Recommendations for the Policymaker

A policymaker with a fixed budget of reduction cost and time frame to act can make his decision using two methods.

If the policymaker is conservative, he can use the first hitting time method. In this method, the policymaker sets a target CO2 concentration level which he will monitor closely. Once the target level is reached the policymaker implements the policy. For the policymaker this is easiest and simplest method.

If the policymaker is faced with many constraints and options, the optimal stopping time method is the alternative solution. He can justify the implementation by choosing the most favourable and cost effective conditions to implement the policy. However, he has to make certain assumptions about the future states of the problem and make recursive deductions to justify his decision.

The optimal stopping times can be in interpreted in terms of CO2 concentration level or actual time. As there is uncertainty in the timing in the stochastic process, it is recommended that the policymaker also monitors CO2 concentration level. The policy is implemented at the actual time or when CO2 concentration level is reached, whichever is earlier. Sometimes the policymaker may find this method difficult to apply because the optimal stopping time is unrealistically

long or the conditions at implementation time are not feasible. Therefore the policymaker should always be prudent and take a precautionary attitude to avoid waiting for too long to act.

The best CO2 reduction rates depend on stopping time methods and not on the reduction policies. For maximum flexibility the policymaker should set the reduction rate as follows:

- first hitting time policy should set the reduction rate at 100%. From this maximum reduction rate the policymaker has the maximum flexibility to adjust the policy downwards.
- optimal stopping time policy should set the reduction rate 50%. From this optimal reduction rate the policymaker can adjust the reduction rate upwards or downwards.

A compromise and balanced approach for the policymaker is to implement the policy using the first hitting time method. The implementation will take some time to take effect and complete, and in the meantime, the CO2 concentration level continues to increase in the atmosphere, even the CO2 emission has ceased. So by the time the CO2 concentration level stabilizes, the optimal stopping time would have been reached.

The policymaker can also apply the results in this research with other approaches in climate change analysis. For example, an increase in temperature implies that CO2 concentration level also increases. This suggests that the potential benefits of reduction policy will also increase, and an early adoption of policy is suggested. If there is 10% probability of the temperature increase, the policymaker could decide to adopt the policy now and enjoy the accompanying benefits that come along with the adoption. These benefits may include better health and less medical costs, protected clean environment, sustainable economy growth, and sufficient food resources. Alternatively, the policymaker may defer the adoption and wait for the 90% of the information to confirm and realize the temperature increase. However, by

deferring the adoption, the policymaker would take the risk that the benefits will disappear and he would be a worse condition than adopting the policy now.

8. CO2 REDUCTION AND RARE EVENTS

In recent years, there have been more catastrophe events in nature, and global climate becomes increasing unpredictable. Moreover, the changes in climate events are also more intense and severe. These result in great economic losses and fatalities (IPCC SREX, 2012).

The CO2 emission model in Chapters 4, 6, and 7 is a continuous time stochastic process. This model is satisfactory for normal events when there are no large or abrupt changes in the process. In nature, there are rare occasions (remote possibilities) of major climatic catastrophes. To investigate these rare events, a discontinuous stochastic process is necessary. In Chapter 5, a jump diffusion model in perpetual time is described with the discontinuous process modelled in Poisson process. This Chapter continues with development of a finite time jump diffusion model and a modified numerical solution is used to generate Monte Carlo simulation paths. First hitting time is used to illustrate the application in this jump diffusion model.

8.1 Jump Diffusion Model in Finite Time

Merton proposed a finite time jump diffusion model for financial options by combining a Brownian motion and Poisson process (Merton, 1976). Merton's paper outlined a general solution equation for option pricing with lognormal jump size distribution but a closed form analytical solution is not available except for two special cases. In his paper, Merton assumes that the jumps are non-systematic risk and are uncorrelated with the market. Therefore, the complete market assumption still holds if the solution is limited to the opportunity set of strategies within the defined problem.

In this research, the jump diffusion model assumes that a complete market exists for a derivative asset to hedge the risk. These non-systemic risks in the jumps are diversifiable, and the remaining risk is market risk in the portfolio. Copeland &

Antikarov employ the same argument for real options which they call marketed asset disclaimer (MAD) (Copeland & Antikarov, 2001). MAD asserts that the project itself, without the real option, can be considered as the marketable asset. In constructing the risk free portfolio, the most suitable security is one that is highly correlated with the underlying project and information is easily available. Therefore the project is the only unique asset which satisfies these criteria.

8.1.1 Mathematical Model

Brownian motion is a continuous time process which is characterized by drift and diffusion components. A discontinuous process is usually represented by Poisson jump process which indicates the sudden arrival of jump events. When these jump events have random magnitudes, or jump sizes, it is called a compound Poisson process. A jump diffusion process can be constructed by combining a Brownian motion continuous process and a compound Poisson discontinuous process.

Jump Diffusion Process = Brownian Motion + Poisson Process

= Drift + Diffusion + Jump Events [1]

The jump diffusion model comprises 3 types of uncertainties: uncertainty in paths of normal random events (volatility or diffusion), arrival time of jump events (frequency of events), and magnitude of jump events (jump sizes). It is assumed that the jump diffusion process is everywhere right-continuous and has left limits everywhere (RCLL), or *càdlàg*. The geometric Brownian motion is given by:

$$dX = \mu X dt + \sigma X dz \qquad [2]$$

where *X* denotes the CO2 concentration level, *Z(t)* denotes a random variable with normal distribution *N(0,1)*, that is mean μ is zero and variance σ^2 is 1.

The discontinuous process comprises two components:

1 A pure Poisson point process, also known as a counting process, which indicates the $N(t)$ number of jumps in a fixed interval of time, with λ the arrival rate or intensity of the jumps;

2 A compound Poisson process, also known as marked point process, is the realization of the Poisson process $N(t)$ together with the respective jump size Y_i. The compound Poisson process is given by $J(t) = \sum_{i=1}^{N(t)} Y_i$.

The jump diffusion process is obtained by adding the two independent processes:

$$\frac{dX}{X} = (\mu - \lambda k)dt + \sigma dz + dJ \qquad [3]$$

$$\frac{dX}{X} = (\mu - \lambda k)dt + \sigma dz + \int_R Y(J)N(dt, dJ) \qquad [4]$$

Equation [4] is a partial integral differential equation.

Rewriting the above equation as

$$\frac{dX}{X} = (\mu - \lambda k)dt + \sigma dz + d\sum_{j=1}^{N(t)} (Y_j - 1) \qquad [5]$$

where Y_i denotes the ratio of benefit values $\frac{X_t}{X_t^-}$ after and before the jump, and $k = \varepsilon(Y - 1)$ denotes the expected value of Y_i.

Note that the expected mean of the new jump diffusion process is now $(\mu - \lambda k)$, the subtraction of λk is to compensate for the drift from the Poisson process to maintain risk neutrality.

A general explicit closed form solution for finite time for equation [5] is not known to exist. Two difficulties in the solution are the effect of time dimension in the solution process, and random jump sizes in the compound Poisson process which needs to be integrated in the PIDE (partial integral differential equation) before solving the differential equation. Numerical solutions are frequently employed to

solve jump diffusion problem. One numerical scheme is to discretize the process using Euler discretization scheme. The CO2 concentration level can then be expressed in the following form:

$$X_{i+1} = X_i \exp^{\left\{\left(\mu-\frac{1}{2}\sigma^2\right)(t_{i+1}-t_i)+\sigma[Z(t_{i+1})-Z(t_i)]\right\}} * \prod_{j=N(t_i)+1}^{N(t_{i+1})} Y_j \quad [6]$$

Alternatively, set *X(t)* to follow a log normal process and obtain a simpler expression for path simulation in Monte Carlo simulation by Euler discretization scheme:

$$X_{i+1} = X_i + \left(\mu - \frac{1}{2}\sigma^2\right)(t_{i+1} - t_i) + \sigma[Z(t_{i+1}) - Z(t_i)] + \sum_{j=N(t_i)+1}^{N(t_{i+1})} \log Y_j \quad [7]$$

From Ito calculus, $Z(t_{i+1}) - Z(t_i) = \sqrt{t_{i+1} - t_i}$, *J* is the Poisson process with intensity *λ*. *J=1* when there is a jump event with probability *λ*, *J=0* when there is no jump event with probability *(1- λ)*. This discretized form in equation [7] can now be used for generation of simulated paths in Monte Carlo numerical simulation.

8.1.2 Literature Review

Cox & Ross describes an early jump diffusion model is based on a binomial lattice method with Poisson jumps in discrete time (J. C. Cox & Ross, 1976). Merton's jump diffusion model combines both continuous time process with compound Poisson process (Merton, 1976). Subsequent extensions to Merton's model are mainly in the treatment of the jump size distribution. These include mean reverting jumps and single jump process (Ball & Torous, 1983), normally distributed jumps with stochastic volatility (Bates, 1991), normal density jumps (Hanson & Westman, 2002), asymmetric log double exponential jumps (S. G. Kou, 2002; S.G. Kou & Wang, 2003, 2004), log double uniform jump (Zhu & Hanson, 2005), double Rayleigh and double uniform model (Synowiec, 2008), and mixed exponential jumps (Cai & Kou, 2011). Among these models, Kou & Wang's double exponential model

can handle both up and down simultaneously and has some closed form analytical solutions (S.G. Kou & Wang, 2004).

Another recent approach is to use the more generalized Levy process which includes Brownian motion and Poisson process. The characteristics of Levy process are infinite number of jumps in continuous time intervals, homogenous and independent increments, and no drift component (Cont & Tankov, 2008). Levy process is gaining popularity because of the flexibility in modelling various distributions and processes; for example, the double exponential model use Levy process.

As for first hitting time with jump diffusion model, there are not many literatures focusing in this topic. Tuckwell & Wan outline a partial integral differential equation without providing a closed form solution (Tuckwell & Wan, 1984). Kou & Wang provide a closed form analytical solution for double exponential distribution jump sizes (S.G. Kou & Wang, 2003). Atiya & Metwally propose a Monte Carlo method with importance sampling for first hitting times with jump events (Atiya & Metwally, 2005).

There are many studies of option pricing with jump diffusion from financial option pricing. However the application of jump diffusion in climate change studies is lacking. This research fills a gap in investigating and answering the research question, what is the probability density function of CO2 concentration level when there is sudden change of CO2 emission rate. The answers will provide better understanding of the probability of loss damages from climatic catastrophe events.

8.2 Numerical Solution of Jump Diffusion Process

When the jump diffusion problem can be represented mathematically in partial integral differential equations and associated boundary conditions, then it could be solve by one of the finite difference methods, such as implicit difference,

explicit difference, or central difference (Duffy, 2006). However the difficulty with finite difference method is the construction of matching mesh between the integration and differentiation boundary. Furthermore the finite difference method cannot indicate the actual stopping time of policy adoption; it can only provide the CO2 concentration level at stopping time.

Lattice tree method is a flexible numerical method for derivative pricing. Cox et al outline the binomial tree method for optimal stopping time (J. C. Cox, et al., 1979). Amin approximates the jump-diffusion process by a multinomial lattice. However the large number of branches at each node make the lattice inefficient (Amin, 1993). Hilliard & Schwartz propose matching the first local moments of the lognormal jumps (Hilliard & Schwartz, 2005). At each sub period, the random path is decomposed into a diffusion component and jump component sequentially. The two weakness of lattice tree method are solving multi dimension problems and improving accuracy with more sub-periods. These will result in many branches and nodes, and the whole scheme becomes unmanageable.

In Chapter 7, Monte Carlo numerical solution, together with least square regression basis method (LSMC), is shown to be able to obtain results in finite time non-jump models. This Chapter continues to explore using LSMC methodology for jump diffusion models in finite time.

There are two methods for generating random paths in Monte Carlo simulation (Glasserman, 2004). The first method is simulating jump times or inter-arrival time. This requires finding the times which the jump events occur and then interpolating the continuous random path between these jump times with Brownian bridge. Atiya & Metwally apply the inter-arrival time method to determine the first hitting time (Atiya & Metwally, 2005). The second method is simulating at fixed dates. This requires partitioning the simulation period into several fixed dates and the jump and diffusion processes are simulated at these fixed dates with Euler time discretization method. Forward events are generated sequentially, and each period

is tested for jump events, and jump sizes are generated whenever there is a jump. Between the two methods, the inter-arrival time method is very efficient for generating random paths of rare events because the number of jumps is small and it is not necessary to test for jump event in every sub period. Appendix 5 presents the results of a study to compare the efficiency of these two methods.

8.2.1 Simulating Fixed Time Discretization Method

The fixed time discretization method is a straight forward method performed explicitly on the stochastic differential equation [6]. The process is subdivided into equal time periods, and in each sub period a new value and number of jump events are obtained. In each jump event, the jump size is found and the new value is updated with the jump size. This method is able to produce accurate results by having more sub-period divisions that is decreasing the time period in each sub division.

Basic Algorithm

Step 1 Simulate a Poisson variable N with jump intensity parameter λ

Step 2 Simulate random samples of jump size $Y_1, \ldots, Y_N$ with probability distribution f_Y

Step 3 Simulate a standard normal variable z

Step 4 Return $X . Y_1 \ldots . Y_N . \exp\left(\left[\mu - 0.5\sigma^2\right]dt + \sigma\sqrt{dt}\right)$

8.2.2 Simulating Jump Diffusion Paths with Modified Inter-Arrival Time Method

In this section a modified method is introduced to take advantage of the efficiency of inter-arrival time period method for rare events. In the modified method, the times of all possible jump events are simulated for the entire duration time period. The jump size is obtained for each jump event. Next the entire diffusion process is simulated, and at each jump event, the CO2 concentration level is updated with the

jump size. This method is particular useful for low jump intensity which has very few jump events.

Modified Algorithm for Generating Inter-Arrival Time Random Paths

Step 1 Initialize parameters

Drift (μ), volatility (σ), initial CO2 concentration level (X_0), event jump size (Y), time period (T), number of sub periods (N), and $dt = T/N$

Jump intensity (λ), mean jump size (μ_y), jump size variance (σ_y)

Step 2 Generate random variate for the Poisson jump event, U

Find the k^{th} jump time $t_k = t_{k-1} - log(U) / \lambda$

Step 3 For each jump event, generate a random jump validate, *dy,* for the event jump size

Calculate the event jump size, Y_k, using the probability distribution of the random jump variate with μ_y and σ_y

Step 4 Generate a random path variate *dz* with normal distribution *N(0,1)* for each sub-period

Step 5 Compute value of CO2 concentration level, X_j , using geometric Brownian motion from the last jump time to next jump time

$$X_j = X_{j-1} exp\left(\left[\mu - 0.5\sigma^2\right]dt + \sigma\sqrt{dt}\right)$$

Step 6 At the k^{th} event jump time, update the diffusion process with the jump process by multiplying the last period CO2 concentration level by the jump size in time k

$$X^* = X_{j-1}.Y_k$$

Step 7 Continue and go to Step 4

This modified method is used to generate random paths in this research.

8.3 Rare Events and Jump Diffusion Model

Rare events are also known as outliers in statistical analysis. These events are located at the extreme tail ends of a probability density function. This contributes to the leptokurtic feature of the probability distributions which tend to have higher peaks around the mean compared to normal distributions, and thicker tails on both ends. The geometric Brownian motion in the CO2 emission model which assumes a normal distribution in the diffusion process is does not have leptokurtic features. However, by incorporating jump events in the geometric Brownian motion, it is possible to reproduce these leptokurtic features.

Two experiments are performed in this section to investigate leptokurtic features in the jump diffusion model. The first experiment is to find the distribution of CO2 concentration levels at a fixed date in future. The second experiment is to find the distribution of CO2 concentration levels at a certain threshold CO2 concentration level. These two events correspond to the benefit levels used in fixed maturity date (for example, European option and optimal stopping time) and first hitting time option respectively.

The parameters of the jump diffusion model are drift (μ) 0.003957, volatility (σ) 0.000479, jump intensity (λ) 0.002 (1 in 500 years), jump size distribution is lognormal jump size distribution, mean jump size is 10X drift of CO2 emission, and jump size variance is 0.1X mean jump size. Initial benefits and exercise or adoption benefits are 1.50×10^5 ppm CO2. For first hitting time option the threshold barrier is assumed to be 3.00×10^5 ppm CO2, (twice the initial benefits or 100% increase from initial benefits), and for fixed time horizon of 500 years.

8.3.1 Probability Density Function at Fixed Date Maturity Time

The simulated paths of the time period are shown in Figure 8.1. The larger jumps can be clearly seen in some of the simulated paths. Although some paths may have more than one jump in each path, on the average the number of jumps per

path is one (1 event in 500 years). The frequency distribution of benefits at fixed date show negative skews on the left and long tails on the right which are typical of log normal distributions (Figure 8.2).

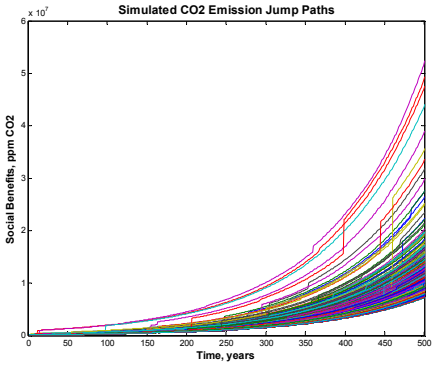

Figure 8-1 Simulated Paths

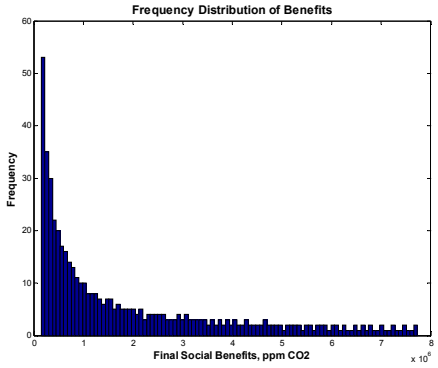

Figure 8-2 Frequency Distributions (T=500)

Maximum log likelihood and parametric method are used to obtain an unknown probability distribution fit of benefit values at fixed date. The best probability fit is Type II generalized extreme value distribution (Table 8.1, Figures 8.3 and 8.4). The frequency distribution shows a positive skewed distribution to the right with a long right tail, which has relatively few high extreme values (Figure 8.3).

Distribution	Generalized extreme value		Lognormal	
Parameter	Estimate	Std. Err.	Estimate	Std. Err.
mu	604581	362333	13.886	0.0510
sigma	623701	46226	1.141	0.0361
k	1.044	0.0828	Not applicable	Not applicable

Table 8-1 Probability Distribution Fit of Fixed Date Maturity Time

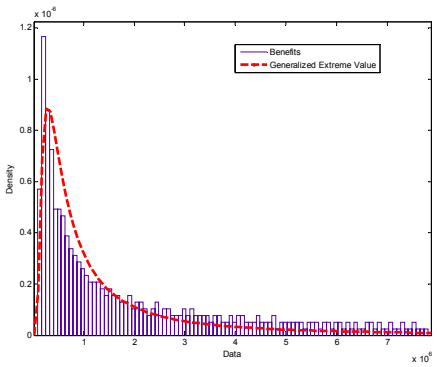

Figure 8-3 PDF of Data and GEV Fit

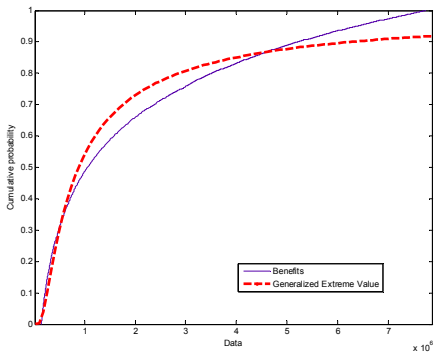

Figure 8-4 CDF of Data and GEV Fit

This probability distribution is a Frechet distribution, which is a member of the generalized extreme value distribution family, and its probability density function is given by:

$$PDF_{GEV} = \left(\frac{1}{\sigma}\right)\exp\left[-\left(1+k\frac{x-\mu}{\sigma}\right)^{-\frac{1}{k}}\right]\left(1+k\frac{x-\mu}{\sigma}\right)^{-1-\frac{1}{k}}$$

where μ denotes the mean, σ denotes variance, $k>0$ denotes shape parameter, and $1+k\frac{x-\mu}{\sigma}>0$.

The Frechet distribution has a long right tail which decreases as a polynomial, such as Student's *t*. For comparison a log normal distribution curve with the same data is shown in Figure 8.5. The CDFs in Figure 8.6 show that catastrophe events will increase the catastrophic damage to 15% (exceeding 5 x 10^6 ppm CO2) of total damages in the lognormal distribution of normal events.

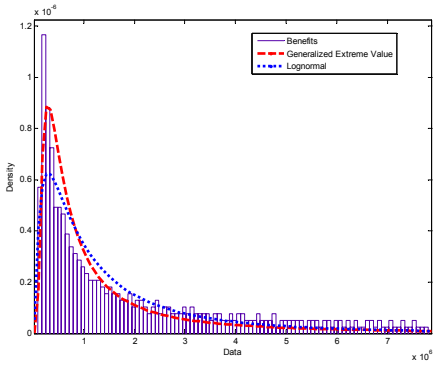

Figure 8-5 PDF of GEV and Lognormal

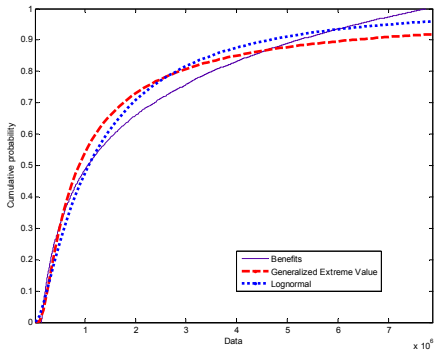

Figure 8-6 CDF of GEV and Lognormal

The significance of the results is that benefit values in the jump diffusion model has a Frechet probability distribution which can be used for studying rare events.

8.3.2 Probability Density Function at First Hitting Time

The same simulated random paths and procedure from the last Section 8.3.1 is used in first hitting time analysis.

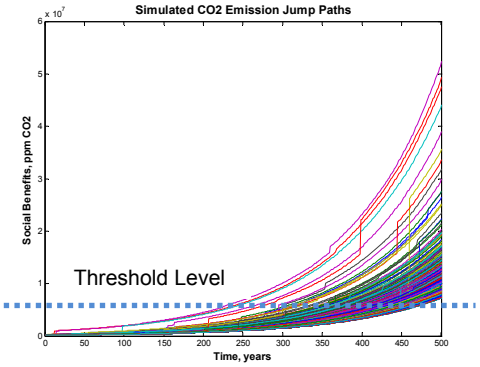

Figure 8-7 Simulated Paths

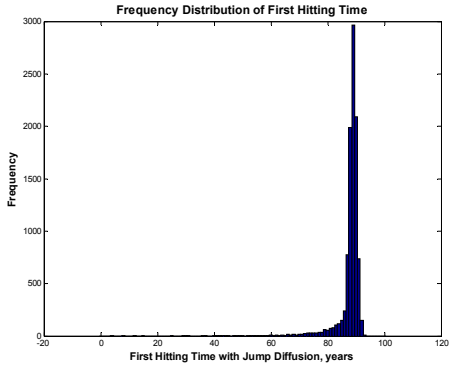

Figure 8-8 Inter Arrival Time (λ=0.002)

The frequency distribution shows a negative skewed distribution to the left with a long left tail, which has relatively few low extreme values (Figure 8.8).

A probability fit of the frequency distribution suggests that extreme value distribution, another member of the generalized extreme value distribution family, is the best distribution fit (Table 8.2, Figures 8.9 and 8.10).

Distribution	**Extreme value**		**Inverse Gaussian**	
Parameter	Estimate	Std. Err.	Estimate	Std. Err.
mu	89.987	0.0207	87.694	0.083
sigma	2.011	0.0170	Not applicable	Not applicable
lambda	Not applicable	Not applicable	9649.57	91.27

Table 8-2 Probability Distribution Fit of First Hitting Time

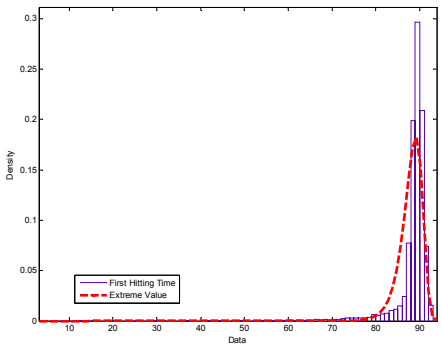

Figure 8-9 PDF of Data and Extreme Value Fit

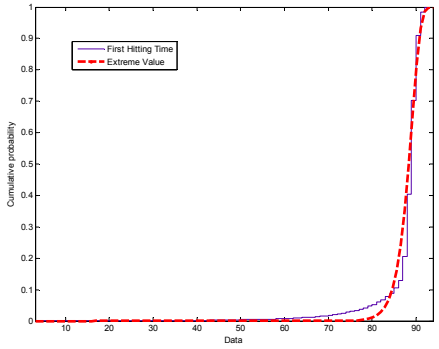

Figure 8-10 CDF of Data and Extreme Value Fit

The probability density function of the extreme value distribution is given by

$$PDF_{EV} = \left(\frac{1}{\sigma}\right)\exp\left(\frac{x-\mu}{\sigma}\right)\exp\left[-\exp\left(\frac{x-\mu}{\sigma}\right)\right]$$

where μ denotes mean, σ denotes variance.

For further analysis the inverse Gaussian distribution is fitted with the same data. The extreme value distribution and inverse Gaussian distribution are plotted in Figures 8.11 and 8.12. It can be seen from CDF in Figure 8.12 that the extreme value distribution has higher probability of hitting the threshold than the inverse Gaussian distribution.

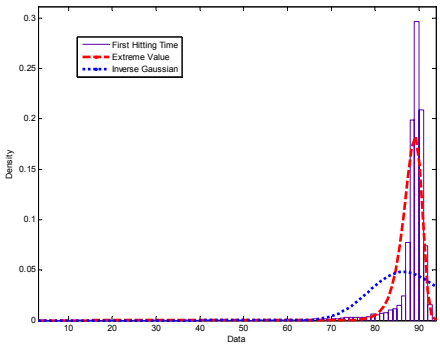

Figure 8-11 PDF of Extreme Value and Inverse Gaussian

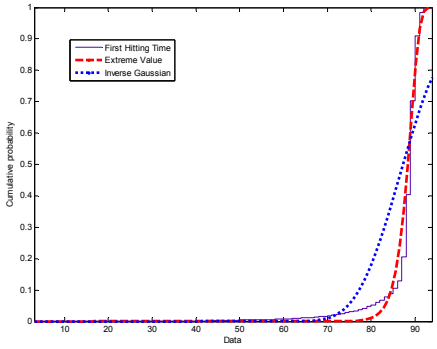

Figure 8-12 CDF of Extreme Value and Inverse Gaussian

The significance of these results is that the first hitting time with jump diffusion model produces rare events which can be approximated with an extreme value distribution.

In summary, the results show that the jump diffusion model and CO2 emission parameters is able to reproduce rare events with extreme value distributions for first hitting time and optimal stopping time.

8.4 Recommendations for the Policymaker

Catastrophe events can be viewed as extreme or jump events which have low probability of occurrence (frequency and variance) and have high impacts (magnitude). Extreme events theory involved complex mathematics and statistical theory. However the policymaker can apply the results of the simulations in this Chapter. For example, the probability density function of CO2 concentration for

optimal stopping time is Frechet distribution. So, the policymaker can directly use a Frechet probability distribution in Monte Carlo numerical simulation of catastrophe events. This simplifies the analytical work of the policymaker, and leaves him with more time for policymaking. Similarly, the Extreme Value distribution can be used in the simulation of catastrophe events involving first hitting time.

9. CATASTROPHE EVENTS AND REAL OPTIONS

In IPCC report of extreme events (IPCC SREX, 2012), it concludes that some extremes in climate change are the result of anthropogenic influences, including increases in atmospheric concentrations of greenhouse gases. The potential danger is that human activity may cause catastrophic tipping points or runaway climate change in which internal positive feedback effects result in the climate to continue changing without further external CO2 increases. In climate records, there are evidences from paleoclimatology analysis of sudden increases of CO2 concentration level caused by CO2 feedback, such as during the transition between glacial and interglacial periods (IPCC AR4, 2007c).

Present global warming may cause slowdown or sudden shutdown of thermo-haline circulation of Gulf Stream which changes in the seawater chemistry and cause release of large amounts of dissolved CO2 gases in ocean waters. Another possibility is the melting of glaciers, ice sheets and frozen ice caps could also cause sudden release huge amounts of CO2 from permafrost. These catastrophe events could result in enormous social costs and global environmental disasters.

In Chapter 8 random rare events are modelled with jump diffusion model. This chapter continues with investigations on the impact of jump events on CO2 reduction policies using the jump diffusion model in finite time with different jump sizes, jump size variances, and jump intensities.

9.1 Rare Events and Catastrophe Events

An accurate classification of rare events and catastrophe events is difficult because of subjective interpretations. IPCC discusses catastrophe event as abrupt change which has such a large impact that the climate system is unable to respond to the change (IPCC AR4 Section 8.7). In addition, the time scale of such event is also important.

Lenton et al (Timonty Lenton et al., 2008) studied and projected the likelihood of several major climate catastrophe events using time scale of event and increase in temperature (Table 9.1).

	Potential Catastrophe	Trigger Global Warming(1)	Timescale(1)	Impact(2)
1	Melting of Arctic summer sea-ice	+0.5-2 C	~10 year	low
2	Collapse of Greenland ice sheet (GIS)	+1-2 C	>300 year	med-high
3	Collapse of West Antarctic ice sheet (WAIS)	+3-5 C	>300 year	high
4	Change in amplitude/frequency/variability of ENSO	+3-6 C	~100 year	med-high
5	Dieback of Amazon rainforest	+3-4 C	~50 year	med
6	Dieback of Boreal forest	+3-5 C	~50 year	med-low
7	Weakening/Shutdown of Atlantic Thermohaline Circulation (THC)	+3-5 C	~100 year	med

Table 9-1 Probability and Impact of Potential Catastrophe Events
References: (1) Lenton 2008, (2) Lenton 2011

In addition Lenton used subjective judgment and assessed the impacts of these catastrophe events relative to thermo-haline circulation (Timonty Lenton, 2011). Impacts are considered on the full time horizon of 1,000 years, assuming minimal discounting of impacts on future generations (Figure 9.1).

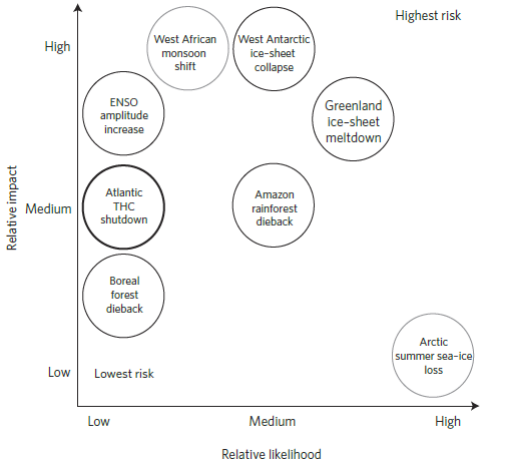

Figure 9-1 Likelihood and Relative Impact of Catastrophe Events
Reference: (Timonty Lenton, 2011)

To develop an analytical quantitative model of catastrophic event requires defining the parametric factors which characterized these abrupt events. Wright & Erickson use three characteristics to classify catastrophe events studies: low probability high impact events, threshold phenomena, and readily resolvable uncertainty (Wright & Erickson, 2003). In low probability high impact events the important criteria is how fast the probability goes to zero as damages approach infinity. Chapter 8 demonstrates that the jump diffusion model is able to represent these low probability events. In addition, the jump intensity can also be varied to increase or decrease the return

period of catastrophe events. High impact damages could be incorporated in the jump diffusion model by increasing the jump sizes. In threshold phenomena category, catastrophe events are characterised as events that might be triggered once a 'safe' level of warming has been surpassed. The features of first hitting time fit the requirements in this category. Finally, for readily resolvable uncertainty, a long duration for study is proposed because the duration of CO2 in the atmosphere could be between 100 and 500 years.

The variable parameters in the jump diffusion model can also be employed to characterize catastrophe events. For example, magnitude of jump size indicates the seriousness of impact in the jump event. The jump size variance indicates the uncertainty of the jump size; a large jump size variance could produce a low probability but very large jump size. And the jump intensity signifies the frequency or return period of the jump events, a short return period of jump events would produce damages more frequently.

Having established the suitability of jump diffusion model for investigating catastrophe events, it is necessary to specify the boundaries of catastrophe events. It is assumed that the urgent need to attend to possible catastrophe events leads to certain adoption of the reduction policy within a time frame of 500 years. In other words the finite time option period is 500 years.

9.2 Literature Review of Real Options Analysis with Jump Diffusion Model in Finite Time

The literature of real options analysis with jump diffusion in finite time, especially in problems involving optimal stopping time, is scarce. The reasons could be in the difficulty in obtaining a closed form analytical solution, and numerical analysis solution is challenging, especially in locating the free boundary solution.

Baranzini et al propose a downward jump of CO2 concentration level in the jump diffusion model to represent implementation of a climate abatement policy to mitigate the damages caused by catastrophe events (Baranzini, et al., 2003). In the paper there are four different scenarios, each with a different monetary cost of climate damages, jump intensity, abatement policies of 0%, 5%, and 10%. The focus of their study is to find the find the optimal threshold level of benefit/cost ratio and the probability of adopting the policy. Their solution for optimal threshold level uses a perpetual time jump diffusion model, and the probability of adopting the policy is the first hitting time of the adoption costs.

Makropoulou et al extend Pindyck's framework for climate policy adoption with Poisson jumps in perpetual time (Makropoulou, et al., 2008). However no closed form solution is presented in the analysis, and, as a result, the application in their example is simplified with several scenarios using fixed jump sizes, fixed jump intensities, and fixed reduction costs.

Chen & Funke (Chen & Funke, 2010) adapt the double exponential jump diffusion model to investigate the optimal stochastic climate sensitivity parameter (θ) in Pindyck's framework (Pindyck, 2000). However their study is for a perpetual time jump diffusion model.

This research fills a research gap in the real options analysis with jump diffusion model using first hitting time and optimal stopping time. It seeks to answer the research question of the impact of catastrophe events on implementation time and flexibility of CO2 reduction policies.

9.3 Applying Jump Diffusion Model to Real Options in CO2 Reduction

In assessing extreme sea level rise, IPCC TAR suggests using decision analytical frameworks beyond the cost-benefit analysis of optimal mitigation levels and with more studies on the impact of uncertainties (IPCC TAR, 2001a).

Furthermore, real options analysis is one analytical method recommended in a report from United Nations Framework Convention on Climate Change for analysing major long-term risks, uncertainty and flexibility (Markandya & Wakiss, 2010). For example, real options analysis is used in the study of London Thames Estuary 2100 flood risk project (Woodward, Gouldby, Kapelan, Khu, & Townend, 2011).

9.3.1 Jump Diffusion Model for Real Options Analysis

To recapitulate, the jump diffusion model in Chapter 8 is used as the CO2 emission model to obtain CO2 concentration level:

$$X_t = X_0\, exp\left[\left(\mu - \frac{1}{2}\sigma^2\right)t + \sigma Z\right]\prod_{j=1}^{N(t)} Y_j \qquad [1]$$

The discretized form of equation [1] is:

$$X_{i+1} = X_i \exp^{\left\{\left(\mu-\frac{1}{2}\sigma^2\right)(t_{i+1}-t_i)+\sigma[Z(t_{i+1})-Z(t_i)]\right\}} * \prod_{j=N(t_i)+1}^{N(t_{i+1})} Y_j \qquad [2]$$

CO2 concentration level *X* causes pollution which results in social costs and damages. The CO2 reduction policy goal is to produce social benefit, *B(X)*, which is equal or greater than the social cost. The social benefit model is same as in Chapters 4 and 7:

$$B(X_t) = \theta X^m \qquad [3]$$

The benefit model becomes:

$$B_i(X) = \left[X_i \exp\left[\left(\mu - \frac{1}{2}\sigma^2\right)\Delta t + \sigma\sqrt{\Delta t}\right] * \prod_{j=1}^{N_j} Y_j\right]^2 \qquad [4]$$

The reduction cost function *K* is derived Section 7.1.2 equation [3]:

$$K = c_1 R^{2.8} \qquad [5]$$

where *R* denotes reduction rate and c_1 = 19.85 is a constant value which depends on the total reduction.

The objective of the reduction policy is to maximize socio-economic benefits payoff. This is the option value adopting the CO2 reduction policy, or the value of the CO2 reduction policy project.

$$Option\ to\ Defer\ Value = B(X_t) - Ke^{-rt} \quad [6]$$

Where *r* denotes the risk free interest rate, *t* denotes time period of the project - elapsed time from the beginning of the project, in other words, *t* is the remaining time to the end of the project.

9.3.2 CO2 Reduction Policies

As in previous chapters, the CO2 reduction policies considered are CO2 emission cutback and CO2 concentration level abatement. For each of these policies, two different stopping times are used, first hitting time and optimal stopping time.

9.3.3 CO2 Reduction Costs

The benefit of adopting CO2 reduction policy in Section 4.6.1 is given by:

Benefit of Adoption = Cost without adoption - Cost with adoption [7]

It is assumed that the CO2 reduction policy must be implemented at the end of time horizon. In this example the time horizon is 500 years. This means the CO2 reduction policy must be implemented by year 500, and the maximum cost of reduction is equal to B_{500}. From equation [5], the parameter value of *c* can be obtained as: $c_1 = B_{500} / R^{2.8}$ where R=100. The reduction cost function is $K = c_1 R^{2.8}$ where 0<*R*<100. The value of c_1 parameter is 19.85, which is the same c_1 used in Section 7.1.2.

9.4 Real Options and Jump Events in CO2 Concentration Levels

The impacts of jump size, jump size variance, and jump intensity on stopping times, benefit values, and option values with the first hitting time and optimal time approaches are investigated in this Chapter.

Monte Carlo numerical solution with modified inter-arrival time method is used to generate the random paths. The real options analysis for optimal stopping time is performed with the least squares regression basis function (LSMC) method. For first hitting time, the stopping time is obtained when the reduction cost is the same as the benefit value cost.

The parameters used in the experiments for the jump events are as follows.

Jump size distribution:	lognormal distribution
Mean jump size [times drift]:	1.0, 2.5, 5.0, 7.5, 10.0, 12.5, 15.0, 17.5, 20.0, 22.5, 25.0 (or a total of 11 mean jump sizes)
Jump size variance [times mean jump size]:	0.10, 0.125, 0.25, 0.50, 0.75, 1.00, 1.25, 1.50, 1.75, 2.0 (or a total of 10 jump size variances)
Jump intensity:	0.001, 0.002, 0.003, 0.004, 0.005, 0.006, 0.007, 0.008, 0.009, 0.010, 0.011
[frequency of jumps]:	0.5, 1.0, 1.5, 2.0, 2.5, 3.0, 3.5, 4.0, 4.5, 5.0, 5.5 (or a total of 11 jump intensities)
Discount Rate:	4 % pa
Reduction Costs [ppm CO2]:	12526, 87234, 271483, 607534, 1134799, 1890716, 2911235, 4231114, 5884124, 7903197
[corresponding reduction rates]:	10%, 20%, 30%, 40%, 50%, 60%, 70%, 80%, 90%, 100%

The investigation is setup in four experiments:

1. CO2 reduction rates and Jump Size

   The experiment with jump size is first performed with zero jump size variance, and repeated with a jump size variance of 1 X drift (CO2 emission rate). In CO2 concentration abatement case, there is no CO2 emission cutback and vice versa. The jump intensity is fixed at 0.002.

2. CO2 reduction rates and Jump Intensity

   This is the same as experiment 1 but the impact of jump intensity is examined instead of jump size. The jump size is fixed at 10 X drift (CO2 emission rate).

3. Jump Size and Jump Size Variance

   In this experiment the joint conditional impacts of jump size and jump size variance factors are studied. The CO2 emission cutback rate is 50% and CO2 concentration abatement is zero, and vice versa. The jump intensity is 0.002.

4. Jump Size and Jump Size Intensity

   This is same experiment 3 except jump size and jump intensity factors are studied. The CO2 emission cutback rate is 50% and CO2 concentration abatement is zero, and vice versa. The jump size variance is 1 X jump size.

The number of simulation paths for experiments 1 and 2 is 100,000. For experiments 3 and 4, it is found necessary to use 1,000,000 simulation paths because of the sensitivities of option value solutions. Also, in experiments 3 and 4, the number of divisions of jump size, jump size variance, and jump intensity are increased to improve the accuracy of the simulation results.

Mean jump size [times drift]:	1.0 to 25.0 in incremental step of 1 (or a total of 25 drifts)
Jump size variance [times mean jump size]:	1.0 to 2.0 in incremental step of 0.1 (or a total of 20 jump size variances)
Jump intensity: [frequency of jumps]:	0.2 to 5.0 jumps in 500years in incremental

steps of 0.2 (or a total of 25 jump intensities)

9.5 Analysis and Discussion of CO2 Reduction Rates and Impact of Jump Sizes, Jump Size Variances, and Jump Intensity

Results from the experiments show that there are common features in the CO2 emission cutback and CO2 concentration abatement. Therefore the discussions are combined and discussed together in terms of stopping times, and option values.

9.5.1 Analysis and Discussion of CO2 Reduction Rates and Jump Sizes

Jump size is a very important factor in catastrophe event. It represents the magnitude of event, and, indirectly, the cost of damages.

Stopping Times

In general, optimal stopping times have longer than first hitting times. The first hitting times increase with CO2 reduction rates, but the first hitting times are not sensitive to changes (Figures 9.2a and 9.2b). Similar results are also obtained for optimal stopping time (Figure 9.2c and 9.2d). This means that stopping times are primarily determined by CO2 reduction rate in both CO2 emission cutback and CO2 concentration abatement.

With 1X jump size variance, the optimal stopping time increases with large jump sizes – this is especially prominent at low CO2 reduction rates (Figures 9.3b and 9.3d). But first hitting times are not sensitive to the volatility (1X drift variance) in jump size. This result implies that stopping time is more sensitive to jump sizes in optimal stopping time than first hitting time at low CO2 reduction rates but this sensitivity is less obvious in higher reduction rates (Figure 9.3).

JUMP SIZE VARIANCE ZERO	
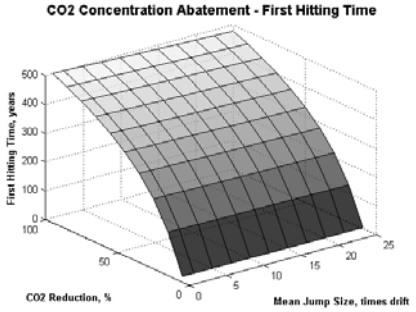	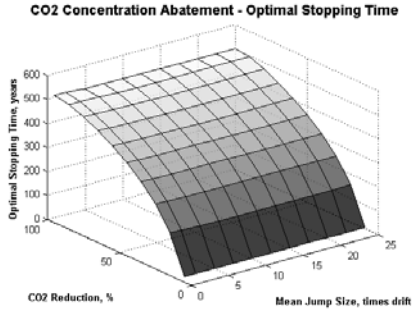
First Hitting Time Figure 9.2a	Optimal Stopping Time Figure 9.2b
CO2 Concentration Abatement	
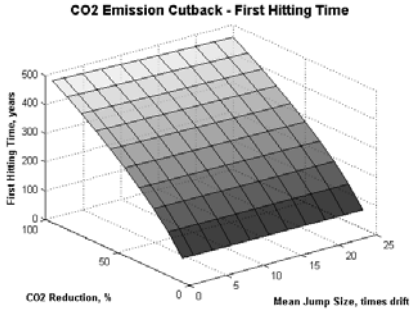	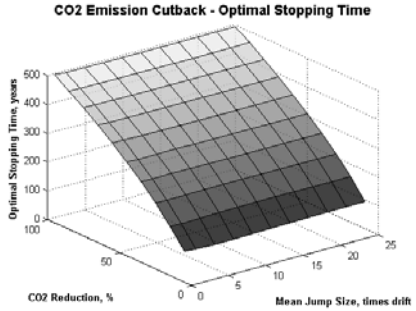
First Hitting Time Figure 9.2c	Optimal Stopping Time Figure 9.2d
CO2 Emission Cutback	

Figure 9-2 CO2 Reduction and Jump Sizes – Stopping Times with Zero Jump Size Variance

JUMP SIZE VARIANCE 1X	
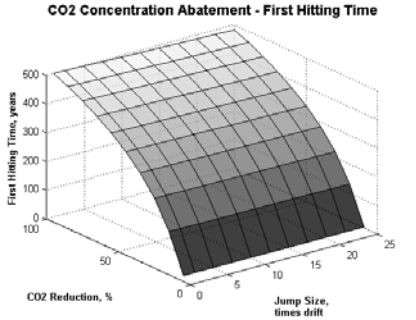	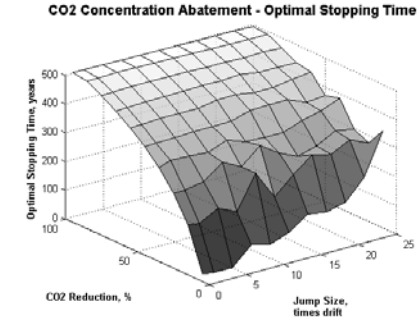
First Hitting Time Figure 9.3a	Optimal Stopping Time Figure 9.3b
CO2 Concentration Abatement	
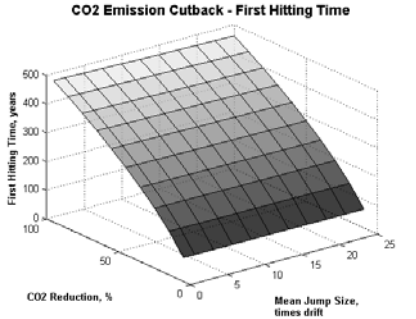	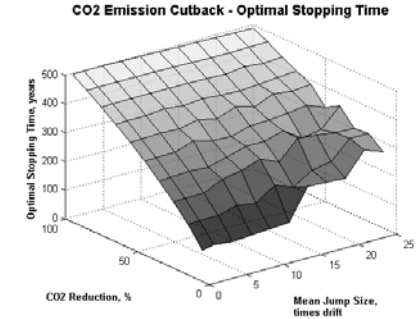
First Hitting Time Figure 9.3c	Optimal Stopping Time Figure 9.3d
CO2 Emission Cutback	

Figure 9-3 CO2 Reduction and Jump Sizes – Stopping Times with 1X Jump Size Variance

JUMP SIZE VARIANCE ZERO

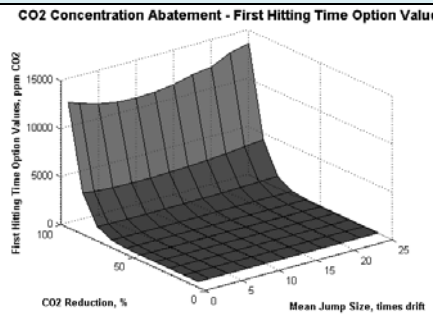

First Hitting Time
Figure 9.4a

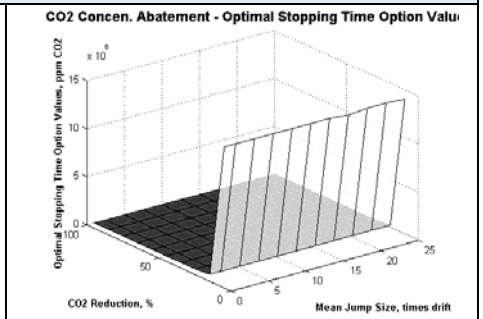

Optimal Stopping Time
Figure 9.4b

CO2 Concentration Abatement

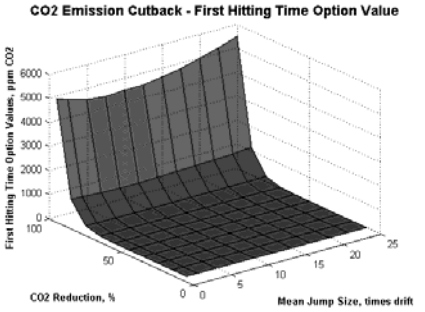

First Hitting Time
Figure 9.4c

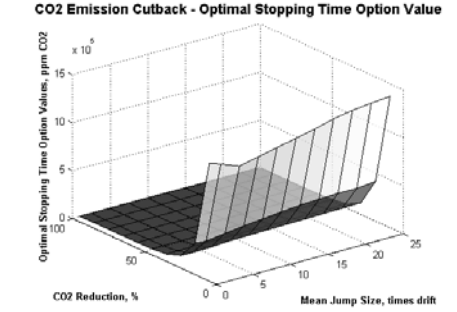

Optimal Stopping Time
Figure 9.4d

CO2 Emission Cutback

Figure 9-4 CO2 Reduction and Jump Sizes – Option Values with Zero Jump Size Variance

JUMP SIZE VARIANCE 1X

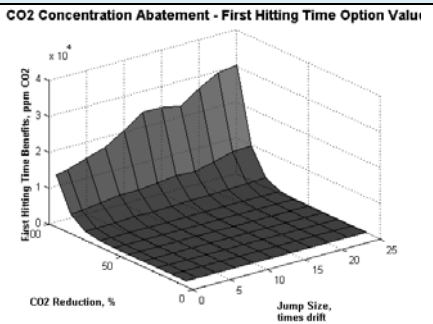

First Hitting Time
Figure 9.5a

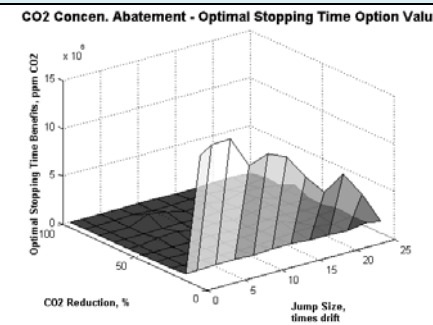

Optimal Stopping Time
Figure 9.5b

CO2 Concentration Abatement

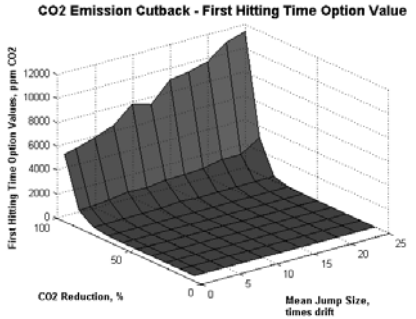

First Hitting Time
Figure 9.5c

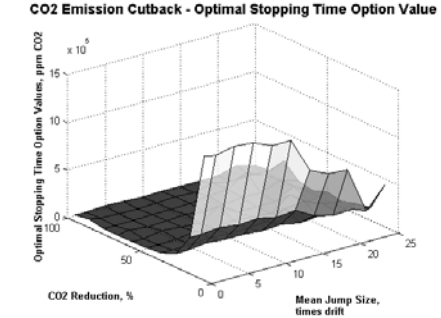

Optimal Stopping Time
Figure 9.5d

CO2 Emission Cutback

Figure 9-5 CO2 Reduction and Jump Sizes – Option Values with 1X Jump Size Variance

Option to Defer Values

In first hitting times there are large option values at high CO2 reduction rates but the first hitting times decease very quickly with reduced CO2 reduction rates (Figures 9.4a and 9.4c). In contrast the option values in optimal stopping times are large at low CO2 reduction rates (Figures 9.4b and 9.4d). The results suggest that at low reduction rates there is little flexibility in first hitting time but greater flexibility in optimal stopping time. These results agree with previous findings in perpetual time model (Chapters 4 and 5) and normal events in finite time (Chapter 7).

Also the option values in CO2 emission cutback are larger than CO2 concentration abatement. In general this implies that there is greater flexibility in CO2 emission cutback policy than CO2 concentration abatement policy. The results are reasonable because there is urgency to manage immediate problems caused by existing CO2 concentration, whereas, there are still uncertainty of the problems from CO2 emission.

When there is uncertainty in jump sizes (1X drift variance) of first hitting time, the larger the jump sizes produce higher option values (Figure 9.5). In contrast, volatility in jump sizes of optimal stopping times reduces option values with higher jump sizes. The optimal stopping time results suggest that the flexibility is reduced when the uncertainty of large jump sizes increases. Also there is little flexibility when high reduction rates are planned using optimal stopping time.

In general CO2 emission cutback policy has greater flexibility than CO2 concentration abatement policy. The adoption time for CO2 concentration abatement policy is earlier than CO2 emission cutback policy. Uncertainty in large jump sizes decreases flexibility of optimal stopping time.

The optimal reduction rate in first hitting time is at 100%. This is the same result as in the findings in Section 7.4.3. In contrast, the optimal reduction rate in optimal stopping time is nearly zero (0%) because of the uncertainty introduced by

catastrophe events. At this rate the policymaker has maximum flexibility to adjust the policy rate only upwards. This suggests that the priority of the policymaker should invest in precautionary measures to prevent catastrophe events and not in reduction policies. Of course, these precautionary measures could also include very drastic changes, for example, a revolutionary non-polluting technology which could replace all fossil fuel energy plants.

JUMP SIZE VARIANCE ZERO	
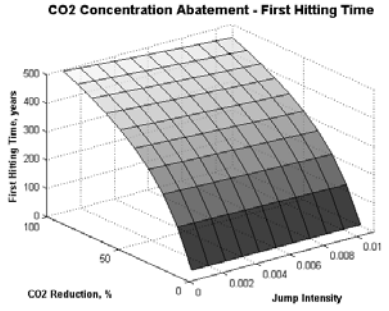	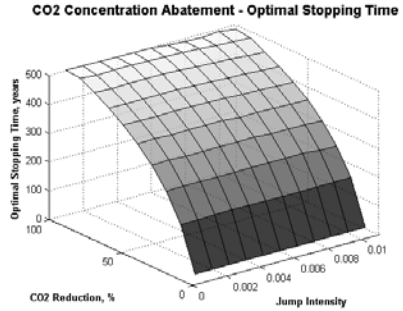
First Hitting Time Figure 9.6a	Optimal Stopping Time Figure 9.6b
CO2 Concentration Abatement	
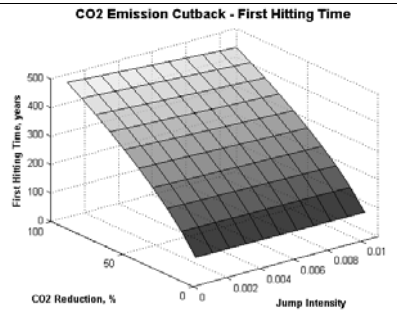	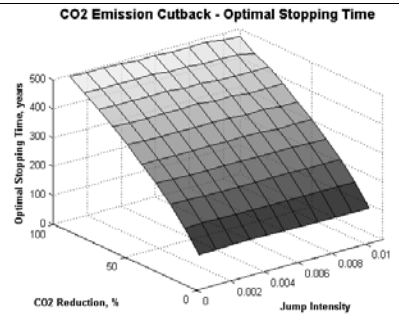
First Hitting Time Figure 9.6c	Optimal Stopping Time Figure 9.6d
CO2 Emission Cutback	

Figure 9-6 CO2 Reduction and Jump Intensity - Stopping Times with Zero Jump Size Variance

JUMP SIZE VARIANCE 1X	
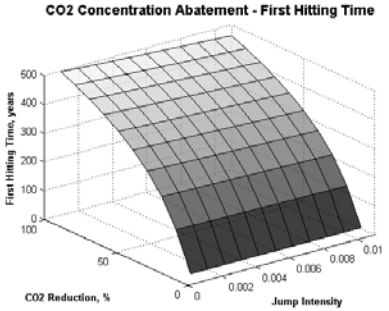	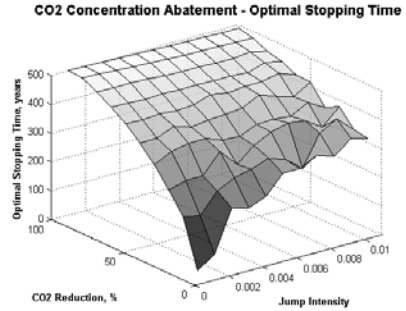
First Hitting Time Figure 9.7a	Optimal Stopping Time Figure 9.7b
CO2 Concentration Abatement	
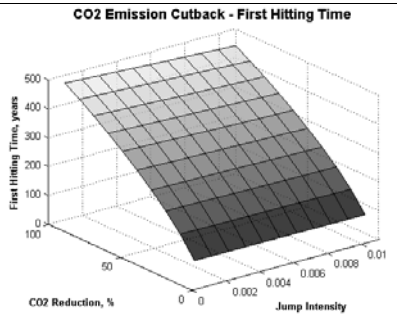	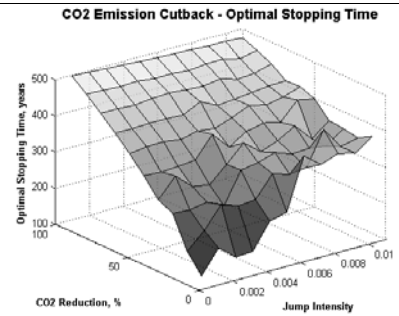
First Hitting Time Figure 9.7c	Optimal Stopping Time Figure 9.7d
CO2 Emission Cutback	

Figure 9-7 CO2 Reduction and Jump Intensity - Stopping Times with 1X Jump Size Variance

JUMP SIZE VARIANCE ZERO

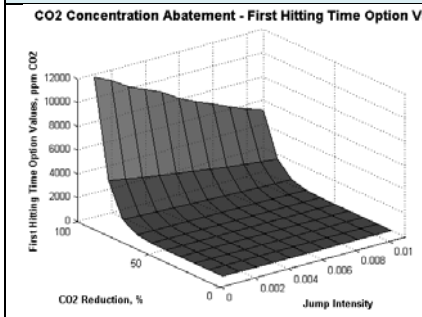

First Hitting Time
Figure 9.8a

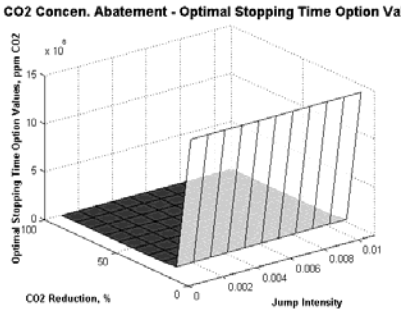

Optimal Stopping Time
Figure 9.8b

CO2 Concentration Abatement

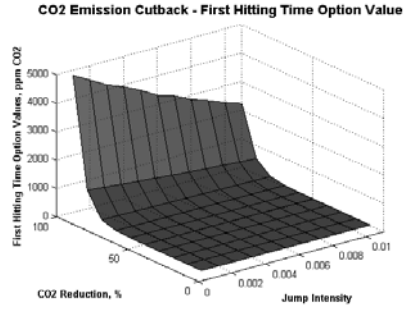

First Hitting Time
Figure 9.8c

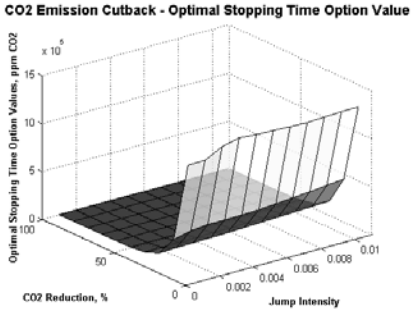

Optimal Stopping Time
Figure 9.8d

CO2 Emission Cutback

Figure 9-8 CO2 Reduction and Jump Intensity - Option Values with Zero Jump Size Variance

JUMP SIZE VARIANCE 1X

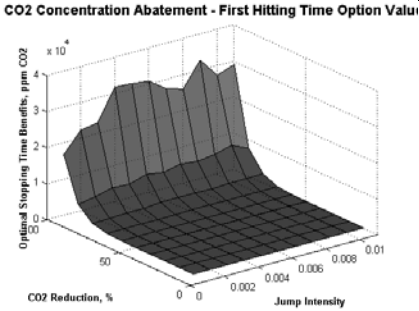

First Hitting Time
Figure 9.9a

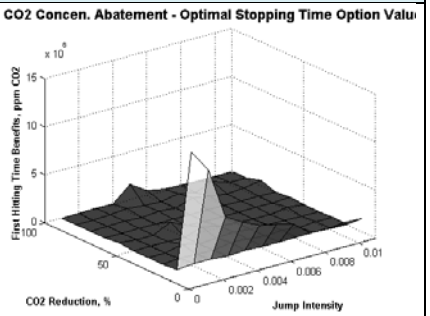

Optimal Stopping Time
Figure 9.9b

CO2 Concentration Abatement

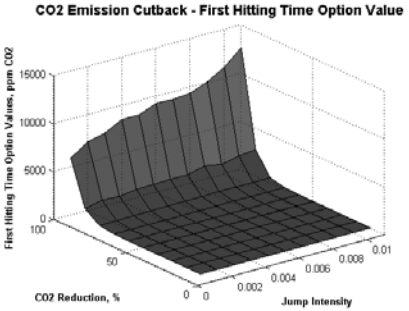

First Hitting Time
Figure 9.9c

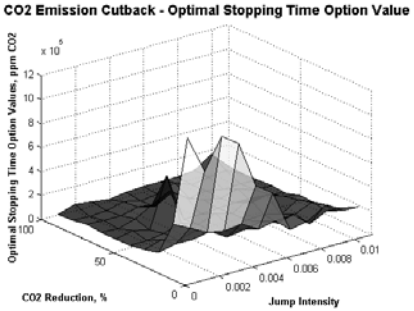

Optimal Stopping Time
Figure 9.9d

CO2 Emission Cutback

Figure 9-9 CO2 Reduction and Jump Intensity - Option Values with 1X Jump Size Variance

9.5.2 Analysis and Discussion of CO2 Reduction Rates and Jump Intensity

Besides specifying a jump size in a catastrophe event, another uncertainty is the frequency of catastrophe event or jump intensity. More frequent catastrophe events result in faster increase in CO2 concentration levels.

Stopping Times

The stopping times of jump intensity with CO2 reduction rates (Figures 9.6 and 9.7) are similar to those of jump size with CO2 reduction rates (Figures 9.2 and 9.3). This suggests that the stopping times effects of jump intensity and jump size are identical. In addition the variance of jump size has the same effects with jump intensity as with jump sizes.

Option to Defer Values

In first hitting times, the option values decrease with increasing jump intensity, especially at high CO2 reduction rates (Figures 9.8a and 9.8c). Otherwise the option values are small for low CO2 reduction rates. For optimal stopping times, there high option values at low CO2 reduction rates and these option values are not sensitive to changes in jump intensity (Figures 9.8b and 9.8d).

In general the option values from jump intensity (Figure 9.8) are lower than from jump size (Figure 9.6). This suggests that there is less flexibility with jump intensity than with jump size. It also implies that the risk aversion of jump intensity is higher than jump size effects.

When 1X jump size variance is introduced with jump intensity, the flexibility is even smaller (Figures 9.9). In optimal stopping time, the flexibility is lowest at high jump intensities (Figures 9.9b and 9.9d).

JUMP SIZE - JUMP SIZE VARIANCE

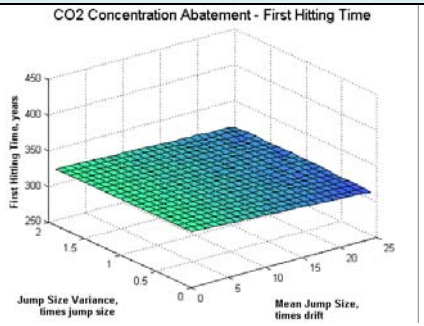

First Hitting Time
Figure 9.10a

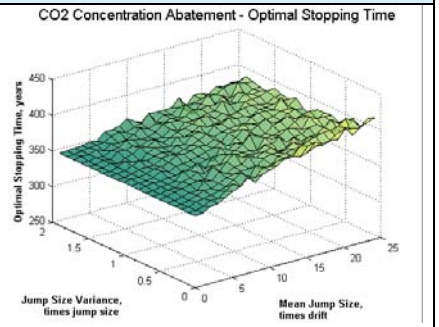

Optimal Stopping Time
Figure 9.10b

CO2 Concentration Abatement

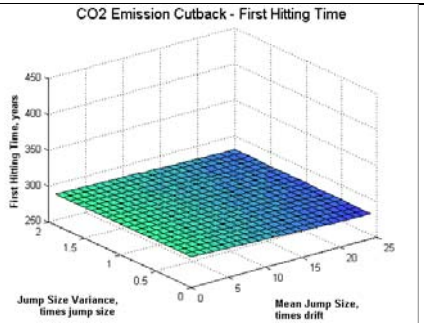

First Hitting Time
Figure 9.10c

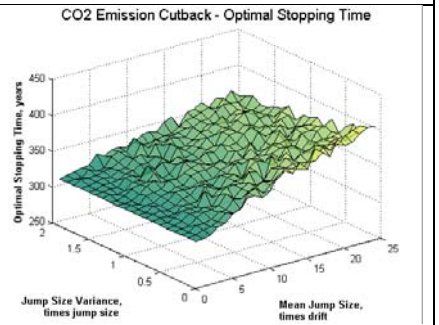

Optimal Stopping Time
Figure 9.10d

CO2 Emission Cutback

Figure 9-10 Jump Size and Jump Size Variance - Stopping Times

JUMP SIZE - JUMP INTENSITY

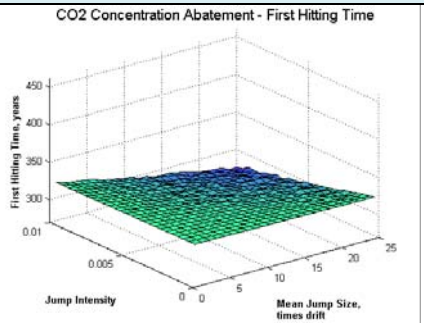

First Hitting Time
Figure 9.11a

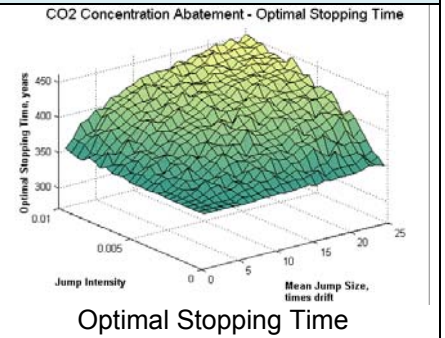

Optimal Stopping Time
Figure 9.11b

CO2 Concentration Abatement

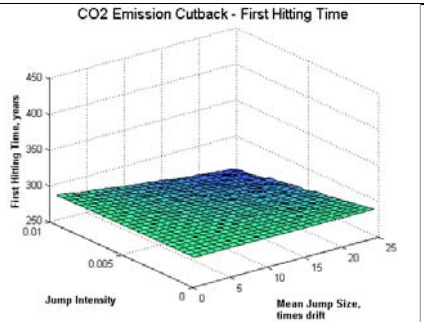

First Hitting Time
Figure 9.11c

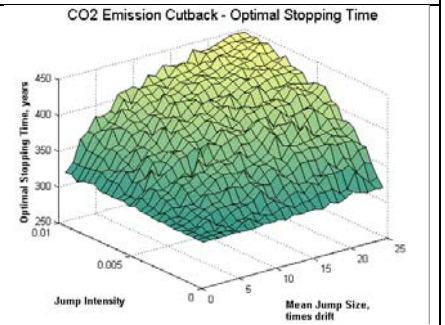

Optimal Stopping Time
Figure 9.11d

CO2 Emission Cutback

Figure 9-11 Jump Size and Jump Intensity - Stopping Times

9.5.2 Analysis and Discussion of Jump Size, Jump Size Variance, and Jump Intensity

Catastrophe events are characterised in this research by the uncertainties and magnitudes of jump size, jump size variance, and jump intensity. The inter-relationships of these three uncertainties with respect to jump size are explored in this section.

Stopping Times

In uncertainty of jump size (jump size vs. jump size variance, an increase in jump size reduces the stopping time of first hitting time (Figures 9.10a and 9.10c). On the other hand, an increase in jump size variance increases the stopping time of first hitting time. However, as the slopes of the plots suggest, the first hitting times are more sensitive to jump size than jump size variance. In contrast, optimal stopping times have the opposite features from first hitting times (Figures 9.10b and 9.10d). An increase in jump size increases the stopping times, and an increase in jump size variance reduces the stopping times. In general, Figure 9.10 shows that the slope of stopping times vs jump size variance is less steep than the slope of stopping times vs jump size. This suggests that the stopping times are more sensitive to jump sizes than to jump size variances.

For jump size and jump intensity, the stopping times in first hitting time decrease with both jump size and jump intensity (Figures 9.11a and 9.11c). On the other hand, the stopping times of optimal stopping time increase with both jump size and jump intensity (Figures 9.11b and 9.11d). The optimal stopping times of CO2 concentration abatement (Figure 9.11b) and CO2 emission cutback (Figure 9.11d) are almost the similar. But the first hitting times of CO2 concentration abatement (Figure 9.11a) is larger than first hitting times of CO2 emission cutback (Figure 9.11c). The results of Figure 9.11 suggest that the significant impact of jump size and jump intensity on stopping times, although the effects are different; in first hitting

time, increase in jump intensity and jump size reduce stopping time, while, in optimal stopping time, increase in jump intensity and jump size increase stopping time.

JUMP SIZE - JUMP SIZE VARIANCE

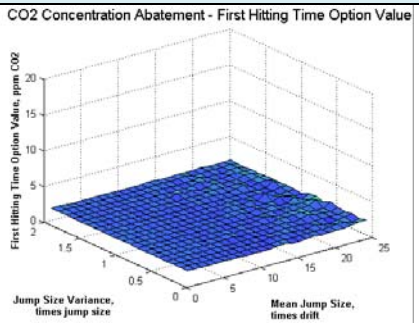

First Hitting Time
Figure 9.12a

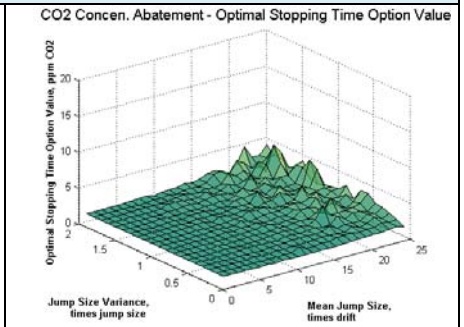

Optimal Stopping Time
Figure 9.12b

CO2 Concentration Abatement

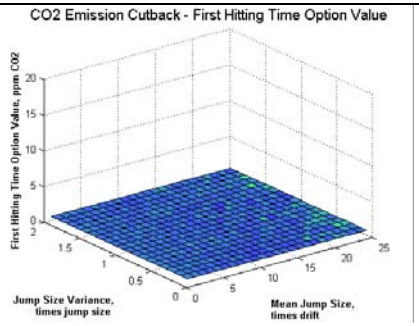

First Hitting Time
Figure 9.12c

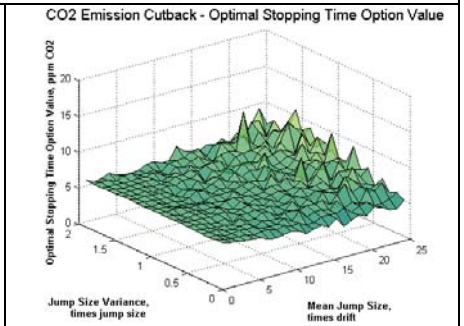

Optimal Stopping Time
Figure 9.12d

CO2 Emission Cutback

Figure 9-12 Jump Size and Jump Size Variance - Option Values

JUMP SIZE - JUMP INTENSITY

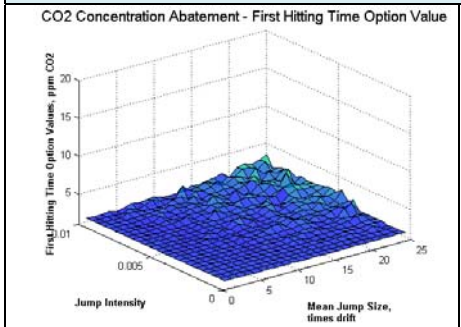

First Hitting Time
Figure 9.13a

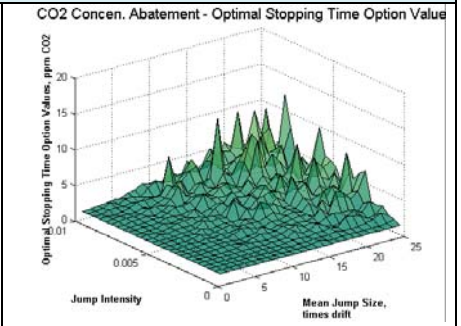

Optimal Stopping Time
Figure 9.13b

CO2 Concentration Abatement

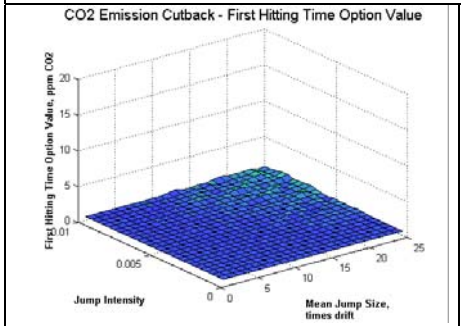

First Hitting Time
Figure 9.13c

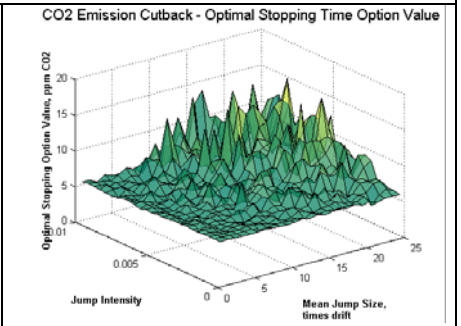

Optimal Stopping Time
Figure 9.13d

CO2 Emission Cutback

Figure 9-13 Jump Size and Jump Intensity - Option Values

Option to Defer Values

Option values from jump size and jump size variance show that increases in jump size or jump size variance increase the incentive to defer adoption of CO2 reduction policy (Figures 9.12b and 9.12d) in optimal stopping time. In other words, the flexibility of both reduction policies increase with both jump size and jump size variance.

The impacts of jump size and jump size variance in first hitting time are not as significant as optimal stopping time. This indicates that the flexibility from optimal stopping time (Figures 9.12b and 9.12d) is larger than first hitting time (Figures 9.12a and 9.12c). In fact the flexibility of first hitting time is relatively insignificant when compared with optimal stopping time.

There is a clearer relationship of impact of option values from jump size and jump intensity (Figure 9.13). Increases in jump size or jump intensity increase the option values and flexibility in both first hitting time and optimal stopping time (Figures 9.13). Largest option values are obtained with large jump size and large jump intensity. This suggests that large uncertainties in jump size and jump intensity also provide more flexibility for the policymaker. Again CO2 concentration abatement (Figures 9.13a and 9.13e) shows lower flexibility thanCO2 emission cutback policies in optimal stopping time (Figures 9.13b and 9.13d).

9.5.3 Evaluation of Catastrophe Events and Normal Events

The results of finite time in normal events of finite time model in Chapter 6 and catastrophe events in this chapter are now studied to investigate the impact of catastrophe events. In both cases, the flexibility decrease with increasing CO2 reduction rates (Figure 9.14), this is the same feature in the perpetual time model. The option values stabilize when CO2 emission cutback is higher than 40%.

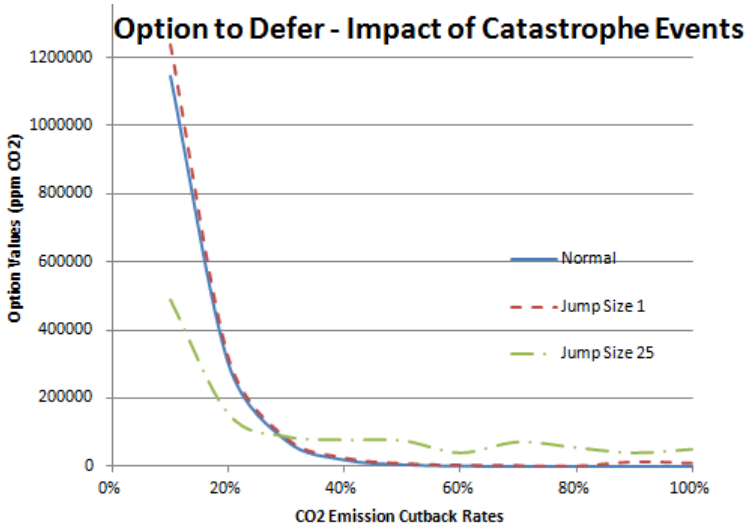

Normal Events and Catastrophe Events
50% CO2 emission cutback, jump size volatility: 1 X jump size,
jump intensity 0.002, discount rate 4%pa, 500 year period

Figure 9-14 Catastrophe and Normal Events - Option Values

When the jump size is small (see jump size 1 time of CO2 emission rate) there is no difference in option value. But with larger jump size events the option values are smaller than normal events with no jump (see jump size 25 times). However the option values stabilize at quite low CO2 reduction rates, 20% to 30% CO2 emission cutback rate. Thereafter the option values of large jump size are higher than normal events.

The results suggest that there is not flexibility with large jump sizes, especially if the reduction rates are small. For the same reduction costs, it is advisable to adopt the reduction policy earlier if large jump sizes are anticipated. However for larger reduction rates, there is little flexibility because of larger uncertainties in the jump events and higher reduction costs. But at the same reduction costs, the normal event option values show even lower flexibility. In such cases, for higher reduction rates, it is prudent to reduce the flexibility of catastrophe events to be the same as the flexibility available in normal events.

In summary, the flexibility is reduced for low reduction rates in the present of catastrophe events. But for high reduction rates, the flexibility of normal events are

used. Therefore, the overall option values are reduced when catastrophe events are combined with normal events.

9.6 Recommendations for the Policymaker

In practice, the policymaker has to make some decisions within a limited time horizon. With catastrophe events, policymaking becomes even more challenging because of many more uncertainties such as magnitude and frequency of catastrophe events. The following recommendations assume that the policymaker has to make and implement the policy within a finite time period.

Between reduction rate and one of the jump factors, the reduction rate affects implementation time more than the jump factor in all cases. An increase in reduction rate results in increase in implementation time.

As for managerial flexibility in implementing the policy, the recommendation varies for each policy. Furthermore, the interaction of two jump factors at the same time complicates the policy situation.

For clarity, the recommendations are placed in separate sections for the conservative policymaker and optimal policymaker.

Conservative Policymaking with First Hitting Time

In a conservative policy, there is very low flexibility for the policymaker as he is required to implement the policy immediately once CO2 concentration level reaches the threshold.

The implementation times are not sensitive to interacting relationship between jump size and jump size variance. However there is slight negative linear correlation in the joint probabilities of jump size and jump intensity on implementation but the effect is insignificant. Overall the implementation time in the conservative policy is less complicated for the policymaker. Once the policy is determined there is lower flexibility for the policymaker to make changes in the policy other than raising the

threshold level for catastrophe events. These new threshold could be reset using procedures in Chapter 8 to find the probability density function. Then the new threshold is determined with the appropriate statistical measures and confidence levels.

Optimal Policymaking with Optimal Stopping Time

In the optimal policy, the jump size and jump intensity are important factors to determine implementation time. For example, in the interacting relationship between jump size and jump size variance, the implementation time increases with jump size but not with jump size variance. And between jump size and jump intensity, increase with either one of these jump factors would increase implementation time.

The optimal policy offers the policymaker flexibility to manage, learn and resolve uncertainties about catastrophe events. The amount of flexibility increases more with larger jump size and jump intensity, than with jump size and jump size variance.

9.7 Contributions and Summary

The impact of jump events on option value depends on the interacting factors of jump size, jump size variance, and jump intensity. This complex relationship is summarised in Table 9.2. Catastrophe events are characterized by very high jump sizes, high jump size variance, and high jump intensity. A combination of high jump size with either high jump size variance or high jump intensity is an extreme event with serious consequences. The results in Table 9.2 provide some interesting guidelines for policy management of extreme climate change events.

CO2 Concentration Abatement Policy	
Low Flexibility (low option values)	High Flexibility (high option values)
▪ Low CO2 reduction rates ▪ First hitting time o all small jump sizes o small jump size with small jump intensity ▪ Optimal stopping time o all small jump sizes o all small jump size variances o all small jump intensities	▪ High CO2 reduction rates ▪ First hitting time o large jump size with large jump size variance ▪ Optimal stopping time o large jump size with large jump size variance
CO2 Emission Cutback Policy	
Low option values (low incentive to defer)	High option values (high incentive to wait)
▪ High CO2 reduction rates ▪ First hitting time o all small jump sizes ▪ Optimal stopping time o all small jump sizes o all small jump size variances o all small jump intensities	▪ Low CO2 reduction rates ▪ First hitting time o large jump size with large jump intensity ▪ Optimal stopping time o large jump size with large jump size variance o large jump size with high jump intensity

Table 9-2 Summary of Impact of Jump Events on Option Values

As discussed in Section 9.5.2, the flexibility of both CO2 concentration abatement and CO2 emission cutback increase with both jump size and jump size variance. However it should be noted that jump size variance directly affects jump size. In other words, both these uncertainties relate to one underlying variable, that is uncertainty of jump size. Therefore the results show importance of jump size in adoption of CO2 reduction policy. Also, large jump size and high jump intensity produces high flexibility values in both CO2 concentration abatement and CO2 emission cutback. This indicates the importance of jump intensity in resolving uncertainties in CO2 reduction policy. Indeed, the magnitude of catastrophe impact (jump size) and probability of catastrophe event (jump intensity) are the key concerns in IPCC worst case scenarios. The results demonstrate the capability of real options in analyzing CO2 reduction policies of catastrophe events in climate change.

10. CONCLUSIONS AND RECOMMENDATIONS

Global warming produces unpredictable and extreme events in climate change. The main cause of global warming is CO2 emission from economic activities. The challenge is how to manage and control CO2 reduction policies to optimize cost effective solutions. The problem is compounded by large uncertainties in CO2 emission process and irreversible nature of decision making. The present research study uses real options analysis to investigate the problems and solutions of the CO2 reduction policies in normal and catastrophe events. Real options analysis provides a means to incorporate information of future events in climate change investments under uncertainty.

10.1 Summary

For real options analysis, the CO2 emission process is modelled as a geometric Brownian motion. Using CO2 observation data, the stochastic parameters of the process are estimated in the stochastic differential equation. It is found that the estimated parameters are vastly different from those obtained using simple regression statistical mean and variance. The CO2 concentration level in the resulting CO2 process model approximates the B1 scenario of IPCC SRES.

Two CO2 reduction policies are considered in the research. The CO2 emission cutback aims to reduce the CO2 emission rate at source and this identical to CO2 mitigation policy in IPCC reports. The CO2 concentration abatement focuses on the reduction of CO2 concentration level already present in the climate system. This is equivalent of CO2 adaption policy in IPCC reports. A perpetual time real options analysis model is developed and closed form analytical solutions are obtained. It is found that low CO2 emission cutback and low discount rates result in higher option value. Also CO2 emission cutback is more cost effective in CO2

reduction than CO2 concentration abatement. In addition, it is found that low discount rates result in a number of discontinuities in the solutions.

To study catastrophe events, a perpetual time jump model is developed and a semi-numerical closed form analytical solution is provided. The results from this model show that small jump size and low jump intensity produce high flexibility in reduction policy adoption. The perpetual time model (with normal and jump events) produces extreme option values and CO2 concentration levels which are not realistic for practical applications.

A finite time model is developed for practical real options analysis of CO2 reduction policies. Two stopping time methods, first hitting time and optimal stopping time, are used to determine the actual time of policy adoption within a specific time period. Numerical solution methods are required for solution of the finite time model. The Monte Carlo numerical simulation is used to generate CO2 concentration level paths, and LSMC is used to obtain optimal stopping time. Similar with the results of perpetual time model, the finite time model also produces high flexibility at low reduction rates and low discount rates. As expected the stopping time of optimal stopping time is longer than first hitting time, and it also has higher benefit values at stopping. The flexibility of CO2 emission cutback is 2 to 3 times larger than CO2 concentration abatement. This result confirms again the higher value of waiting in CO2 emission cutback reduction policy.

To complete the investigation in finite time, catastrophe events are modelled with jump diffusion model. An efficient and fast method, using inter-arrival time properties of Poisson jump events, is developed to generate simulation paths in Monte Carlo numerical method. The probability distribution of benefit values in first hitting time and optimal stopping time are found to have extreme value probability density function distributions.

To understand the impact of jump events on flexibility to adopt reduction policy, experiments are performed with jump size, jump size variance, and jump

intensity. Flexibility is observed to increase with either jump size or jump intensity, but jump size variance has little impact on flexibility. The most flexibility in optimal stopping time are from low reduction rates and low jump size, whereas, the highest flexibility in first hitting time are from high reduction rates and high jump size. However, flexibility in optimal stopping times are 100 times larger than first hitting times. This implies that the flexibility and incentive to defer policy adoption is high with optimal stopping time because of deeper uncertainties of these rare events and motivation to obtain more information to resolve these uncertainties.

The results also suggest that when operating on low budget (low reduction costs or low reduction rates) there is less flexibility and incentive to defer in the presence of catastrophe events. This is because catastrophe events reduce option values and value of waiting at low reduction rates.

Comparing the difference of option values of catastrophe events and normal events, it is shown that at high reduction rates the flexibility value of catastrophe events is higher than those with normal events. This suggests that deep uncertainties together with high reduction costs create high flexibility and an incentive to defer adoption of reduction policy than would otherwise with normal events. Notwithstanding this analytical interpretation, a prudent policy would indicate that a more urgent and proactive action is required by adopting the reduction policy as soon as possible.

10.2 User Guide for Practical Policy Making

For the policymaker, a quick summary of the important findings of this research is described below with a flowchart (on the right) of the basic application procedures.

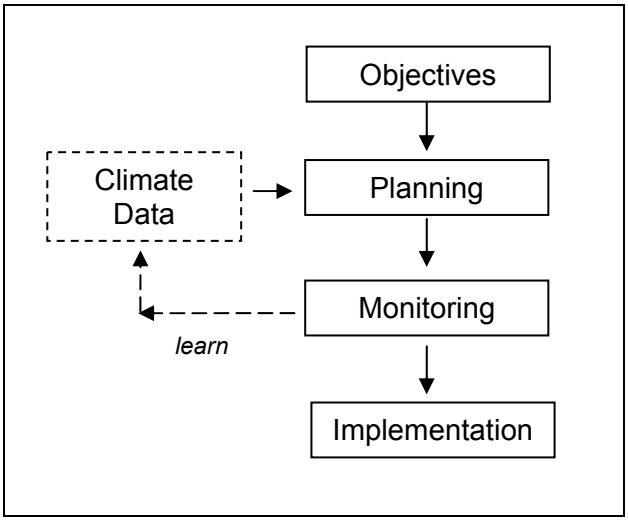

Objectives

- Decide on CO2 reduction method: whether it is for CO2 emission cutback or CO2 concentration abatement
- Decided whether Conservative or Optimal Policies

Planning - Important Factors to Consider

- Decide on time horizon – longer time horizon have more uncertainty and irreversibility impact
- Decide on how much of CO2 emission to reduce
- Determine on the budget for implementation costs
- Estimate the probable magnitude and frequency of sudden increase of CO2 emission

Investigation and Evaluation

- Use discount rate 4% p.a. for preliminary investigation – not so sensitive
- Perform sensitivity analysis with a range of discount rates.
- Perform real options analysis and find out what flexibility value are available and option value
- Use option value to find out what is value of information. Use value of information for trade-off between increasing implementation cost and investing in Research and Development

- Quick analysis of impact of catastrophe can be performed with Extreme Value probability density function of CO2 concentration and Monte Carlo simulation
- For catastrophe events focus more on magnitude of sudden increase CO2 emission

Monitoring

- Update CO2 concentration level regularly and update drift and volatility parameters and learn from new information
- Perform real options analysis to update CO2 policy targets and implementation costs
- Monitor sudden increases of CO2 emission rates as these may signal impending catastrophe events

Implementation

- Be realistic with CO2 policy targets. Some policies are unattainable because of long implementation time
- Be prepared for catastrophe events. Stay cautious and prudent
- Adaptation policy requires to be implemented fully and immediately as costs will increase with delays
- Even small percentage of CO2 emission cutback will save plenty of higher costs in future
- For an optimal time policy with fixed time period for implementation, increase in CO2 reduction rate will require increase in the time for implementation. At the same time, the managerial flexibility will decline because there is shorter time left.

10.3 Contributions

This research introduces several interesting and novel features in real options analysis and related climate change studies. A short summary of the novelties in the research are described below.

The research develops a stochastic process model for CO2 emission with parameters which are estimated from observed CO2 concentration data. It shows that these parameters are different from usual parameters obtained from climate science models.

Both CO2 emission cutback and CO2 concentration abatement are incorporated into a stochastic process model. A closed form analytical solution is derived for perpetual time. The model and solution can also be used for catastrophe events by incorporating jump events.

In finite time problems, first hitting time is used as one of the stopping time. The other stopping time is optimal stopping time. These stopping times represent conservative and optimal policies for CO2 reduction. Longstaff Schwartz Monte Carlo numerical method is demonstrated for pricing option to defer projects in real options analysis of finite time problems.

Catastrophe events are investigated extensively with uncertainty in jump sizes, variance in size, and frequencies

The research contributes to a better understanding of timing and effectiveness of CO2 reduction policies in normal and catastrophe events.

10.4 Limitations

The research is theoretical study of CO2 reduction policies with real options analysis. There will be assumptions and imitations in modelling to facilitate solutions which may not be entirely accurate. These are listed below under climate and modelling headings.

Climate

This research considers only net CO2 concentration in the atmosphere and does take into account CO2 decay factors, CO2 in oceans and other CO2 sinks such CO2 in permafrost and soils. As the net CO2 concentration is used in the research, the model does not take into account physical science of climate system, such as

ocean circulation, for climate change projections. Although CO2 concentration is a main contributor to climate forcing, the research does not take into account the effect of other greenhouse gases such as nitrous oxide and methane. Clouds and water vapour are also important climate forcing factors which are not considered in this research as it is too complex even for climate science modelling.

Modelling

The stochastic process model assumes that drift and volatility parameters in stochastic differential equation are stable over time. In reality these parameters may change over long periods of time with economic growth and technology innovations. The value of project using no arbitrage approach assumes that long term assets are available to hedge the project. The reduction cost function is highly simplified and may not be realistic and the discount rate used in the analysis is unknown. These uncertainties are mitigated to certain extent using sensitivity analysis of reduction rates and discount rates in the research.

A main problem of using Monte Carlo numerical method in jump diffusion model solution (for catastrophe events) is the overshooting of value solution across the free boundary at adoption time. This problem happens when a jump occurs at the same time as the stopping time. Although the stopping time can be captured accurately once the stopping time is reached, the large incremental jump value overshoots across the adoption boundary. This causes an overestimation or excess value above the boundary which in turn results in a higher value to be used in the calculation of option value. This problem can be minimized by using smaller sub periods in the simulated path and reducing the excess value.

10.5 Validity

The CO2 emission model used in the research projects CO2 concentration level to 2100 which are compatible to a certain extent of the CO2 concentration level

in IPCC B1 scenario to 2100. Higher CO2 concentration levels could be reproduced in the CO2 emission model using larger drift rates and volatility by adjusting the confidence levels of these estimated parameters.

The option values produced the results of the real options analysis model similar characteristics and properties of financial option pricing models. This confirms the validity of the analysis procedure.

The results of the research are intuitively reasonable:

- Low discount rate and CO2 reduction rate produce low opportunity cost, high flexibility, and defers adoption time;
- CO2 adaptation requires immediate action because of urgency of problem while CO2 mitigation has longer adoption time because of uncertainty in the process;
- Optimal CO2 reduction rate in finite time for:
    - first hitting time is near full reduction (100%) because there is few uncertainties and only flexibility is downwards adjustment;
    - optimal stopping time is mid reduction (50%) because there is greater uncertainties and flexibility can be either upwards of downwards adjustment;
- large jump size and jump intensity introduces higher option values because of deeper uncertainties;
- catastrophe events have earlier stopping times than normal events because catastrophe events result in greater damages and more urgency.

10.6 Further Research

The potential areas of future research and investigation are described below.

Damage Cost Function Variations

A different value of the value of θ parameter in the benefit function $B = \theta X^m$ for catastrophe events could be investigated and compare with the same parameter for

normal events. This may indicate the economic impact sensitivity of catastrophe events to equivalent flow of CO2 concentration to social costs (θ).

For catastrophe events, the probability distribution of CO2 concentration levels is shown to be either a Frechet or Extreme Value Theory function. It is possible to use a general form of these distribution functions in the damage loss function, for example, an exponential type function with variables in jump size and jump intensity.

Integrate temperature with CO2 concentration level

A recent research trend is to use temperature increase in the cost damage function. Weitzman proposes a loss function which relates directly to increase in temperature (M.L. Weitzman, 2010):

$$L(\Delta T)=exp\ [\ -\beta(\Delta T)^2]$$

where β is a parameter, $L(\Delta T)$ is the damage loss function, ΔT is the temperature increase. Using this approach real options analysis and temperature increase could be used together to study CO2 reduction policies.

Sequential Real Option Analysis in Finite Time

This will require two optimizations to be performed back to back. For example, set an arbitrary time for the first exercise time. Start from the last period and to arrive at the optimal stopping time for the first period. This procedure allows additional learning to take place before making the final decision (Trigeorgis, 1996; Weeds, 2002). Sequential investment can also be studied as continuous investments with new information arrival (Majd & Pindyck, 1987).

Principal component analysis of jump factors

The jump diffusion studies with Monte Carlo numerical method produce a large amount of statistical data. These raw data can be further analysed using structural equation modelling (SEM) to determine the relative importance of the jump factors.

Multivariate distribution simulation using Metropolis-Hastings algorithm

The jump diffusion studies employ contain 3 variables in its jump events: jump size, jump size variation, and jump size. In this case a multivariate distribution simulation may be a more efficient for studying the analysis.

Generalized Extreme Value Theory Distribution

The jump size distribution could be replaced easily with other probability density distribution in the numerical analysis. For example, using with the extreme value distribution (a three parameter probability distribution) will provide fresh insight into the types of jump properties which affect policymaking.

Copula Analysis with Real Options Analysis

Copula analysis is relatively new in real options analysis. It is widely used in pricing credit derivatives and has been used in civil and environmental engineering studies (Salvadori, de Michele, Kottegoda, & Rosso, 2007). This methodology would be useful for investigating extreme events from marginal probability and probability dependence of jump factors. This methodology could also be applied in a two factor real options analysis, for example, probabilistic dependence of CO2 reduction cost and CO2 concentration levels.

Additional Practical Applications

For practical applications, the framework and procedures described in this thesis could be used to study of impact of mitigation and adaptation policies in other problems affected by climate change.

One example is sea level rise caused by global warming. In this example, the sea level height replaces CO2 concentration. Catastrophe events are caused by collapse of Antarctica ice shelf and melting of ice sheets. Damages are related to flooding of cities.

Another example is agriculture crop failures caused by extreme weather changes. In this example, rain precipitation or temperature replaces CO2 concentration.

10.7 Final Remarks

Although it would be impossible to develop a perfect model and analysis, these models do have their usefulness. It has been said that, "*All models are wrong, some models are useful*" (Box & Draper, 1987). Even if the models may seem to be incorrect, these models could still contribute to scientific research. As Karl Popper puts it, *"In so far as a scientific statement speaks about reality, it must be falsifiable; and in so far as it is not falsifiable, it does not speak about reality."*(Popper, 1962).

Global warming is an urgent problem and there are many views and proposed solutions to the problem. *"There is an air of unreality in debating these arcane points when the world is changing in such dramatic ways right in front of our eyes because of global warming."* (Gore & Melcher Media., 2006).

We must not let uncertainties deter us to keep on exploring, researching and investigating even though we may never have the perfect answer and solution. Every discovery step in science is new knowledge for a better environment for future generations.

REFERENCES

Ackerman, F., DeCanio, S. J., Howarth, R. B., & Sheeran, K. (2009). Limitations of integrated assessment models of climate change. *Climatic Change, 95*(3), 297-315.

Ahn, S. R., Bae, H. O., Koo, H. K., & Lee, K. (2011). A survey on American options: old approaches and new trends. *Bull. Korean Math. Soc, 48*(4), 791-812.

Alesii, G. (2008). Assessing Least Squares Monte Carlo for the Kulatilaka Trigeorgis General Real Options Pricing Model (D. o. P. a. A. M. Physics and Natural Sciences, Trans.): Universit´a di L'Aquila, Faculty of Mathematics, Via Vetoio (Coppito 1), Coppito di L'Aquila 67010 AQ, Italy.

Amin, K. I. (1993). Jump diffusion option valuation in discrete time. *Journal of Finance*, 1833-1863.

Amram, M., & Kulatilaka, N. (1999). *Real options: Managing strategic investment in an uncertain world*: Harvard Business School Press.

Arrow, K. J., & Fisher, A. C. (1974). Environmental preservation, uncertainty, and irreversibility. *The Quarterly Journal of Economics, 88*(2), 312-319.

Atiya, A. F., & Metwally, S. A. K. (2005). Efficient estimation of first passage time density function for jump-diffusion processes. *SIAM Journal on Scientific Computing, 26*(5), 1760-1775.

Ball, C. A., & Torous, W. N. (1983). A simplified jump process for common stock returns. *Journal of Financial and Quantitative Analysis, 18*(1), 53-65.

Baranzini, A., Chesney, M., & Morisset, J. (2003). The impact of possible climate catastrophes on global warming policy. *Energy Policy, 31*(8), 691-701.

Barone-Adesi, G., & Whaley, R. E. (1987). Efficient analytic approximation of American option values. *Journal of Finance*, 301-320.

Barraquand, J., & Martineau, D. (1995). Numerical valuation of high dimensional multivariate American securities. *Journal of Financial and Quantitative Analysis, 30*(3).

Bates, D. S. (1991). The crash of'87: Was it expected? The evidence from options markets. *Journal of Finance*, 1009-1044.

Bernanke, B. S. (1983). Irreversibility, uncertainty, and cyclical investment. *The Quarterly Journal of Economics, 98*(1), 85-106.

Black, F., & Scholes, M. (1973). The pricing of options and corporate liabilities. *The Journal of Political Economy*, 637-654.

Box, G. E. P., & Draper, N. R. (1987). *Empirical model-building and response surfaces*. New York: Wiley.

Boyle, P. P. (1977). Options: A Monte Carlo approach. *Journal of Financial Economics, 4*(3), 323-338.

Brach, M. A., & Paxson, D. A. (2001). A gene to drug venture: Poisson options analysis. *R&D Management, 31*(2), 203-214.

Brennan, M. J., & Schwartz, E. S. (1985). Evaluating natural resource investments. *Journal of Business*, 135-157.

Broadie, M., & Glasserman, P. (1997). Pricing American-style securities using simulation. *Journal of Economic Dynamics and Control, 21*(8-9), 1323-1352.

Cai, N., & Kou, S. (2011). Option pricing under a mixed-exponential jump diffusion model. *Management Science, 57*(11), 2067.

Chao, H. P. (1995). Managing the Risk of Global Climate Catastrophe: An Uncertainty Analysis. *Risk Analysis, 15*(1), 69-78.

Chen, Y.-F., & Funke, M. (2010). Global Warming And Extreme Events: Rethinking The Timing And Intensity Of Environmental Policy: University of Dundee, Economic Studies.

Cline, W. R. (1992). *The economics of global warming*: Peterson Institute.

Cline, W. R. (2011). *Carbon Abatement Costs and Climate Change Finance*. Washington: Peterson Institute for International Economics.
Cobb, C. W., & Douglas, P. H. (1928). A theory of production. *The American Economic Review, 18*(1), 139-165.
Cont, R., & Tankov, P. (2008). *Financial modelling with jump processes* (2nd rev. ed.). Boca Raton, Fla. u.a.: Chapman & Hall/CRC.
Copeland, T. E., & Antikarov, V. (2001). *Real options : a practitioner's guide*. New York: Texere.
Cortazar, G. (2001). Simulation and Numerical Methods in Real Options Valuation. In E. S. Schwartz & L. Trigeorgis (Eds.), *Real options and investment under uncertainty : classical readings and recent contributions* (pp. 871 p.). Cambridge, Mass.: MIT Press.
Cox, D. R., & Miller, H. D. (1965). The theory of stochastic processes (Vol. 134): Chapman and Hall.
Cox, J. C., & Ross, S. A. (1976). The valuation of options for alternative stochastic processes. *Journal of Financial Economics, 3*(1), 145-166.
Cox, J. C., Ross, S. A., & Rubinstein, M. (1979). Option pricing: A simplified approach. *Journal of Financial Economics, 7*(3), 229-263.
Dellink, R. B. (2005). *Modelling the costs of environmental policy : a dynamic applied general equilibrium assessment*. Cheltenham, UK ; Northampton, MA: Edward Elgar.
Dixit, A. K. (1993). *The Art of Smooth Pasting*. Reading England: Harwood Academic Publishers.
Dixit, A. K., & Pindyck, R. S. (1994). *Investment under uncertainty*. Princeton, N.J.: : Princeton University Press.
Duffy, D. J. (2006). *Finite difference methods in financial engineering : a partial differential equation approach*. Chichester, England ; Hoboken, NJ: Wiley.
Epstein, L. G. (1980). Decision making and the temporal resolution of uncertainty. *International Economic Review, 21*(2), 269-283.
Gerber, H. U., & Shiu, E. S. W. (1998). Pricing perpetual options for jump processes. *North American Actuarial Journal, 2*(3).
Geske, R., & Johnson, H. E. (1984). The American put option valued analytically. *Journal of Finance*, 1511-1524.
Gjerde, J., Grepperud, S., & Kverndokk, S. (1999). Optimal climate policy under the possibility of a catastrophe. *Resource and Energy Economics, 21*(3), 289-317.
Glasserman, P. (2004). *Monte Carlo methods in financial engineering*. New York: Springer.
Gollier, C., & Treich, N. (2003). Decision-making under scientific uncertainty: The economics of the precautionary principle. *Journal of Risk and Uncertainty, 27*(1), 77-103.
Gore, A., & Melcher Media. (2006). *An Inconvenient Truth : the planetary emergency of global warming and what we can do about it*. Emmaus, Pa.: Rodale Press.
Graham, D. A. (1981). Cost-Benefit Analysis Under Uncertainty. *The American Economic Review, 71*(4), 715-725.
Green Book. (2011). The Green Book- Appraisal and Evaluation in Central Government: HM Treasury
Grenadier, S. R., & Weiss, A. M. (1997). Investment in technological innovations: An option pricing approach. *Journal of Financial Economics, 44*(3), 397-416. doi: 10.1016/s0304-405x(97)00009-3
Hallegatte, S., Shah, A., Lempert, R., Brown, C., & Gill, S. (2012). Investment decision making under deep uncertainty - application to climate change *Policy Research Working Paper* (pp. 41): The World Bank.
Hanson, F., & Westman, J. (2002). Stochastic analysis of jump-diffusions for financial log-return processes. *Stochastic Theory and Control*, 169-183.

Hardin, G. (1968). The Tragedy of the Commons. *Science, 162*(3859), 1243-1248.
Harrison, J. M. (1985). *Brownian motion and stochastic flow systems* (1st ed.). New York: : Wiley.
Harvey, F., & Vidal, J. (2011). Durban deal will not avert catastrophic climate change, *The Guardian*. Retrieved from http://www.guardian.co.uk/environment/2011/dec/11/durban-climate-change-deal?intcmp=239
Haug, E. G. (2007). *The complete guide to option pricing formulas* (2nd ed.). New York: McGraw-Hill.
Heal, G., & Kriström, B. (2002). Uncertainty and climate change. *Environmental and Resource Economics, 22*(1), 3-39.
Higham, D. J. (2001). An algorithmic introduction to numerical simulation of stochastic differential equations. *SIAM review*, 525-546.
Hilliard, J. E., & Schwartz, A. (2005). Pricing European and American derivatives under a jump-diffusion process: A bivariate tree approach. *Journal of Financial and quantitative Analysis, 40*(3), 671.
Hull, J. (2012). *Options, futures, and other derivatives* (8th ed.). Harlow, England: Pearson Education Ltd.
Ingersoll, J. E. (1987). *Theory of financial decision making*. Totowa, N.J.: : Rowman & Littlefield.
IPCC. (2007). The Physical Science Basis. Contribution of Working Group I to the Fourth Assessment Report of the Intergovernmental Panel on Climate Change *Cambridge University Press, Cambridge, United Kingdom and New York, NY, USA* (Vol. 996, pp. 2007).
IPCC AR4. (2007a). Climate change 2007 : impacts, adaptation and vulnerability : contribution of Working Group II to the fourth assessment report of the Intergovernmental Panel on Climate Change (pp. ix, 976 p. : ill. (some col.), maps ; 928 cm. + 971 CD-ROM (974 973/974 in.)). Cambridge, U.K. ; New York :: Cambridge University Press.
IPCC AR4. (2007b). Climate change 2007 : mitigation of climate change : contribution of Working Group III to the Fourth Assessment Report of the Intergovernmental Panel on Climate Change (pp. x, 851 p. : ill. ; 828 cm.). Cambridge :: Cambridge University Press.
IPCC AR4. (2007c). Climate change 2007 : the physical science basis : contribution of Working Group I to the Fourth Assessment Report of the Intergovernmental Panel on Climate Change (pp. viii, 996 p. : col. ill., col. maps ; 929 cm. + 991 CD-ROM (994 993/994 in.)). Cambridge ; New York :: Cambridge University Press.
IPCC SAR. (1996). Climate change, 1995 : impacts, adaptations, and mitigation of climate change: scientific-technical analyses : contribution of WGII to the second assessment report of the Intergovernmental Panel on Climate Change (Vol. 914950, pp. x, 878 p. : ill., maps (some col.) ; 829 cm.). Cambridge [England] ; New York, NY, USA: Cambridge University Press.
IPCC SRES. (2000). *Special Report on Emissions Scenarios: Summary for Policymakers*: IPCC, Geneva, Switzerland.
IPCC SREX. (2012). IPCC, 2012: Managing the Risks of Extreme Events and Disasters to Advance Climate Change Adaptation. A Special Report of Working Groups I and II of the Intergovernmental Panel on Climate Change In C. B. Field, V. Barros, T.F. Stocker, D. Qin, D.J. Dokken, K.L. Ebi, M.D. Mastrandrea, K.J. Mach, G.-K. Plattner, S.K. Allen, M. Tignor & P. M. Midgley (Eds.), (pp. 582). Cambridge, UK.
IPCC TAR. (2001a). Climate Change 2001: Impacts, Adaptation and Vulnerability. IPCC Third Assessment Report. Cambridge: Cambridge University Press.
IPCC TAR. (2001b). Climate Change 2001: Synthesis Report-Summary for Policymakers (pp. 20). Cambridge: Cambridge University Press.

Jacka, S. (1991). Optimal stopping and the American put. *Mathematical Finance, 1*(2), 1-14.
Kann, A., & Weyant, J. P. (2000). Approaches for performing uncertainty analysis in large-scale energy/economic policy models. *Environmental Modeling and Assessment, 5*(1), 29-46.
Karlin, S., & Taylor, H. M. (1975). *A first course in stochastic processes* (2d ed.). New York: : Academic Press.
Kim, I. J. (1990). The Analytic Valuation of American Options. *Review of Financial Studies, 3*(4), 547-572.
Kodukula, P., & Papudesu, C. (2006). *Project valuation using real options: a practitioner's guide*. Plantation, Florida: J Ross Pubishing.
Koh, W., & Paxson, D. (2007). Real R&D Options in Paradise and Purgatory. *SSRN eLibrary*.
Kolstad, C. D., & Toman, M. (2005). Chapter 30 The Economics of Climate Policy. In M. Karl-Göran & R. V. Jeffrey (Eds.), *Handbook of Environmental Economics* (Vol. Volume 3, pp. 1561-1618): Elsevier.
Kou, S. G. (2002). A Jump-Diffusion Model for Option Pricing. *Management Science, 48*(8), 1086-1101. doi: 10.1287/mnsc.48.8.1086.166
Kou, S. G., & Wang, H. (2003). First passage times of a jump diffusion process. *Advances in Applied Probability, 35*(2), 504-531.
Kou, S. G., & Wang, H. (2004). Option pricing under a double exponential jump diffusion model. *Management Science*, 1178-1192.
Kwok, Y. K. (2008). Mathematical models of financial derivatives *Springer Finance* (pp. xv, 530 p. ill. 525 cm.).
Lenton, T. (2011). Early Warning of Climate Tipping Points. *Nature Climate Change 1*(4), 201-109.
Lenton, T., Held, H., Kriegler, E., Hall, J., Lucht, W., Rahmstorf, S., & Schellnhuber, H. J. (2008). Tipping Elements in the Earth's Climate System. *Proceedings of the National Academy of Sciences, 105*(6), 1786-1793.
Lin, T., Ko, C., & Yeh, H. (2007). Applying real options in investment decisions relating to environmental pollution. *Energy Policy, 35*(4), 2426-2432.
Lin, X. S. (2006). *Introductory stochastic analysis for finance and insurance*. Hoboken, N.J.: John Wiley.
Longstaff, F. A., & Schwartz, E. S. (2001). Valuing American options by simulation: A simple least-squares approach. *Review of Financial Studies, 14*(1), 113-147.
MacMillian, L. (1986). An analytical approximation for the American put prices. . *Advances in Futures and Options Research 1*, 119–139.
Majd, S., & Pindyck, R. S. (1987). Time to build, option value, and investment decisions. *Journal of Financial Economics, 18*(1), 7-27.
Makropoulou, V., Dotsis, G., & Markellos, R. N. (2008). Environmental Policy Implications of Extreme Variations in Pollutant Stock Levels and Socioeconomic Costs. *SSRN eLibrary*.
Manne, A. S., & Richels, R. G. (1991). Buying greenhouse insurance. *Energy policy 19*(6), 543-552
Markandya, A., & Wakiss, P. (2010). Potential costs and benefits of adaptation options: A review of existing literature (pp. 83). Geneva: United Nations Framework Convention on Climate Change.
McDonald, R., & Siegel, D. (1986). The value of waiting to invest. *The Quarterly Journal of Economics, 101*(4), 707.
McKean Jr, H. P. (1965). Appendix: A free boundary problem for the heat equation arising from a problem in mathematical economics. *Industrial Management Review, 6*(2), 32-39.
McKinsey, C. (2009). Pathways to a Low-Carbon Economy: Version 2 of the Global Greenhouse Gas Abatement Cost Curve, from https://solutions.mckinsey.com

Meadows, D. H., Meadows, D. L., Randers, J., & Behrens, W. W. (1972). *The limits to growth* (Vol. 381): Universe books New York.
Merton, R. C. (1973). Theory of Rational Option Pricing. *Bell Journal of Economics and Management Science, 4*(1), 141-183.
Merton, R. C. (1976). Option pricing when underlying stock returns are discontinuous. *Journal of Financial Economics, 3*(1-2), 125-144.
Mordecki, E. (1999). Optimal stopping for a diffusion with jumps. *Finance and Stochastics, 3*(2), 227-236.
Myers, S. C. (1977). Determinants of corporate borrowing. *Journal of Financial Economics, 5*(2), 147-175.
Narain, U., Hanemann, M., & Fisher, A. (2007). The irreversibility effect in environmental decisionmaking. *Environmental and Resource Economics, 38*(3), 391-405.
Neftci, S. N. (2000). *An introduction to the mathematics of financial derivatives* (2nd ed.). San Diego: Academic Press.
NOAA. (2012). The NOAA Annual Greenhouse Gas Index (AGGI), from http://www.esrl.noaa.gov/gmd/aggi/
Nordhaus, W. D. (1991). The cost of slowing climate change: a survey. *The Energy Journal, 12*(1), 37-66.
Nordhaus, W. D. (1994). *Managing the global commons: the economics of climate change*.
Nordhaus, W. D. (2010). RICE-2010 Model. New Haven: Yale University.
Paddock, J. L., Siegel, D. R., & Smith, J. L. (1988). Option valuation of claims on real assets: the case of offshore petroleum leases. *The Quarterly Journal of Economics, 103*(3), 479-508.
Pennings, E., & Lint, O. (1997). The option value of advanced R & D. *European Journal of Operational Research, 103*(1), 83-94.
Peterson, S. (2006). Uncertainty and economic analysis of climate change: A survey of approaches and findings. *Environmental Modeling and Assessment, 11*(1), 1-17.
Picchini, U. (2007). SDE toolbox: Simulation and estimation of stochastic differential equations with MATLAB, from http://sdetoolbox.sourceforge.net/
Pindyck, R. S. (1991). Irreversibility, uncertainty, and investment: National Bureau of Economic Research.
Pindyck, R. S. (2000). Irreversibilities and the timing of environmental policy. *Resource and Energy Economics, 22*(3), 233-259.
Pindyck, R. S. (2002). Optimal timing problems in environmental economics. *Journal of Economic Dynamics and Control, 26*(9-10), 1677-1697.
Popper, K. R. (1962). *Conjectures and Refutations ; the Growth of Scientific Knowledge*. New York: Routledge & K. Paul.
Ramsey, F. P. (1928). A mathematical theory of saving. *The Economic Journal, 38*(152), 543-559.
Rubinstein, M., & Reiner, E. (1991). Breaking down the barriers. *Risk, 4*(8), 28-35.
Sabour, S. A. A., & Poulin, R. (2006). Valuing real capital investments using the least-squares Monte Carlo method. *The Engineering Economist, 51*(2), 141-160.
Salvadori, G., de Michele, C., Kottegoda, N. T., & Rosso, R. (2007). *Extremes in Nature: An Approach Using Copulas* (Vol. 56). Berlin: Springer.
Saphores, J.-D. M. (2004). Environmental uncertainty and the timing of environmental policy. *Natural Resource Modeling, 17*(2), 163-190.
Saphores, J.-D. M., & Carr, P. J. (2001). Real Options and the Timing of Implementation of Emission Limits under Ecological Uncertainty. In M. J. Brennan & L. Trigeorgis (Eds.), *Project flexibility, agency, and competition : new developments in the theory and application of real options* (pp. viii, 357 p.). New York: Oxford University Press.

Schwartz, E. S. (1977). The Valuation of Warrants: Implementing a New Approach. *Journal of Financial Economics, 4*, 79-94.
Schwartz, E. S., & Moon, M. (1999). Evaluating Research and Development Investments. In M. J. Brennan & L. Trigeorgis (Eds.), *Project flexibility, agency, and competition : new developments in the theory and application of real options* (pp. viii, 357 p.). New York: Oxford University Press.
Scripps Institution of Oceanography. Monthly atmospheric CO2 concentrations (ppm) derived from flask air samples Retrieved 20 March 2012, from http://scrippsco2.ucsd.edu/data/atmospheric_co2.html
Silverman, B. W. (1986). *Density estimation for statistics and data analysis* (Vol. 26): Chapman & Hall/CRC.
Snell, J. (1952). Applications of Martingale System Theorems. *Transactions of the American Mathematical Society, 73*(2), 293-312.
Solomon, S., Plattner, G. K., Knutti, R., & Friedlingstein, P. (2009). Irreversible climate change due to carbon dioxide emissions. *Proceedings of the National Academy of Sciences, 106*(6), 1704.
Stern, N. H., Peters, S., Bakhshi, V., Bowen, A., Cameron, C., Catovsky, S., . . . Dietz, S. (2006). *Stern Review: The economics of climate change* (Vol. 30): HM treasury London.
Synowiec, D. (2008). Jump-diffusion models with constant parameters for financial log-return processes. *Computers & Mathematics with Applications, 56*(8), 2120-2127.
Tilley, J. A. (1993). Valuing American options in a path simulation model. *Transactions of the Society of Actuaries, 45*(83), 104.
Trigeorgis, L. (1993). The nature of option interactions and the valuation of investments with multiple real options. *Journal of Financial and Quantitative Analysis, 28*(01), 1-20.
Trigeorgis, L. (1996). *Real options : managerial flexibility and strategy in resource allocation*. Cambridge, Mass.: : MIT Press.
Tuckwell, H. C., & Wan, F. Y. M. (1984). First-passage time of Markov process to moving barriers. *Journal of Applied Probability*, 695-709.
UNFCCC, U. (2009). Kyoto Protocol Reference Manual on Accounting of Emissions and Assigned Amount. Bonn, Germany: UNFCC.
Wald, A. (1945). Sequential tests of hypotheses. *Ann Math Statist, 16*, 117-186.
Weeds, H. (2002). Strategic Delay in a Real Options Model of R&D Competition. *The Review of Economic Studies, 69*(3), 729-747. doi: 10.1111/1467-937X.t01-1-00029
Weitzman, M. L. (1998). Why the far-distant future should be discounted at its lowest possible rate. *Journal of Environmental Economics and Management, 36*(3), 201-208.
Weitzman, M. L. (2010). Some Dynamic Economic Consequences of the Climate Sensitivity Inference Dilemma *Handbook of Environmental Accounting* (pp. 187-206): Edward Elgar Publishing.
Weitzman, M. L., & Gollier, C. (2010). How should the distant future be discounted when discount rates are uncertain? *Economic Letters, 107*(3), 350-353.
Wigley, T. M. L., Richels, R., & Edmonds, J. A. (1996). Economic and environmental choices in the stabilization of atmospheric CO2 concentrations. *Nature, 379*(6562), 240-243.
Woodward, M., Gouldby, B., Kapelan, Z., Khu, S. T., & Townend, I. (2011). Real Options in flood risk management decision making. *Journal of Flood Risk Management, 4*(4), 339-349. doi: 10.1111/j.1753-318X.2011.01119.x
Wright, E. L., & Erickson, J. D. (2003). Incorporating catastrophes into integrated assessment: science, impacts, and adaptation. *Climatic Change, 57*(3), 265-286.

Zhu, Z., & Hanson, F. B. (2005). *A Monte-Carlo option-pricing algorithm for log-uniform jump-diffusion model*.

APPENDIX 1

Derivation of Differential Equation with No Arbitrage

In this derivation the risk neutrality approach is used to construct a replicating portfolio. The replicating portfolio comprises the value of the CO2 reduction project, and traded options on CO2 emission. These options are currently available on ICE (IntercontinentalExchange Inc., NYSE:ICE). ICE Futures Europe is the leading market for carbon dioxide (CO2) emissions. Furthermore, it is assumed that the social benefits or social costs can be hedged with insurance derivative contracts, such as catastrophe bonds.

No Exercise - No Adopt Region

Let V = value of NOT ADOPTING the CO2 reduction project (NAP), X = CO2 concentration level, μ = drift of CO2 emission, σ = standard deviation, r= risk free interest rate, θ and m are parameters in social cost function.

CO2 emission (GBM process) $\mathrm{dX} = \mu \mathrm{X dt} + \sigma \mathrm{X dz}$ [1]

First Portfolio Π_1 is a replicating portfolio comprising η units of V, (η/r) units of θX^m and one unit of X. This portfolio represents the value of investment plus social cost.

$$\Pi_1(\mathrm{t}) = \mathrm{E_t}\left[\eta \mathrm{V(t)} + \mathrm{X(t)} + \left(\frac{\eta}{\mathrm{r}}\right)\theta \mathrm{X^m(t)}\right] \quad [2]$$

Ito's Lemma

$$\mathrm{dV} = \frac{\mathrm{dV}}{\mathrm{dX}}\left(\mu \mathrm{X dt} + \sigma \mathrm{X dz}\right) + \frac{1}{2}\frac{\mathrm{d^2V}}{\mathrm{dX^2}}\left(\mathrm{X dt} + \sigma \mathrm{X dz}\right)^2 \quad [3]$$

Substitute [1] in [2]

$$\mathrm{dV} = \mu \mathrm{X}\frac{\mathrm{dV}}{\mathrm{dX}}(\mathrm{dt}) + \sigma \mathrm{X}\frac{\mathrm{dV}}{\mathrm{dX}}(\mathrm{dz}) + \frac{1}{2}\frac{\mathrm{d^2V}}{\mathrm{dX^2}}(\sigma \mathrm{X})^2(\mathrm{dt}) \quad [4]$$

From [2]

$$\mathrm{d}\Pi_1 = \mathrm{E_t}\left[\eta \mathrm{dV} + \mathrm{dX} + \left(\frac{\eta}{\mathrm{r}}\right)\theta \mathrm{dX^m}\right] \quad [5]$$

Substitute [4] & [1] in [5]

$$\mathrm{d}\Pi_1 = \eta\left(\mu \mathrm{X}\frac{\mathrm{dV}}{\mathrm{dX}} + \sigma \mathrm{X}\frac{\mathrm{dV}}{\mathrm{dX}}(\mathrm{dz}) + \frac{1}{2}\frac{\mathrm{d^2V}}{\mathrm{dX^2}}(\sigma \mathrm{X})^2\right)\mathrm{dt} + \left(\mu \mathrm{X dt} + \sigma \mathrm{X dz}\right) + \left(\frac{\eta}{\mathrm{r}}\right)\theta\left(\mu \mathrm{X dt} + \sigma \mathrm{X dz}\right)^m \quad [6]$$

Stochastic calculus $(\mathrm{dt})^2 = 0, (\mathrm{dz})^2 = \mathrm{dt},\ (\mathrm{dt})(\mathrm{dz}) = 0,\ \mathrm{E_t}(\mathrm{dz}) = 0$

Also it can be shown from the above stochastic relationships that $(\mu X dt+\sigma X dz)^m = 0$ for all values of m equal or greater than 2

Simplifying

$$d\prod_1 = \eta\left(\mu X\frac{dV}{dX}+\frac{1}{2}\frac{d^2V}{dX^2}(\sigma X)^2\right)dt + \mu X(dt) \quad [7]$$

We eliminate μ by setting Hedging Ratio $\eta = -\left(\frac{dV}{dX}\right)^{-1}$ [8]

$$d\prod_1 = \eta\mu X\frac{dV}{dX}(dt)+\eta\frac{1}{2}\frac{d^2V}{dX^2}(\sigma X)^2(dt)+\mu X(dt)$$

$$d\prod_1 = \eta\mu X\frac{dV}{dX}(dt)+\eta\frac{1}{2}\frac{d^2V}{dX^2}(\sigma X)^2(dt)+\mu X(dt)$$

$$d\prod_1 = -\left(\frac{dX}{dW}\right)\mu X\frac{dV}{dX}(dt)+\eta\frac{1}{2}\frac{d^2V}{dX^2}(\sigma X)^2(dt)+\mu X(dt)$$

$$d\prod_1 = -\mu X(dt)+\eta\frac{1}{2}\frac{d^2V}{dX^2}(\sigma X)^2(dt)+\mu X(dt)$$

$$d\prod_1 = \eta\frac{1}{2}\frac{d^2V}{dX^2}(\sigma X)^2(dt) \quad [9]$$

The second portfolio $\prod_2$ comprised η units of V, (η/r) units of θX^m, and one unit of X.

Note that the second portfolio has same portfolio composition as the first portfolio.

Second Portfolio comprises has risk free return.

Second Portfolio

$$\prod_2 = r\left[\eta V + X + \left(\frac{\eta}{r}\right)\theta X^m\right] \quad [10]$$

$$d\prod_2 = r(\eta V)(dt)+rX(dt)+\eta\theta X^m(dt) \quad [11]$$

Assume that the *value* of project *X(dt)* under consideration is discounted by the policymaker with discount rate of ρ , but the *growth value* of project *V(dt)* is discounted with risk free rate of *r* because the policymaker has no control of interest rate of assets which are traded in the market.

$$d\prod_2 = r(\eta V)(dt)+(\rho)X(dt)+\eta\theta X^m(dt) \quad [12]$$

For no arbitrage, equate Portfolios $d\prod_1 = d\prod_2$ of equations [9] and [11]

$$\eta\frac{1}{2}\frac{d^2V}{dX^2}(\sigma X)^2(dt)=r(\eta V)(dt)+(\rho)X(dt)+\eta\theta X^m(dt)$$

$$r(\eta V)+(\rho)X+\eta\theta X^m=\eta\frac{1}{2}\frac{d^2V}{dX^2}(\sigma X)^2 \quad [13]$$

$$r(\eta V)+\eta\theta X^m=-X(\rho)+\eta\frac{1}{2}\frac{d^2V}{dX^2}(\sigma X)^2 \quad [14]$$

Substitute [8] in [12]

$$rV+\theta X^m=(\rho)X\frac{dV}{dX}+\frac{1}{2}\sigma^2\frac{d^2V}{dX^2}X^2 \quad [15]$$

Exercise-Adopt Region

Let *W* = value of ADOPTING the CO2 reduction project (AP), *X* = CO2 concentration level, α*μ* = drift of CO2 emission after adoption of policy, *σ* = standard deviation, *r*= risk free interest rate, *θ* and *m* are parameters in social benefits function.

CO2 emission (GBM process) $dX=\alpha\mu Xdt+\sigma Xdz$ [16]

First Portfolio Π_1 is a replicating portfolio comprising *η* units of *W,* (*η/r)* units of θX^m and one unit of *X*. This portfolio represents the value of investment (AP) plus social benefits.

$$\Pi_1(t)=E_t\left[\eta W(t)+X(t)\left(\frac{\eta}{r}\right)\theta X^m(t)\right] \quad [17]$$

Ito's Lemma

$$dW=\frac{dW}{dX}(\alpha\mu Xdt+\sigma Xdz)+\frac{1}{2}\frac{d^2W}{dX^2}(Xdt+\sigma Xdz)^2 \quad [18]$$

Substitute [16] in [18]

$$dW=\alpha\mu X\frac{dW}{dX}(dt)+\sigma X\frac{dW}{dX}(dz)+\frac{1}{2}\frac{d^2W}{dX^2}(\sigma X)^2(dt) \quad [19]$$

From [17]

$$d\Pi_1=E_t\left[\eta dW+dX+\left(\frac{\eta}{r}\right)\theta dX^m\right] \quad [20]$$

Substitute [16] & [19] in [20]

$$d\Pi_1=\eta\left(\alpha\mu X\frac{dW}{dX}+\sigma X\frac{dW}{dX}(dz)+\frac{1}{2}\frac{d^2W}{dX^2}(\sigma X)^2\right)dt+(\alpha\mu Xdt+\sigma Xdz)+\left(\frac{\eta}{r}\right)\theta(\alpha\mu Xdt+\sigma Xdz)^m \quad [21]$$

Stochastic calculus

$$(dt)^2=0,(dz)^2=dt,\ (dt)(dz)=0,\ E_t(dz)=0$$

Also it can be shown from the above stochastic relationships that $(\alpha\mu X dt+\sigma X dz)^m = 0$ for all values of m equal or greater than 2

Simplifying

$$d\prod_1 = \eta\left(\alpha\mu X\frac{dW}{dX}+\frac{1}{2}\frac{d^2W}{dX^2}(\sigma X)^2\right)dt+\alpha\mu X(dt) \quad [22]$$

We eliminate μ by setting Hedging Ratio $\eta = -\left(\frac{dW}{dX}\right)^{-1}$ [23]

$$d\prod_1 = \eta\alpha\mu X\frac{dW}{dX}(dt)+\eta\frac{1}{2}\frac{d^2W}{dX^2}(\sigma X)^2(dt)+\alpha\mu X(dt)$$

$$d\prod_1 = -\left(\frac{dX}{dW}\right)\alpha\mu X\frac{dW}{dX}(dt)+\eta\frac{1}{2}\frac{d^2W}{dX^2}(\sigma X)^2(dt)+\alpha\mu X(dt)$$

$$d\prod_1 = -\alpha\mu X(dt)+\eta\frac{1}{2}\frac{d^2W}{dX^2}(\sigma X)^2(dt)+\alpha\mu X(dt)$$

$$d\prod_1 = \eta\frac{1}{2}\frac{d^2W}{dX^2}(\sigma X)^2(dt) \quad [24]$$

The second portfolio $\prod_2$ comprised η units of W, (η/r) units of θX^m, and one unit of X. Note that the second portfolio has same portfolio composition as the first portfolio. Second Portfolio comprises has risk free return.

Second Portfolio

$$\prod_2 = r\left[\eta W + X + \left(\frac{\eta}{r}\right)\theta X^m\right] \quad [25]$$

$$d\prod_2 = r(\eta W)(dt)+rX(dt)+\eta\theta X^m(dt) \quad [26]$$

Assume that the *value* of project $X(dt)$ under consideration is discounted by the policymaker with discount rate of ρ , but the *growth value* of project $W(dt)$ is discounted with risk free rate of r because the policymaker has no control of interest rate of assets which are traded in the market.

$$d\prod_2 = r(\eta W)(dt)+(\rho)X(dt)+\eta\theta X^m(dt) \quad [27]$$

For no arbitrage, equate Portfolios $d\prod_1 = d\prod_2$ of equations [26] and [28]

$$\eta\frac{1}{2}\frac{d^2W}{dX^2}(\sigma X)^2(dt) = r(\eta W)(dt)+(\alpha\rho)X(dt)+\eta\theta X^m(dt)$$

$$r(\eta W)+(\alpha\rho)X+\eta\theta X^m = \eta\frac{1}{2}\frac{d^2W}{dX^2}(\sigma X)^2 \quad [28]$$

$$r(\eta W) + \eta\theta X^m = -(\alpha\rho)X + \eta\frac{1}{2}\frac{d^2W}{dX^2}(\sigma X)^2 \qquad [29]$$

Substitute [23] in [29]

$$rW + \theta X^m = (\alpha\rho)X\frac{dW}{dX} + \frac{1}{2}\sigma^2\frac{d^2W}{dX^2}X^2 \qquad [30]$$

Remarks

In Section 2.8.1 with Business As Usual (BAU) approach, the risk neutral policymaker discount rate is given by equation [54] in Section 2.8.1, that is, the discount rate is $\rho = \mu$.

Then equation [15] for No Adopt Project becomes

$$rV + \theta X^m = \mu X\frac{dV}{dX} + \frac{1}{2}\sigma^2\frac{d^2V}{dX^2}X^2 \qquad [31]$$

And equation [30] for Adopt Project becomes

$$rW + \theta X^m = \alpha\mu X\frac{dW}{dX} + \frac{1}{2}\sigma^2\frac{d^2W}{dX^2}X^2 \qquad [32]$$

APPENDIX 2

General Solution of Linear Second Order Non Homogenous with Variable Coefficients Ordinary Differential Equation

General Form of ODE

The second order ordinary differential equation to be solved is in the form:

$$\frac{1}{2}\sigma^2 X^2 \frac{d^2V}{dX^2} + \mu X \frac{dV}{dX} - rV = X^m \qquad \text{[A2.1]}$$

Homogenous Solution

Guess the solution is $V_h = AX^\beta$

Substitute this into the homogenous solution as solve for β,

$$\beta_1, \beta_2 = \frac{-\left(\mu - \frac{1}{2}\sigma^2\right) \pm \sqrt{\left(\mu - \frac{1}{2}\sigma^2\right)^2 + 2\sigma^2 r}}{\sigma^2} \qquad \text{[A2.2]}$$

And $\mu > \sigma > 0$, and $0 > \beta_1 > \beta_2$

Homogenous Solution is:

$$V_h = A_1 X^{\beta_1} + A_2 X^{\beta_2} \qquad \text{[A2.3]}$$

Where A_1 and A_2 are constants to be determined. Note that β_2 value is very small (minus infinity). This will cause the complete solution to explode, therefore A_2 must be zero.

Particular Solution

Method of Variation of Parameters

Guess the particular solution $V_p = u_1(X) X^{\beta_1} + u_2(X) X^{\beta_2}$ [A2.4]

The method of variation of parameters provides 2 additional equations to equation [A2.4]:

$$u'_1(X) X^{\beta_1} + u'_2(X) X^{\beta_2} = 0 \qquad \text{[A2.5]}$$

$$u'_1(X)\beta_1 X^{\beta_1-1} + u'_2(X)\beta_2 X^{\beta_2-1} = X^m \qquad \text{[A2.6]}$$

Solve for $u'_1(X)$ and $u_1(X)$,

Multiply [A2.6] by X, $$u'_1(X)\beta_1 X^{\beta_1} + u'_2(X)\beta_2 X^{\beta_2} = X^{m+1} \qquad \text{[A2.7]}$$

Subtract [A2.7] from [A2.5] $$u'_1(X)\beta_1 X^{\beta_1} - u'_1(X) X^{\beta_1} = X^{m+1}$$

$$u'_1(X) = \frac{1}{(\beta_1 - 1)} X^{m+1-\beta_1} \qquad \text{[A2.8]}$$

Integrating $$u_1(X) = \frac{1}{(\beta_1 - 1)(m+2-\beta_1)} X^{m+2-\beta_1} \qquad \text{[A2.9]}$$

Solve for $u'_2(X)$ and $u_2(X)$,

Subtract [A2.7] from [A2.5] $$u'_2(X)\beta_2 X^{\beta_2} - u'_2(X) X^{\beta_2} = X^{m+1}$$

$$u'_2(X) = \frac{1}{(\beta_2 - 1)} X^{m+1-\beta_2} \qquad \text{[A2.10]}$$

Integrating $$u_2(X) = \frac{1}{(\beta_2 - 1)(m+2-\beta_2)} X^{m+2-\beta_2} \qquad \text{[A2.11]}$$

Substitute [A2.9] and [A2.11] in [A2.4]

$$V_p = \frac{1}{(\beta_1 - 1)(m+2-\beta_1)} X^{m+2-\beta_1}.X^{\beta_1} + \frac{1}{(\beta_2 - 1)(m+2-\beta_2)} X^{m+2-\beta_2}.X^{\beta_2}$$

$$V_p = X^{m+2}\left[\frac{1}{(\beta_1 - 1)(m+2-\beta_1)} + \frac{1}{(\beta_2 - 1)(m+2-\beta_2)}\right] \qquad \text{[A2.12]}$$

To simplify let $$C_1 = \left[\frac{1}{(\beta_1 - 1)(m+2-\beta_1)} + \frac{1}{(\beta_2 - 1)(m+2-\beta_2)}\right] \qquad \text{[A2.13]}$$

Therefore [A2.12] becomes $$V_p = C_1 X^{m+2} \qquad \text{[A2.14]}$$

Total Solution

$$V = V_h + V_p \qquad \text{[A2.15]}$$

Substitute [A2.3] and [A2.14] in [A2.15]

$$V = A_1 X^{\beta_1} + C_1 X^{m+2} \qquad \text{[A2.16]}$$

Where

$$\beta_1, \beta_2 = \frac{-\left(\mu - \frac{1}{2}\sigma^2\right) \pm \sqrt{\left(\mu - \frac{1}{2}\sigma^2\right)^2 + 2\sigma^2 r}}{\sigma^2}$$

$$C_1 = \left[\frac{1}{(\beta_1 - 1)(m + 2 - \beta_1)} + \frac{1}{(\beta_2 - 1)(m + 2 - \beta_2)}\right]$$

APPENDIX 3

Complete Solution of Real Options Analysis Model

Boundary Conditions

To recapitulate, the policy regions are defined as:

NO ADOPT $$V = A_1 X^{\beta_1} + C_1 X^{m+2} \quad \text{[A3.1]}$$

ADOPT $$W = A_3 X^{\beta_3} + C_2 X^{m+2} \quad \text{[A3.2]}$$

Boundary Condition 1 Value Matching

At the point of investment, *X=X**;

$$V\left(X^*\right) = nW\left(X^*\right) - K \quad \text{[A3.3]}$$

$$A_1 K^{\beta_1} + C_1 K^4 = n\left(A_3 X^{\beta_3} + C_2 X^4\right) - K \quad \text{[A3.4]}$$

The abatement level is *n*, where *1 > n > 0*, where *n=0* for full abatement, and *n=1* for no abatement. For partial abatement, to reduce the cost damages to *n* level will require abatement of the order of *(1-n)* of the level. A partial abatement for n<1 will result in a discontinuity at *X=X**, which is similar to downward jump from *V(X*)* to *nV(X*).*

Boundary Condition 2 Smooth Pasting

Point of contact of two curves is tangential for continuous transition at *X=X**. Notwithstanding the possible discontinuity from Boundary Condition 1, it is a valid assumption to have the two curves to have the same slope at *X=X**.

$$\frac{dV}{dX^*} = \frac{dW}{dX^*} \quad \text{[A3.5]}$$

$$\frac{dV}{dX^*} = A_1\beta_1 X^{*\beta_1 - 1} + (m+2) C_2 X^{*(m+1)} \quad \text{[A3.6]}$$

And

$$\frac{dW}{dX^*} = A_3\beta_3 X^{*\beta_3 - 1} + (m+2) C_2 X^{*(m+1)} \quad \text{[A3.7]}$$

Equating [A3.6] and [A3.7]

$$A_1\beta_1 K^{\beta_1-1} + (m+2)C_1K^{(m+1)} = A_3\beta_3 K^{\beta_3-1} + (m+2)C_2K^{(m+1)} \quad \text{[A3.8]}$$

Final Analytical Solution

From boundary condition equations [A3.4] and [A3.8], there are two equations to solve for two unknowns A_1 and A_3:

$$A_1K^{\beta_1} + C_1K^{(m+2)} = n\left(A_3K^{\beta_3} + C_2K^{(m+2)}\right) - K \quad \text{[A3.9]}$$

$$A_1\beta_1 K^{\beta_1-1} + (m+2)C_1K^{(m+1)} = A_3\beta_3 K^{\beta_3-1} + (m+2)C_2K^{(m+1)} \quad \text{[A3.10]}$$

Solving for A_1:

Multiply [A3.10] by nK/β_3,

$$A_1 n\frac{\beta_1}{\beta_3}K^{\beta_1} + (m+2)C_1\frac{n}{\beta_3}K^{(m+2)} = A_3nK^{\beta_3} + (m+2)C_2\frac{n}{\beta_3}K^{(m+2)} \quad \text{[A3.11]}$$

Subtract from [A3.9] $-A_1K^{\beta_1} - C_1K^{(m+2)} = -A_3nK^{\beta_3} - C_2nK^{(m+2)} + K$ [A3.12]

Then

$$A_1 n\frac{\beta_1}{\beta_3}K^{\beta_1} - A_1K^{\beta_1} + C_1K^{(m+2)}\left([m+2]\frac{n}{\beta_3} - 1\right) = C_2nK^{(m+2)}\left(\frac{[m+2]}{\beta_3} - 1\right) + K$$

$$A_1K^{\beta_1}(n\beta_1 - \beta_3) = C_1K^{(m+2)}(\beta_3 - n[m+2]) + C_2K^{(m+2)}([m+2] - \beta_3) + K\beta_3$$

$$A_1 = \frac{K^{(m+2)-\beta_1}}{\beta_3 - n\beta_1}\left[C_1(n[m+2] - \beta_3) + C_2n([m+2] - \beta_3) - \frac{\beta_3}{K^{(m+1)}}\right] \quad \text{[A3.13]}$$

Solving for A_3 :

Multiply [A3.9] by β_1/K,

$$A_1\beta_1 K^{\beta_1-1} + C_1\beta_1 K^{(m+1)} = A_3n\beta_1 K^{\beta_3-1} + C_2n\beta_1 K^{(m+1)} - \beta_1 \quad \text{[A3.14]}$$

Subtract from [A3.10]

$$-A_1\beta_1 K^{\beta_1-1} - (m+2)C_1K^{(m+1)} = -A_3\beta_3 K^{\beta_3-1} - (m+2)C_2K^{(m+1)} \quad \text{[A3.15]}$$

Then

$$A_3 K^{\beta_3 - 1}\left(n\beta_1 - \beta_3\right) + C_2 K^{(m+1)}\left(n\beta_1 - \left[m+2\right]\right) - \beta_1 = C_1 K^{(m+1)}\left(\beta_1 - \left[m+2\right]\right)$$

$$A_3 K^{\beta_3}\left(\beta_3 - n\beta_1\right) = C_1 K^{(m+2)} n\left(\left[m+2\right] - \beta_1\right) + C_2 K^{(m+2)}\left(n\beta_1 - \left[m+2\right]\right) - K\beta_1$$

$$A_3 = \frac{K^{(m+2)-\beta_3}}{\beta_3 - n\beta_1}\left[C_1\left(\left[m+2\right] - \beta_1\right) - C_2\left(\left[m+2\right] - n\beta_1\right) - \frac{\beta_1}{K^{(m+1)}}\right] \qquad \text{[A3.16]}$$

APPENDIX 4

Solution of Ordinary Differential Equation of Jump Diffusion Model

General Form of ODE

The second order ordinary differential equation to be solved is in the form:

$$\frac{1}{2}\sigma^2 X^2 \frac{d^2V}{dX^2} + \mu X \frac{dV}{dX} - V(\lambda + r) + \lambda\left[V(\varphi - 1)\right] = X^2 \qquad \text{[A4.1]}$$

Where λ is the frequency the jump or Poisson process intensity. $\varphi = (V_{n+1} / V_{n-1})$, and φ is the proportionate increase of CO2 concentration after the jump.

Homogenous Solution

We guess the solution is $V_h = AX^{\beta}$, and substitute this into the homogenous solution as solve for β,

$$\frac{1}{2}\sigma^2\beta^2 + \left(\mu - \frac{1}{2}\sigma^2\right)\beta - (r + \lambda) + \lambda(\varphi - 1)^{\beta} = 0 \qquad \text{[A4.2]}$$

Case 1 $1>\varphi>0$

There is a negative or downward jump, that is, $V_n > V_{n+1}$, which results in a sudden decrease in value of project. This is an improbable situation in nature, therefore we ignore this case.

Case 2 $\varphi = 1$

There is no jump, $\varphi=1$, and the last term is simply λ. Then equation [A4.2] will reduce to the same form as a no-jump continuous process solution.

Case 3 $\varphi = 0$

If $V_{n+1} = 0$, that is the value of project reduces to zero after the jump, then $\varphi=0$.

If β is positive, then the last term is zero, and the solution is:

$$\beta_1, \beta_2 = \frac{-\left(\mu - \frac{1}{2}\sigma^2\right) \pm \sqrt{\left(\mu - \frac{1}{2}\sigma^2\right)^2 + 2\sigma^2(r + \lambda)}}{\sigma^2} \qquad \text{[A4.3]}$$

If β is negative, the last term is undefined, because division by zero is implied.

Case 4 $\varphi>1$

This is a positive or upward jump. Equation [A4.2] can be solved for β value by numerical method. By evaluating equation [A4.2] with various φ values, we can investigate the impact of catastrophe events due the corresponding jump sizes.

The homogenous solution form is given by:

$$V_h = A_1 X^{\beta_1} + A_2 X^{\beta_2} \qquad [A4.4]$$

where β_1 and β_2 are obtained from [A4.3] or [A4.4], and A_1 and A_2 are constants to be determined as described in Appendix 3. Note that β_2 value is very small (minus infinity). This will cause the complete solution to explode, therefore A_2 must be zero.

APPENDIX 5

Comparison of Inter-Arrival Time and Fixed Time Simulation

The numerical example evaluates the efficiency and performance of Monte Carlo numerical solution in a jump diffusion process using the fixed time discretization method and inter arrival time method.

The parameters of the jump diffusion model are drift (μ) 0.003956817 ppm CO2 pa, volatility (σ) 0.000479211 ppm CO2, jump intensity (λ) 0.002 (1 in 500 year), jump size distribution is lognormal jump size distribution, mean jump size is 10 x drift, jump size variance is 0.1 x jump size, and time duration of 500 years. Initial benefits and exercise or adoption benefits are 149,916 ppm CO2 at 299,832 ppm CO2 respectively (that is 2X initial benefits level).

The results are shown below.

	Inter Arrival Time [A]	**Fixed Time Discretization [B]**	**Difference (A-B)/B**
Jump Intensity	0.002	0.002	
Simulation Paths	10000	10000	
Minimum Benefits, 10^6 ppm CO2	7.33	7.27	0.83%
Maximum Benefits, 10^6 ppm CO2	82.46	50.83	62.23%
Average Benefits, 10^6 ppm CO2	8.55	8.55	0%
Average number of jump per path	1.01	1.01	0%
First Hitting Times Level	299832	299832	
No FHT with jumps, %	100	100	0.00%
Mean FHT with jumps, years	87.64	87.71	-0.08%
Std Dev of FHT with jumps	5.30	5.19	2.12%
Simulation Time, seconds	25.34	518.10	-95.11%

Simulation Paths

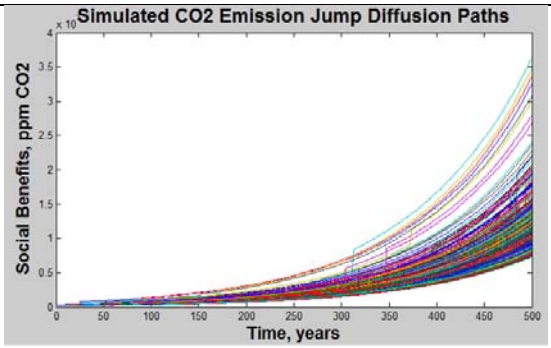

Figure 1

Inter Arrival Time (λ=0.002)

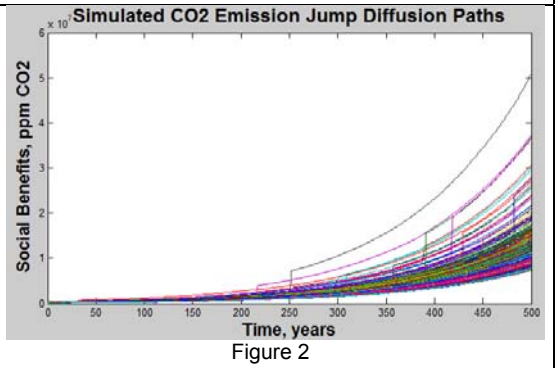

Figure 2

Fixed Time Discretization (λ=0.01)

Density Function at Fixed Time (year 500)

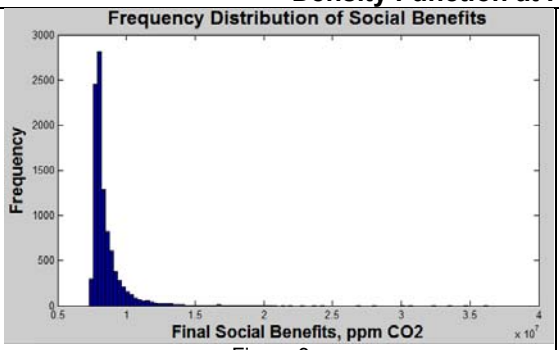

Figure 3

Inter Arrival Time (λ=0.002)

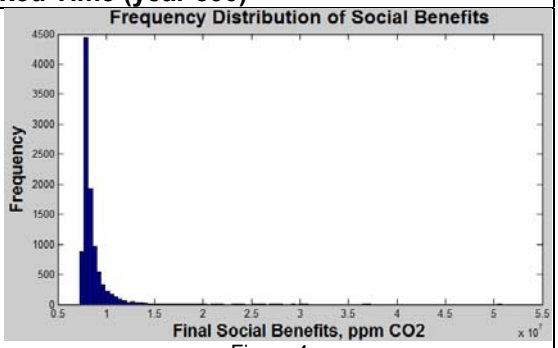

Figure 4

Fixed Time Discretization (λ=0.01)

Frequency Distribution of Social Benefits at end of year 500

Transition Density for First Hitting Time

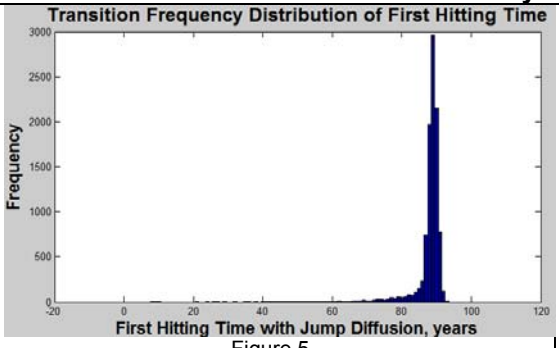

Figure 5

Inter Arrival Time (λ=0.002)

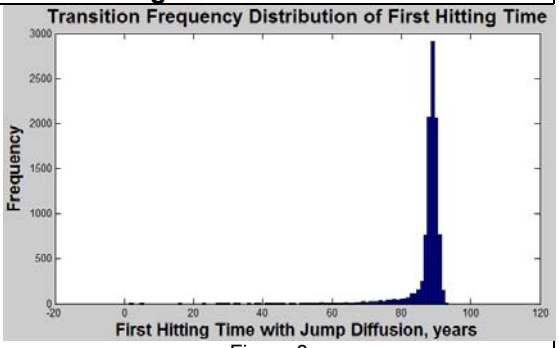

Figure 6

Fixed Time Discretization (λ=0.01)

Frequency Distribution of Social Benefits at 299382 ppm CO2

APPENDIX 6

Longstaff Schwartz's Least Square Regression Basis Algorithm

LSCM method requires forward simulation of random paths. Then, starting at the final time period, each path is evaluated to see if the option would be exercised, and the associated cash flows are recorded. The algorithm then backs up one time period, and the paths are examined to see which are "in the money", that is a positive payoff. For each path that could be exercised, the algorithm performs a linear regression. The least-squares approach for the linear regression results in a function that relates the current option value to the value of continuing. LSCM assumes a simple quadratic regression function given by:

$$Continuing = \beta_0 + \beta_1 * exercise + \beta_2 * exercise^2$$

The function is then evaluated for each path that is in the money, and compared with the value of immediate exercising. The cash flow matrix is then updated to reflect the paths which would be exercised in the current time period, and the algorithm proceeds to the next previous time period.

Once all time periods have been examined, the stopping rule or location of each path can be compiled and the cash flow matrix will contain the gains realized by the exercising the option. The algorithm is efficient because LSCM method only performs the regression when the option is in the money.

Algorithm

Step 1 Compute the simulation matrix of benefit values, *XS*, using the CO2 concentration level, with M paths and N time steps.

Step 2 Compute the cash flows for each path for call option:

$$CF(j) = \max\left\{XS_j(t) - K, 0\right\}$$

Step 3 Back up one time period; set *i=i-1*

Step 4 Compute if the option is in the money for each path *j*. For each path:

a. Let *V* be the vector containing asset prices XS_i and *Y* be the vector containing the corresponding cash flows received at (*i+1*) time period, which have been discounted backward to the i^{th} time period.

b. Regress using least-squares approach to estimate the value of continuing using the equation : $Continuing = \beta_0 + \beta_1 * exercise + \beta_2 * exercise^2$

This will result in the conditional expectation function E[*Y*|*XS*].

c. Compute the value of continuing using E[*Y*|*XS*] and the value of immediately exercising using equation: $CF(j) = \max\{XS_j(t) - K, 0\}$

d. Determine whether to exercise the option immediately or hold the option until the next time period, based on which gives the higher expected value. Establish the current cash flows conditional on not exercising prior to time period *i* using:

$$C_i(j) = \begin{cases} Cash\ Flow; & if\ cash\ flow \geq E[Y \mid XS] \\ 0 \quad ; & otherwise \end{cases}$$

e. Compute the present value of the cash flows $P_i(j)$ given by:

$$P_i(j) = C_i(j) + e^{-r\Delta t} P_i(j)$$

where r is discount rate, Δt is time step (1 year in our model)

Step 5 If at time period one terminate, else go back to Step 3.

Step 6 Compute the average of $C_0(j)$ for call option value.

Compute first hitting time and early exercise time from histogram containing exercise periods.

There are two main contributors to the computational effort required for the LSCM algorithm are computing the CO2 concentration level and solving the least-squares regression equations. For the CO2 concentration level computation of Step 1, a concentration level must be computed for every path *M* and every time period *N*, so the running time is O(*MN*). To solve the least-squares regression equation of Step 4

a 3X3 matrix must be solved, and the least-squares regression equation might potentially be solved a total of N times, i.e. 3^2N. Therefore, the running time for the least-squares regression equation portion is O(N), and the running time for the entire least squares algorithm is O(MN).

APPENDIX 7

Finite Time Model for Multiple Gases in CO2-eq

With multiple gases, such as CO2-eq in GHG, it is necessary to evaluate each gas as a separate asset and combine the results to obtain a general solution. Therefore a finite time solution using numerical method is feasible.

The outline of the solution is as follows:

Gas (before reduction)	Gas (after reduction)	Reduction Cost
$X_1 = f(\mu_1,\sigma_1)$	$Y_1 = f(\mu'_1,\sigma'_1)$	K_1
$X_2 = g(\mu_2,\sigma_2)$	$Y_2 = f(\mu'_2,\sigma'_2)$	K_2
.	.	.
.	.	.
$X_n = n(\mu_n,\sigma_n)$	$Y_n = f(\mu'_n,\sigma'_n)$	K_n

Total GHG conc before reduction: $X = \Sigma(X_1 + X_2 + \ldots\ldots + X_n)$

Total GHG conc after reduction: $Y = \Sigma(Y_1 + Y_2 + \ldots\ldots + Y_n)$

Value of Benefits before reduction $- \theta X^m$

Value of Benefits after reduction $- \theta Y^m$

Benefits of Reduction Project: $B = -\theta X^m + \theta Y^m$

Total GHG Reduction Cost: $K = \Sigma(K_1 + K_2 + \ldots\ldots + K_n)$

Condition for Adoption: Damage Cost = Benefits of Project - Reduction Cost

or Net Benefits = Reduction Cost

that is, $\theta X^m = \theta Y^m - K$

The above adoption condition is sufficient to solve for first hitting time. For optimal stopping time the backward induction process is necessary to optimize the final solution.

It would be difficult to assess the overall impact of an ensemble of LLGHG models on the results because each LLGHG may have a different gas emission rate

and function. It is likely that the CO2-eq is higher than atmospheric CO2. In this case, the net benefits will increase and the option value is higher.

As an example, consider the following hypothetical case. CO2-eq concentration is twice the CO2 concentration, and the reduction costs are also double for CO2-eq.

	Concentration		Benefits			Red	
	Before	After	Before	After	Net	Cost	Option Value
CO2	10	8	100	64	36	10	26
CO2-eq	20	16	400	256	144	20	120

The higher benefits in CO2-eq suggest that is beneficial to adopt the policy early, or employ the benefits in further research and development so as to resolve the uncertainty at an early period.